APPLICATION OF RAW AND MODIFIED CARBON NANOTUBES FOR ADSORPTION OF BTX COMPOUNDS FROM WATER

BY

Aamir Abbas

A Thesis Presented to the
DEANSHIP OF GRADUATE STUDIES

KING FAHD UNIVERSITY OF PETROLEUM & MINERALS

DHAHRAN, SAUDI ARABIA

In Partial Fulfillment of the
Requirements for the Degree of

MASTER OF SCIENCE

In

CHEMICAL ENGINEERING

May, 2015

KING FAHD UNIVERSITY OF PETROLEUM & MINERALS

DHAHRAN- 31261, SAUDI ARABIA

DEANSHIP OF GRADUATE STUDIES

This thesis, written by **Aamir Abbas** under the direction his thesis advisor and approved by his thesis committee, has been presented and accepted by the Dean of Graduate Studies, in partial fulfillment of the requirements for the degree of **MASTER OF SCIENCE IN CHEMICAL ENGINEERING.**

Dr. Basim Ahmed Abussaud
(Advisor)

Dr. Mohammed Ba-Shammakh
Department Chairman

Dr. Nadhir A. H. Al-Baghli
(Member)

Dr. Salam A. Zummo
Dean of Graduate Studies

Dr. Halim H. Redhwi
(Member)

23/6/15
Date

Dr. Mohamamd Mozahar Hossain
(Member)

Dr. Muataz Ali H. Atieh
(Member)

Dedicated to my family, friends and teachers

ACKNOWLEDGMENTS

All thanks to Almighty Allah for providing me opportunity to complete master degree in Chemical Engineering. I am greatly thankful to King Fahd University of Petroleum and Minerals for admission and awarding scholarship. I am also thankful to department of Chemical Engineering for providing excellent educational and research facilities.

I am cordially thankful to my advisor Dr. Basim A. Abussaud for encouragement, guidance and help in each and every step. I am greatly thankful to my co-advisor Dr. Nadhir A. H. Al-Baghli for his kind support. I would like to thank very courteous teacher and committee member Dr. Muataz Ali Atieh for his unceasing support throughout research. I am really grateful to my committee member Dr. Halim H. Redhwi for his support and time. I am also obliged to Dr. Mohammad Mozahar Hossain for his support and guidance.

I really appreciate and thankful to Mr. Jerwin, Engr. M. Abdulaziz Elgzoly and Mr. Sayed Amanullah for training of equipment and help in characterization of samples. I am highly thankful to Dr. Shaikh Abdur Razzak for authorization to his lab and really appreciate Mr. Muhammad Saad for helping me in analysis in Dr. Sheikh's lab.

I am also thankful to all my friends of Heterogeneous group for their support and providing me company. Special thanks to my parents and other family members for their generous prayers, never-ending support and encouragement to achieve my goals.

Last but not the least; I am thankful to everyone who helped me directly or indirectly in completion of this work.

TABLE OF CONTENTS

LIST OF TABLES

LIST OF FIGURES

LIST OF ABBREVIATIONS

CNTs	:	Carbon Nanotubes
SWCNTs	:	Single Wall Carbon Nanotubes
MWCNT	:	Multi Wall Carbon Nanotubes
NPs	:	Nanoparticles
BTX	:	Benzene, Toluene and Xylene
p-Xylene	:	Para-xylene
WHO	:	World Health Organization
EPA	:	Environmental Protection Agency
SEM	:	Scanning Electron Microscope
EDX	:	Energy Dispersive X-ray
XRD	:	X-ray Diffraction
TGA	:	Thermogravimetric Analysis
BET	:	Brunauer–Emmett–Teller
ppm	:	Parts per Million (10^{-6})
ppb	:	Parts per Billion (10^{-9})
rpm	:	Revolution per Minute
D-R	:	Dubinin- Rendenkuvich

ABSTRACT

Full Name : Aamir Abbas

Thesis Title : Application of Raw and Modified Carbon Nanotubes for Adsorption of BTX Compounds from Water

Major Field : Chemical Engineering

Date of Degree : May 2015

Raw and impregnated carbon nanotubes (CNTs) were used for the removal of benzene, toluene and xylene (BTXs) from industrial waste water. Iron, zinc and aluminum oxide nanoparticles were impregnated on the surface of CNTs. The synthesized adsorbents were characterized using nitrogen adsorption, x-ray diffraction (XRD), scanning electron microscope (SEM), energy dispersive x-ray (EDX) and thermogravimetric analysis (TGA). Nitrogen adsorption results showed that all synthesized adsorbents followed type (V) isotherm behavior. Brunner Emit Teller (BET) surface area analysis showed a remarkable increase in the surface area of all impregnated CNTs. The SEM-EDX analysis showed uniform dispersion of the metal oxides on CNTs. The TGA results confirmed the thermal stability of all adsorbents upto 450 °C.

Batch adsorption experiments were conducted at various conditions for the removal of BTXs using synthetic wastewater samples. Contact time, adsorbent dosage and initial concentration of BTXs were observed to have a significant effect on the removal efficiency and adsorption capacity of BTXs. Comparing the removal efficiency of benzene on different adsorbents under similar experimental conditions showed that the removal was highest as 71% for aluminum oxide impregnated CNTs and lowest as 52% for raw CNTs. Similar removal efficiency of 66% was observed for the removal of

toluene using both raw and impregnated CNTs under identical experimental conditions. Highest removal efficiency of 89% was achieved for p-xylene removal using raw and aluminum oxide impregnated CNTs under identical experimental conditions.

Pseudo first order, pseudo second order and intraparticle diffusion model were used to fit all kinetic adsorption data. The pseudo first order model was best for the adsorption of benzene. Values of pseudo first order model constant ranged from 0.005 to 0.007 min^{-1} while, the values of equilibrium adsorption capacity ranged from 1.6 to 2.4 mg/g. Pseudo second order model was found best to describe the toluene and p-xylene adsorption. Values of the pseudo second order model constant ranged from 70 to 2200 µg mg^{-1} min^{-1} while the values of equilibrium adsorption capacity ranged from 40 to 110 mg/g for toluene adsorption. Values of pseudo second order model constant ranged from 278 to 466 µg mg^{-1} min^{-1} while the values of equilibrium adsorption capacity ranged between 86 to 91 mg/g for p-xylene.

Langmuir, Freundlich and Dubinin-Rendenkuvich (D-R) isotherm models were used to fit the equilibrium adsorption data for BTX. The Langmuir isotherm model gave best fit for equilibrium adsorption of benzene. Values of Langmuir constant ranged from 0.5 to 3000 µL/mg while equilibrium adsorption capacity ranged from 517 to 1215 mg/g. Freundlich isotherm model was best to describe the adsorption of toluene and p-xylene. Values of Freundlich isotherm constant ranged from 6 to 14500 µL/mg and values of heterogeneity parameter ranged from 0.24 to 0.48 for toluene adsorption. Values of Freundlich isotherm constant ranged from 1 to 1.4 L/mg while the values of heterogeneity parameter ranged from 0.9 to 0.98 for p-xylene adsorption.

ملخص الرسالة

الاسم الكامل: عامر عباس

عنوان الرسالة: استخدام الأنابيب الكربونية المتناهية الصغر الخامة والمطعمة بأكاسيد المعادن في إزالة البنزين والتولوين والزيلين من المياه

التخصص: الهندسة الكيميائية

تاريخ الدرجة العلمية: مايو 2015

تم استخدام الأنابيب الكربونية المتناهية الصغر الخام والمطعمة بأكاسيد الحديد والزنك والالومنيوم لازالة مركبات البنزين والتولوين والزيلين من مياه الصرف الصناعية. تمت معاينة المواد الممتزة المصنعة باستخدام عدة تقنيات مثل قياس مدى قابليتها لامتزاز النيتروجين والمسح المجهري الالكتروني والتحليل الوزني الحراري والتحليل الطيفي لأشعة اكس وتحليل حيود الأشعة السينية.أظهرت نتائج امتزاز النيتروجين أن جميع المواد الممتزة المصنعة تتبع سلوك النموذج الرابع. كما أظهرت نتائج تحليل مساحة السطح وجود زيادة ملحوظة على أسطح كل الأنابيب الكربونية المطعمة. أثبتت نتائج المسح المجهري الالكتروني والتحليل الطيفي لأشعة اكس أن هناك توزيع متساو لجزيئات أكاسيد المعادن على سطح الأنابيب الكربونية. من ناحية أخرى، أكدت نتائج التحليل الوزني الحراري وجود استقرار حراري لجميع عينات المواد الممتزة حتى درجة حرارة 450 درجة مئوية.

تمت التجارب على عينات مختلفة تم تحضيرها باستخدام مياه صرف مصنعة لدراسة إزالة مركبات البنزين والتولوين والزيلين. لوحظ من النتائج أن هناك تأثير كبير لمدة التلامس وجرعة المادة الممتزة والتركيز المبدئي للملوثات على كفاءة عملية الامتزاز وسعتها. من خلال مقارنة كفاءة عملية إزالة البنزين باستخدام الأنابيب الكربونية الخام والمطعمة بأكاسيد المعادن تحت نفس الظروف تبين أن أعلى نسبة إزالة كانت 71% باستخدام الأنابيب الكربونية المطعمة بأكسيد الالومنيوم بينما كانت اقل نسبة عند استخدام الأنابيب الكربونية الخام. من ناحية أخرى، كانت نسبة إزالة التولوين 66% باستخدام الأنابيب

الكربونية الخام والمطعمة على حد سواء عند توفر نفس الظروف. أما فيما يتعلق بالزيلين فقد بلغت أعلى نسبة إزالة 89% وذلك عند استخدام الأنابيب الكربونية الخام والمطعمة بأكسيد الألومنيوم.

تم استخدام النموذج الشبيه بالدرجة الأولى والنموذج الشبيه بالدرجة الثانية ونموذج الانتشار الجزيئي الداخلي لنمذجة بيانات الامتزاز الحركي وقد أظهرت النتائج أن النموذج الشبيه بالدرجة الأولى كان هو أفضل نموذج في حالة امتزاز البنزين وقد تراوحت قيم ثوابت النموذج بين 0,005 و 0,007 في الدقيقة بينما تراوحت قيم التوازن لسعة الامتزاز بين 1,6 و 2,4 ملجم/ جم. من ناحية أخرى كان النموذج الشبيه بالدرجة الثانية هو الأفضل لوصف عملية الامتزاز للتولوين والزيلين. في حالة امتزاز التولوين، تراوحت قيم الثوابت بين 70 الى 2200 ميكروجرام/ (مليجرام.دقيقة) بينما تراوحت قيم التوازن لسعة الامتزاز بين 40 إلى 110 ملجم/جم .وأخيرا في حالة امتزاز الزيلين تراوحت قيم الثوابت بين 278 إلى 477 ميكروجرام/ (ملجم.دقيقة) في حين تراوحت قيم التوازن لسعة الامتزاز بين 86 إلى 91 ملجم/جم.

تم استخدام ثلاث نماذج لدراسة مدى ملائمتها لتمثيل النتائج التي تم الحصول عليها وهي نموذج لانجميور ونموذج فريندلخ وأخيرا نموذج دبنن _ رينذنكوفيتش (D-R) . بينت النتائج أن نموذج لانجميور كان الأنسب لتمثيل نتائج البنزين وقد تراوحت قيم ثوابت النموذج ما بين 0,5 الى 3000 ميكروليتر/مليجرام فيما تراوحت قيم التوازن لسعة الامتزاز ما بين 517 إلى 1215 مليجرام/جرام. كما بينت النتائج ان نموذج فريندلخ كان هو الأنسب لتمثيل نتائج التولوين والزيلين. تراوحت قيم ثوابت نموذج فريندلخ ما بين 6 الى 14500 ميكروليتر/مليجرام وقيم معامل عدم التجانس ما بين 0,24 الى 0,48 في حالة إمتزاز التولوين.

من ناحية اخرى، تراوحت قيم ثوابت نموذج فريدنلخ في حالة امتزاز الزيلين ما بين 1 إلى 1,4 ليتر/مليجرام بينما تراوحت قيم معامل عدم التجانس بين 0,9 الى 0,98.

CHAPTER 1

INTRODUCTION

1.1 Background

Benzene, toluene and xylenes (BTX) are primary aromatic hydrocarbons. They are used for producing many organic chemicals, synthetic fibers, plastic resins and plasticizers [1]. The origin of these compounds lies in petroleum industry; they are naturally found in crude and also produced by two methods in refinery. One of those methods is the catalytic reforming of naphthenes and paraffins (almost 50% of benzene, 90% of toluene and 95% of mixed xylene are derived by this method) while other one is pyrolysis of gasoline by steam cracking (almost 25% benzene and 10% toluene obtained by this process). BTX are also obtained from coal tar by extraction and distillation. These are building blocks of many modern day used products. They are widely used in petro-chemical industry as raw material for producing polymers, plastic, rubber etc.

Benzene is the feedstock for production of important chemicals including styrene, phenol, nylon and aniline. Benzene is also used for producing detergent alkylate, maleic anhydride and chlorobenzene [2], also utilized as solvent in inks, paints and plastics. Toluene is also used as solvent in paints, cleaners and degreasers and can be utilized for surface coatings. It is also used for explosives and as a raw material in polyurethanes. Xylene is also widely used as a solvent in different ways in paints removers, cleaners,

inks. It exists as clear liquid and can be found in three different isomeric forms which are para-xylene, ortho-xylene and meta-xylene. P-xylene is used for manufacturing of tere-phthalic acid (PTA) which is used for producing polyester resins while o-xylene is used for producing phthalic anhydride which is utilized for making flexible polyvinyl chloride (PVC), m-xylene is converted to iso-phthalic acid, used for making polyester resins [1,3].

During all these industrial processes large amount of BTX is dissolved in water because of their relatively high water solubility. Traces of BTX (ppm level) remain in water due to their hydrophilic nature and their presence has been observed several kilometers way in downstream water of an industry.

Hazards and toxicity of BTX:

The primary route of exposure of BTX to humans is inhalation, although these can also be absorbed through skin. These are toxic compounds and can cause damage to central nervous system. Benzene is more dangerous in a way that it causes Leukemia and anemia leading to cancer [3]. Table 1.1 indicates the exposure limits, hazard associated and sources of BTX.

1.2 Motivation for Work

Water is one of the most important and essential need of humans. With the increase in population and also tremendous urbanization, the need for clean and pure water is enhancing day by day. But unfortunately we are lacking in the sources of fresh water. Natural water resources are being polluted by human activities and industrial wastes. According to a report of World Health Organization (WHO) in 2012; about 780 million people on earth still lack access to improved drinking water resources. Also, the

traditional methods of water treatment are not able to provide water with sufficient purity. So, it is need of time to look for such processes which can treat and provide efficient amount of clean water [4,5].

Table 1-1: BTX Contamination Level and restrictions [6]

Component	**Maximum (allowed) contaminant level**	**Maximum Contaminant Level Goal (MCLG)**	**Risks associated with health**	**Source**
Benzene	0.005 mg/L or 5 ppb	Zero	Loss of platelets (Increased Cancer risk), Skin, Eyes, Central nervous system damage	Discharge from industries, Gas storage tanks leakage, Landfills
Toluene	1mg/L or 1 ppm	1 mg/L or 1 ppm	Causes kidney, liver and nervous system problems	Discharge of petroleum refineries
Xylenes	10 mg/L or 10 ppm	10 mg/L or 10 ppm	Nervous system damage	Discharge of petroleum refineries and different chemical factories

CHAPTER 2

LITERATURE REVIEW

There have been many studies on removal of BTX from water using different techniques which involve physical, chemical and biological techniques. Physical techniques are carbon adsorption, filtration, and adsorption by zeolites while chemical oxidation and photo-catalytic remediation are chemical techniques; biological techniques involve bioremediation and bioleaching. Out of all these techniques, adsorption mechanism is more promising and used commercially for removal of BTX from water [7,8].

Since their discovery in 1991 by Iijima [9], CNTs have become attractive in all scientific and research communities. They have unique physical, chemical and structural properties. It is observed that due to their unique properties, CNTs have a great potential in all fields. They are being studied to be used in almost every field of research which includes medical, electronics, chemistry, catalysis and water treatment [5].

Several forces act simultaneously when CNTs are used as adsorbents for different pollutants. These forces include hydrophobic effect, hydrogen bonding, electrostatic interaction, л-л interaction, л-л electron donor acceptor interaction. Hydrophobic nature of CNTs surface causes strong interaction between them and nonpolar organic chemicals. Abundant л-electrons present on the surface of CNTs cause better contact with the л-electrons present on molecular plane of aromatic pollutants by л-л interface. This л-л electron interface is long ranged and involves van der Waals forces [5,10,11].

CNTs aggregation has a strong effect on adsorption efficiency. This aggregation tendency decreases with increasing number of walls or with decreasing nano-curvature. Generally for CNTs aggregation follows this order; Multiwall carbon nanotubes < Double wall carbon nanotubes < Singe wall carbon nanotubes [5].

2.1 CNTs Characteristics

Carbon nanotubes are graphitic carbon sheets rolled in hollow cylinders with diameters in nano-meters and length varies from nanometers to micrometers. Graphitic carbon is sp^2 hybridized solid phase carbon having three of four valence electrons covalently bonded in two dimensional planes while fourth one acts as delocalized among all atoms present as a weak л bond in three dimensions. Hydrophobicity, high and specific surface area, hollow and layered structure of CNTs make them good adsorbent. The following parameters were observed to play an important role in adsorption of aromatic organic compounds on CNTs.

- п-electron donor and acceptor interaction
- Pore volume, pore size distribution
- Specific surface area
- Functional groups present on the surface of CNTs

It is observed that CNTs may get aggregated, so following areas act as adsorption sites outer most surface, interstitial channels, inner cavities and grooves between CNTs bundle as shown in Figure 2.1 [12]. Adsorption sites of MWCNT were located on the innermost and outermost surfaces because the interlayer spacing between coaxial tubes is

impenetrable to organic compounds. Organic compounds attach first to high energy adsorption sites and then to all low energy sites [13].

In aqueous phase; water chemistry, physicochemical properties of CNTs and adsorbate play vital role.

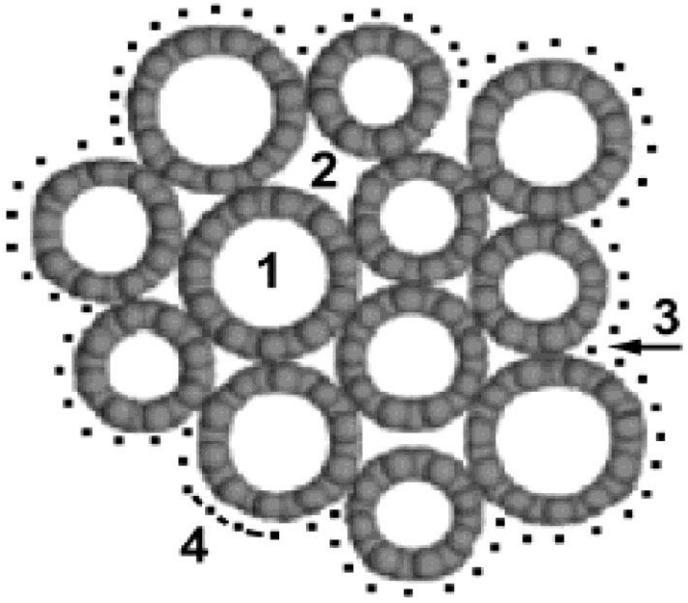

Figure 2-1: Schematic of a typical CNT bundle and its adsorption sites (1) inner cavities, (2) interstitial channels, (3) external grooves, (4) outermost surface [12]

There are two types of CNTs reported in literature. They are single wall carbon nanotubes (SWCNTs) or multiwall carbon nanotubes (MWCNTs). Single wall nanotubes consist of only one graphitized carbon layer rolled in hollow cylinder while multi wall carbon nanotubes consists of many layers. Based on this difference they have different characteristics like inner and outer diameter, length of CNTs, pore volume, and pore distribution and specific surface area [14].

CNTs are pretreated before using as an adsorbent. This includes acid wash using HCl, HNO_3, H_2SO_4, heat treatment and ultrasonication. CNTs surface can be modified by oxidation and can also be functionalized. Functionalization of CNTs occurs at sidewalls, on defected sides and at the ends of tubes through covalent and non-covalent attachment of functional groups. Mostly, CNTs surface is oxidized by oxygen containing groups OH, COOH and C=O. Oxidation provides CNTs hydrophilic moieties and removes impurities, amorphous carbon and hemispherical caps. Different studies indicate the importance of CNT type as well as the oxidizing agent and its strength on alteration of CNT surface chemistry that is change in the surface area. In addition to SSA, Cho et al. [15] reported no change in structure or length distribution of CNTs after oxidation. However, Wu [16] reported a decrease in the diameter of MWCNTs after oxidation and attributed the modification of this diameter to the removal of the amorphous carbon from the surface.

2.2 Impact of Different Properties on Organic Compounds Removal

It is important to study the effect of CNTs surface properties, role of solution chemistry and nature of organic compounds on their removal through adsorption process. Here these effects are discussed in detail.

2.2.1 Effect of CNTs properties on adsorption of organic compounds

CNTs physical properties play important role during adsorption of different organic compounds. The following factors were observed to affect adsorption

- Water cluster formation around oxygen containing functional group
- Metal catalysts used during synthesis of CNTs

- Presence of amorphous carbon on and inside CNTs which impede penetration of adsorbate.
- Nano-curvature and diameter of CNTs also influence adsorption. By increasing the diameter of CNTs; the decrease in adsorption capacity was observed.

CNTs physical properties as well as surface chemistry can also influence the organic compounds adsorption.

Oxidation of CNTs surface

The unintended oxidation of the surface during manufacturing and/or in the environment, and the intentional oxidation with treatment are some possible causes of CNT surface oxidation. It was observed in several studies that there was an overall decrease in adsorption with an increase in surface oxygen content. Two mechanisms have been proposed to explain these observations:

i. The presence of oxygen on the CNT surface makes adsorption of water molecules energetically more favorable relative to organic compounds adsorption, which results in water clusters that deplete the available surface area for organic compounds
ii. The presence of oxygen on CNT surface localizes the л- electrons, which reduces the л-л interactions between the CNT graphitic surface and benzene rings of aromatic organic compounds.

Similar findings were presented and discussed for activated carbon. Yu et al. [17] reported a remarkable increase (~100%) in adsorption capacities of toluene, ethylbenzene and m-xylene with increasing surface oxygen content per specific surface area, up to 8%,

for MWCNTs. The increase was attributed not only to the increase in the dispersion of CNTs but also to the increase in the available adsorption sites. However, it was found that by further increasing the oxygen content per specific surface area (up to 18%), a decreasing trend in the adsorption capacity was observed. This behavior was explained by water cluster formation effect dominating over the CNT dispersion for organic compounds adsorption [18].

2.2.2 Influence of organic compound properties on their adsorption

Following properties of organic compounds and forces act as driving forces for adsorption of organic compounds on the surface of CNTs [19,20]

- Hydrophobic forces are very important factor in adsorption of aromatic hydrocarbons on CNTs surface. Hydrophobicity, an important adsorbate property, is represented by octanol-water portioning co-efficient (K_{OW}) or aqueous solubility (S_W). It was observed that molecular size of adsorbate directly affect adsorption efficiency as hydrophobic affinity cannot overcome steric hindrances.
- Physical and chemical forces between CNTs and organic molecules
- Non-specific forces; resulting from affinity of electron rich and electron deficient regions of uncharged molecules; usually known as van der Waals forces. Their intensity depends on size of molecules, polarizability and electric charge.
- л-л interaction resulting from the interaction between л-electrons of graphitic carbon and л-electrons of aromatic hydrocarbons. Л-electron density of aromatic hydrocarbons is also another important property which influences their adsorption on CNTs surface. It was observed by researchers that hydrocarbons with more

benzene rings had more adsorption and it was attributed to stronger conjugation potential of more rings resulting with stronger л-л interactions.

- Hydrogen bonding; which results from electrostatic interaction of –OH group containing aromatics hydrocarbons and functionalized CNTs surface. Hydrogen bonding is a dipole-dipole interaction and it is caused by an interaction between hydrogen atom and an electronegative element on CNTs functionalized group. It was reported by one of the author [21] that for phenol adsorption the position of hydroxyl group on phenol also plays an important role. He observed higher adsorption when hydroxyl group was attached on meta-position rather than ortho or para position. It is observed that if adsorption is controlled by hydrogen bonding; by decreasing pH adsorption increases.
- Sometimes it was observed that in the presence of л-л interaction adsorption was not upto a good level. So, molecular configuration or surface conformation of organic compounds is also an important parameter.

2.2.3 Effect of solution properties on organic compounds adsorption

The initial pH of the background solution is another major factor controlling adsorption. For organic acids, if pH < pK_a, the non-dissociated species for organic bases dominate the solution and vice versa. Therefore, the influence of background solution pH and ionic strength depends upon the ionizability and the electron donor acceptor ability of organic compounds. The pH change also influences the protonation/deprotonation state of the functional groups on CNT surfaces. Deprotonation of acidic functional groups may increase the density of negatively charged functional groups that may create repulsive forces between negatively charged SOCs or may promote л-electron donor ability of

CNT surface and enhance л-л electron donor interactions between CNTs and organic compounds. The formation of water clusters decreasing hydrophobicity and reduction of hydrogen bond formation decreasing adsorption affinity are other possible mechanisms for this increase in either repulsive forces or the promotion of electron donor ability [22,23]. The variance of the ionic strength of natural waters can be another factor that may influence adsorption of organic compounds. Organic compounds are less soluble in aqueous salt solutions, which are known as the salting-out effect. Salting-out may enhance the hydrophobic interactions of organic compounds with CNTs [23,24].

Adsorption of organic compounds by CNTs is predominantly a temperature-dependent process in which physical sorption occurs mostly as an exothermic process releasing energy. It was observed by different studies that CNT adsorption capacity decreased as the temperature was increased. It was also revealed that adsorption thermodynamics depends upon the nature of the predominant sorption mechanism [17].

2.3 Carbon Nanotubes and Activated Carbon: Comparison

Graphitic carbon is the backbone of both CNTs and activated carbon. Both CNTs and activated carbon have similar chemical characteristics such as hydrophobicity, л-electrons rich surface. Activated carbon consists of rigid pore structure with a lot of micro, meso and macro pores where adsorption occurs; while CNTs have hollow cylindrical shape with micro-pores on their surface and are usually aggregated with each other due to л-л stacking and van der Waals forces. This aggregation in CNTs provides four different sites for adsorption which are external surface, inner cavity of open-ended CNTs, groves and interstitial channels between bundles [25].

Carbon nanotubes were reported to exhibit higher or comparable adsorption capacity than activated carbons in several studies while opposite findings were also reported in others. This was explained on the basis of nature of compounds and also surface chemistry of water. Adsorption kinetics on CNTs have been reported to be faster than on activated carbons [26].

Conventional adsorbents have lower adsorption efficiency due to limited surface area or active sites, the lack of selectivity, and the slow adsorption kinetics [4].

2.4 Removal of Organic Compounds (BTX) from Water

In this section, different techniques used for the removal or reduction of organic compounds from water will be described.

2.4.1 Advanced oxidation process combined with biological process

Advanced oxidation process has been used by many researchers for treatment of water containing organic pollutants [27]. This method was reported as highly competitive because this can remove organic compounds having high chemical stability and low biodegradability which cannot be treated by conventional methods. This method needs high energy for complete conversion of compounds with increasing treatment time. So, it is mostly used in combination with biological treatment [28] in order to achieve complete mineralization of compounds at lower cost. Advanced oxidation process is mainly used as pre-treatment when biologically persistent compounds are converted to biodegradable compounds. And later, these intermediates formed by chemical oxidation are completely converted by micro-organisms.

However, this method has some limitations which are as follows

- Sometimes chemical oxidation process generates such intermediates which are less biodegradable.
- There is lack of selectivity to convert more bio-resistant compounds.
- Selection of treatment conditions is also a problem e.g. sometimes it can generate such an effluent which has less metabolic value for micro-organisms.
- Compounds used as oxidant e.g. ozone or hydrogen peroxide and catalyst e.g. metals, metal oxides and salt are toxic for micro-organisms so they need to be eliminated from the media before charging for biological process.
- Sometimes toxicity of original effluent grows during early treatment due to formation of toxic intermediates which are harmful for biological systems.
- Different oxidation process leads to different intermediates so we need different biological system for their convergence.
- pH needs to be set around 6.5 to 7.5 for biological process but Ozone has good efficiency around 9 pH while Fenton gives good result around pH value of 3. So, after this treatment neutralization is required [29].

2.4.2 Photo-Catalysis

Photo-catalysis is also important method used for removal or degradation of different organic compounds. Photo-catalysis is used mainly for oxidation of organic compounds. Bahmani et al. [30] carried photo catalytic oxidation of BTEX using H_2O_2 along with UV lamps in a batch reactor. They carried out different experiments by using H_2O_2 separately, UV separately and then combining both. It is observed by going through

different works that photo-catalytic technique is quite expensive. A photo-catalyst should be resistant to corrosion and stable under reaction conditions [31,32].

2.4.3 Adsorption

Different materials have been used for adsorption of different pollutants from water which include zeolite, resins and activated carbons; but most commonly used material for adsorption on industrial and commercial scale is activated carbon [33–41]. The benefits associated with large scale use of activated carbon are chemical inertness, thermal stability, and better pollutant removal efficiency. But, problems associated with AC in water treatment are not only slow adsorption kinetics but also difficulty in regeneration. Later, activated carbon fibers were developed to overcome these problems and adsorption kinetics was improved due to openings on the surface [42]. After that, carbon nanotubes emerged as third generation adsorbents. All adsorption sites are located on inner and outer surface of CNTs; which make them better adsorbent [43]. The more porous structure of CNTs is better for adsorption in terms of diffusion of pollutants. Based on stronger interactions of chemicals and nanotubes, tailored surface chemistry, high equilibrium rates and high sorption capacity; CNTs were considered as superior sorbents for a wide range of organic and inorganic contaminants than the conventionally used activated carbons [5].

Few recent studies for removal of BTX from water are reported in Table 2.1. Various scientists reported different adsorption capacities with activated carbon [44,45], activated carbon fiber [46], single wall and multi wall carbon nanotubes [18,47–49] using experimental conditions of 20 ^{o}C to 30 ^{o}C temperature, pH range of 5 to 7 and different initial concentration of adsorbates.

Table 2-1: Summary of different adsorbent and their adsorption capacity

Source	Contaminants present	Adsorbent used and Conditions	Langmuir constant / Adsorption capacity (mg/g)	
Mangun et al. (2001) [50]	Benzene, Toluene, Ethyl-Benzene and m-Xylene	Activated carbon fibers PH 7 Temperature 20 ^{o}C	Benzene – 66 Toluene – 85 Ethyl-Benzene – 237 m-Xylene – 185	
Wibowo et al. (2007) [44]	Benzene, Toluene	Activated carbon pH 7 Temperature – 30 ^{o}C	Benzene – 183.3 Toluene – 194.1	
Chen et al. (2007) [51]	Benzene, Toluene	Single wall CNTs pH 7 Temperature 30 ^{o}C	Benzene – 60.1 Toluene – 103.2	
Chin et al. (2007) [52]	O-xylene, p-xylene	Single wall CNTs Temperature 25 ^{o}C pH 5.4 Amount 50 mg	p-Xylene – 77.5 O-Xylene – 68.5	
Su et al. (2010) [53]	Benzene, toluene, ethyl-Benzene and m-xylene	Activated carbon, MWCNTs oxidized with NaOCl pH 7 Temperature 25 ^{o}C	Activated carbon	Modified MWCNTs
			B – 217.32 T – 221.13 E– 250.65 m-X -301.4	B- 247.87 T – 279.81 E– 342.67 m-X-413.77
Yu et al. (2012) [54]	Toluene, Ethyl Benzene and Xylene	Raw MWCNTs and also modified by KOH pH 6 Temperature 20 ^{o}C	Toluene – 87.12 Ethyl Benzene – 322.05 m-Xylene – 247.83	

YU and MA et al. (2012) [17]	Toluene, Ethyl Benzene and Xylene isomers	Raw MWCNTs and MWCNTs oxidized by NaOCl pH 7	As grown MWCNTs	Modified MWCNTs
			T – 44.9 E – 61.16 p-X – 76.15 m-X –76.86 o-X – 61.86	T – 59.48 E – 85.49 p-X – 103.4 m-X –109.8 o-X – 97.39

After discovery of carbon nanotubes, different studies have been conducted to study their effect on adsorption of many contaminants. It has been observed by researchers that CNTs are very good adsorbents and have adsorption capacity even better than activated carbon [44,53,55]. In the recent years, modification of CNTs surface with different groups was also investigated. It is seen that defective surface of CNTs as well as modified CNTs surface with different groups and oxides, provide enhancement in adsorption activities due to more active sites availability and enhanced bonding interactions [15,23,26,44,54,56,57]. Currently, it is seen that by impregnating CNTs with different metal oxide nanoparticles, dispersion of CNTs enhances and they provide more sites for adsorption of contaminants hence leading to increase in removal efficiency. Different contaminants such as heavy metals and some organic compounds have been removed from waste water using metal oxides impregnated CNTs [58–62].

According to best of our knowledge, not even a single study have been published for removal of BTX from water using metal oxide impregnated CNTs. Based on this conclusion, we have carried out this work for removal of BTX using advanced adsorbents, CNTs impregnated with various metal oxides.

2.5 Objectives of the Study

The main objectives of this study are as follows,

1) To impregnate carbon nanotubes with different metal oxides.
2) To characterize the raw and impregnated CNTs with SEM, EDX, TGA and Zeta potential.
3) To remove BTX from water using raw and modified carbon nanotubes.
4) To optimize the adsorption parameters such as dosage of adsorbent, contact time, shaking rpm, pH of solution and initial concentration of adsorbate on the removal efficiency.
5) To study the thermodynamics and kinetics of adsorption phenomena.

CHAPTER 3

RESEARCH METHODOLOGY

This chapter describes the methodology used to achieve the objectives of study. Here, we have discussed the materials preparation, characterization techniques used to analyze the adsorbents and equipments used to analyze the concentration of adsorbate. Last part of the chapter deals with kinetics and isotherms models used for fitting of experimental data.

3.1 Materials and Preparation

Commercially grade carbon nanotubes were purchased from Cheap Tubes. The purity of CNTs was >95% while length, outer diameter and specific surface area were 10–30 micrometer, 10–20 nanometer and 200 m^2/g, respectively. Metallic salts (Iron Nitrate, Zinc Nitrate and Aluminum Nitrate) and solvents (Ethanol, benzene, toluene and xylene isomers, nitric acid and sodium hydroxide) were purchased from Sigma Aldrich. All chemicals were of analytical grade and used without any further treatment.

3.1.1 Adsorbents preparation

Multiwall carbon nanotubes (MWCNTs) were impregnated with different metal oxides which are

1) Iron Oxide
2) Zinc Oxide
3) Aluminum Oxide

In order to prepare a sample of required weight, e.g. 20 g with 10 weight percent salt contents of iron nitrate or zinc nitrate or aluminum nitrate; 18 g of MWCNTs were weighed and sufficient amount (500 ml) of ethanol was added in the beaker containing CNTs for proper dispersion. The sample was ultra-sonicated using tip sonicator in order to break agglomeration and also to distribute CNTs properly in alcohol. The sample was sonicated for 30 minutes at frequency of full cycle and amplitude of 60%.

Required amount of salt was weighed meanwhile (2 g for 10% and 0.2 g for 1% sample) and it was dissolved in sufficient amount of ethanol (100 ml for 2 g and 50 ml for 0.2 g). Stirring was also performed to dissolve metallic slats in ethanol. After 30 minutes of sonication of CNTs, salt solution was also added to CNTs and sonicated for another 30 minutes at same conditions of frequency and amplitude to make sure proper distribution of metallic salts on CNTs surface.

After completion of sonication process, sample consisting of CNTs and metallic salt distributed in ethanol was placed in an oven for drying at 80 to 90 ^{o}C. It was checked after different intervals and removed from oven when it was completely dried.

Dried cake obtained was crushed, transferred to crucible and placed in furnace for calcination process. Sample was calcined in furnace by heating at 350 ^{o}C for 4 hours.

After calcination process, sample was cooled and metal oxide impregnated CNTs were removed from furnace and placed in sample bag for future use.

3.1.2 Adsorbate solution preparation

For adsorption batch experiments, solutions of desired concentration of organic compounds were prepared. For this purpose, pure organic solvents purchased from Sigma-Aldrich were used to prepare stock solution of higher concentration e.g. 100 ppm in distilled deionized water (resistivity of 18 MΩ.cm) and diluted to required solution concentration for experiments. Amount of organic compound required for preparing solution was measured very effectively and accurately using micro-pipettes. Magnetic stirrer was used for proper mixing, distribution and concentration of solution.

3.1.3 Adsorption batch experiments

For adsorption experiments, accurately weighed amount of adsorbents was added to the flasks, and then flasks were filled with organic chemicals solution. These flasks were placed on shaker at specific shaking speed for specified time at room temperature. After completion of time provided for adsorption, filtration (using Whatman filter paper No. 1 of 11 micron pore size) of solution was carried out to separate adsorbent and sample were collected in specific vials for analysis of concentration using GC-MS.

In order to avoid any losses due to volatilization during experimentation; solution was filled completely in flasks and no headspace was left. Experiments were also conducted without adding any adsorbent to check the adsorption of benzene on surface of glass flask and loss due to volatilization.

3.2 Characterization

It is necessary to characterize the materials using different techniques. Here, we have discussed the characterization of CNTs and concentration analysis of BTX.

3.2.1 Characterization of impregnated CNTs

In order to get confirmation of loading of metal oxides nanoparticles on MWCNTs, prepared materials were analyzed by different techniques. Following characterization techniques were used.

Scanning Electron Microscopy (SEM) (ASTM- E 2809)

It is very important to know the surface morphology and characteristics of a material. Morphology and surface analysis was performed using FESEM. Samples were prepared for analysis by coating with Platinum metal with a 5 nm thickness. Coated samples were analyzed using scanning electron microscope (TESCAN MIRA 3 FEG-SEM) with energy of 15 KV and magnification of 63.6 KX.

Energy-dispersive X-ray Spectroscopy (EDX) (ASTM- E 1508)

EDX was performed in order to look for qualitative analysis of elements present in all samples. TESCAN MIRA 3 FEG-SEM was used for this analysis.

Thermogravimetric Analysis (TGA) (ASTM- E 1131)

Thermogravimetric analysis is important in order to look for degradation temperature and purity of samples. TA Instrument (K.U. Leuven SDT Q600) was used for TG analysis of all materials. Alumina pan were used for sampling, while materials were degraded in the

presence of zero air from room temperature to 900 ºC at constant heating rate of 10 ºC per minute. The flow rate of purge gas (zero air of 99.9 % purity) was 100 ml/minute while pressure was adjusted as 1 bar.

X-Ray Diffraction (XRD)

XRD is an important analysis for looking at crystal nature and phase of metal oxide in a sample. This analysis was performed using 2-theta range of 10 to 100, with step of 0.02^{o} and step time of 1 second.

Zeta Potential Measurement

Zeta potential is an important factor in order to look for charge distribution around adsorbent particles at various pH. Zeta potential of all materials was performed using Zeta Nano-Sizer of Malvern. The sample were prepared by dissolving 10 mg of adsorbent in 100 ml of deionized water (resistivity of 18 MΩ.cm) and ultra-sonicated for 30 minutes. Samples were filled in sample bottles and analyzed for determining zeta potential. In order to get good result, all measurements were repeated three times with 100 cycles in each measurement.

3.2.2 Concentration of solution

BTX concentration was analyzed at the start and end of adsorption experiments using GCMS and COD analysis. These techniques are discussed in detail here.

Concentration analysis using GCMS

Concentration of benzene solution was determined using gas chromatograph mass spectrometer (GC 7890A and MS 5975C, Agilent Inc. USA). GC-MS headspace auto

multi-sampler was used for sample injection. The capillary column (DB-1) was used with specification of 30 m length, 320 µm inner diameter and 1 µm column width. Split mode was used for sample injection with 50 ratios 1 and volume of sample injected was 1000 µL. The temperature of oven was 40 ^{o}C at the start and later raised to 180 ^{o}C with the heating rate of 35 ^{o}C per minute, injection inlet temperature was 200 ^{o}C and auxiliary temperature was 280 ^{o}C while syringe temperature used was 100 ^{o}C.

COD measurement

Concentration analysis using COD was performed with COD analyzer (Hach Inc. Model 3900). COD concentration analysis chemicals were provided by the company. For analysis, 2 ml of sample (to be analyzed) was added to bottle, shaked well and placed in furnace for digestion at temperature of 148 ^{o}C for 2 hours. After digestion, samples were cooled at room temperature and analyzed using UV spectrometer analyzer with 420 nm wavelengths. Standard sample of deionized water was analyzed and COD was turned as zero for that sample then other measurements were carried out.

3.3 Kinetics Study

The adsorption capacity of BTX on CNTs surface was calculated by using following equation [38]

$$q = \frac{(C_0 - C)}{m} * V \quad (3.1)$$

In this equation q is the adsorption capacity (mg/g) of adsorbent, C_0 and C represents the initial and final concentration of adsorbate in sample (mg/l), respectively. V is the volume of solution (ml) and m indicates the amount of adsorbent (g).

Percentage removal was found using following relation [38].

$$Removal\ (\%) = \frac{C_0 - C}{C_0} * 100 \quad (3.2)$$

3.3.1 Adsorption kinetics models

Most widely used kinetics model for adsorption are pseudo first order model and pseudo second order model. Pseudo first order model of Lagergren is presented by the following equation [63,64].

$$log(q_e - q_t) = log(q_e) - \frac{k_1 t}{2.303} \quad (3.3)$$

q_e and q_t indicate the amount of adsorbate (mg/g) adsorbed at equilibrium and various time "t" respectively, k_1 (min^{-1}) is the rate constant of this model. In order to determine the values of k_1 and q_e linear plot of $\log(q_e - q_t)$ vs. t was used.

The linear form of pseudo second order is given as [64,65],

$$\frac{t}{q_t} = \frac{1}{k_2 q_e^2} + \frac{t}{q_e} \quad (3.4)$$

q_e and q_t are the amount of adsorbate adsorbed (mg/g) on the surface of CNTs at equilibrium and at various time "t" respectively. k_2(g/(mg min)) is the rate constant for pseudo second order kinetic model. The values of q_e and k_2 can be determined from slope and intercept of linear plot of t/q vs. t.

In order to get more information for internal diffusion inside adsorbent, intraparticle diffusion model is used. Linear form of intraparticle diffusion model is provided in this equation following [17,64,65]

$$q_t = k_{id}\, t^{0.5} + C \tag{3.5}$$

Where, k_{id} is intraparticle diffusion rate constant with units as mg/g $min^{-0.5}$ and C (mg/g) is intercept which can be calculated by plotting q_t vs. $t^{0.5}$.

3.3.2 Adsorption isotherm models

For adsorption isotherms study, Langmuir, Freundlich and Dubinin-Radushkevitch (D-R) are widely used to fit the experimental data. Langmuir model is used for interpretation of homogenous single layer adsorption. Langmuir model [65,66] is presented by following equation,

$$q_e = \frac{q_m K_L\, C_e}{1 + K_L\, C_e} \tag{3.6}$$

Linear form of Langmuir model is provided as follows,

$$\frac{q_e}{C_e} = q_m K_L - q_e K_L \tag{3.7}$$

Here q_e represents the concentration of adsorbate on the surface of adsorbent and C_e indicates the concentration in water when equilibrium was reached. q_m is the maximum adsorption capacity and K_L is the Langmuir adsorption equilibrium constant (L/mg).

From equation 6, K_L and q_m can be obtained from the non-linear model fitting of q_e and C_e.

Freundlich isotherm model [66,67] is provided as,

$$q_e = K_F\, C_e^{\,1/n} \tag{3.8}$$

Linear form of model is presented as,

$$log(q_e) = log(K_F) + {}^{1}\!/_{n}\, log(C_e) \tag{3.9}$$

K_F is Freundlich constant related to adsorption capacity with units (mg/g)(L/mg)$^{1/n}$ and 'n' is Freundlich constant related to adsorption intensity of the adsorbents, it is dimensionless. By using the non-linear model fit plot of (q_e) vs. (C_e), the values of K_F and 'n' can be obtained.

D-R model was used to show that adsorption of BTX molecules with CNTs surface is physical or chemical. Equation of D-R model [17,66] is as follows

$$q_e = q_m\, e^{-B\,\varepsilon^2} \tag{3.10}$$

Here, B (moles^2/kJ^2) is related to mean free energy of adsorption, q_m(mg/g) is saturation capacity. ε is Polanyi potential and calculated as

$$\varepsilon = R\,T\,\ln\left(1 + \frac{1}{C_e}\right) \tag{3.11}$$

Where R (kJ/mole/K) is the gas constant and T (K) is absolute temperature. Mean free energy of adsorption (E_a) for one mole of adsorbate, by moving from infinity to adsorption site is calculated as follows

$$E_a = 1/(2B^{0.5}) \tag{3.12}$$

Value of E_a can provide information about adsorption mechanism. When 1 mole of a material is transferred to adsorption site, value between 1-8 kJ/mole indicates physical adsorption, value between 8-16 kJ/mole shows adsorption due to ion exchange while the value between 20-40 kJ/mole provides indication of chemisorption [17,36,68].

In order to avoid the error occurring due to use of linearized form of models, non-linear regression analysis was performed for all models using Mathematica 9.0 [69].

CHAPTER 4

RESULTS AND DISCUSSION

CHARACTERIZATION AND ADSORPTION

In the first part of this chapter, the results of different characterization techniques have been discussed. In the second part of chapter, results of different adsorption parameters affecting the removal efficiency of BTX from water have been discussed in detail.

4.1 Characterizations of Materials

The adsorbent materials were characterized using different techniques in order to confirm the morphology and other properties such as thermal stability, phase of a material and surface area. Morphology was analyzed suing scanning electron microscope (SEM). Qualitative elemental analysis of prepared materials was performed using energy dispersive x-ray (EDX) spectrum. The purity and degradation behavior was studied by using thermogravimetric analysis. X-ray diffraction (XRD) analysis was used to study the crystalline nature of materials. Zeta potential was measured using Malvern Zeta-Sizer. All these characterization are described in detail here.

4.1.1 Scanning electron microscope (SEM) analysis

Figures 4.1 and 4.2 show the SEM images of raw CNTs and different metal oxides nanoparticles impregnated CNTs. It could be observed that carbon nanotubes have tubular geometry and no change in morphology was noted after impregnation with metal

oxide nanoparticles. It is observed from Figure 4.2 that after impregnation with iron oxide nanoparticles, dispersion of CNTs improved and agglomeration was observed to be decreased. Similarly, with aluminum oxide nanoparticles impregnation, CNTs were more distributed and less agglomerated. Metal oxides nanoparticles distributed on the surface of CNTs are shown in circles. It was seen that some agglomeration occurred in zinc oxide nanoparticles impregnation while for iron and aluminum oxide nanoparticles, distribution was quite good and homogeneous.

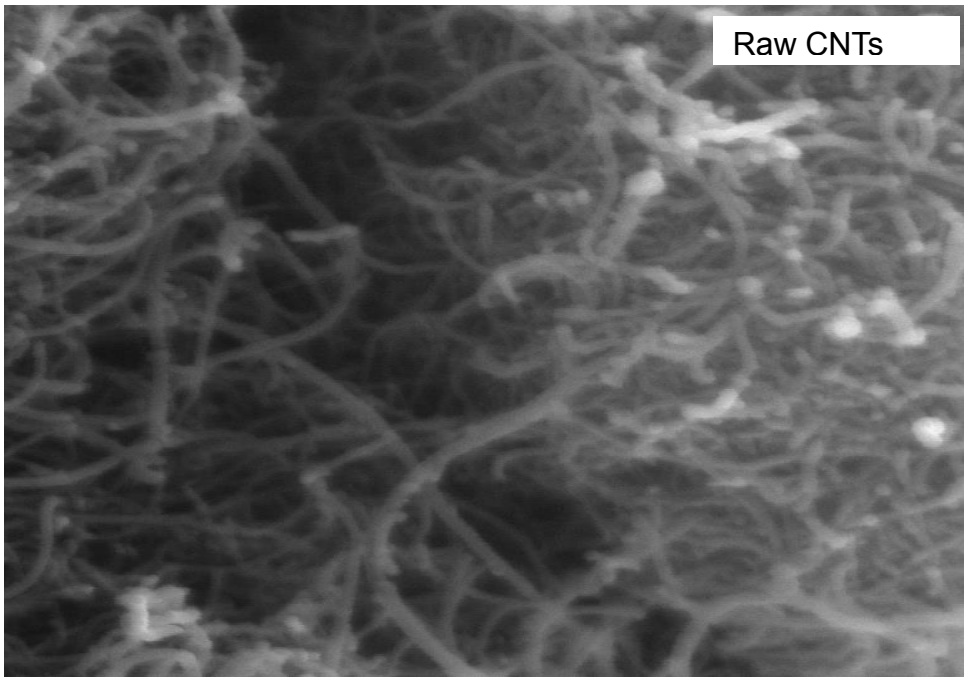

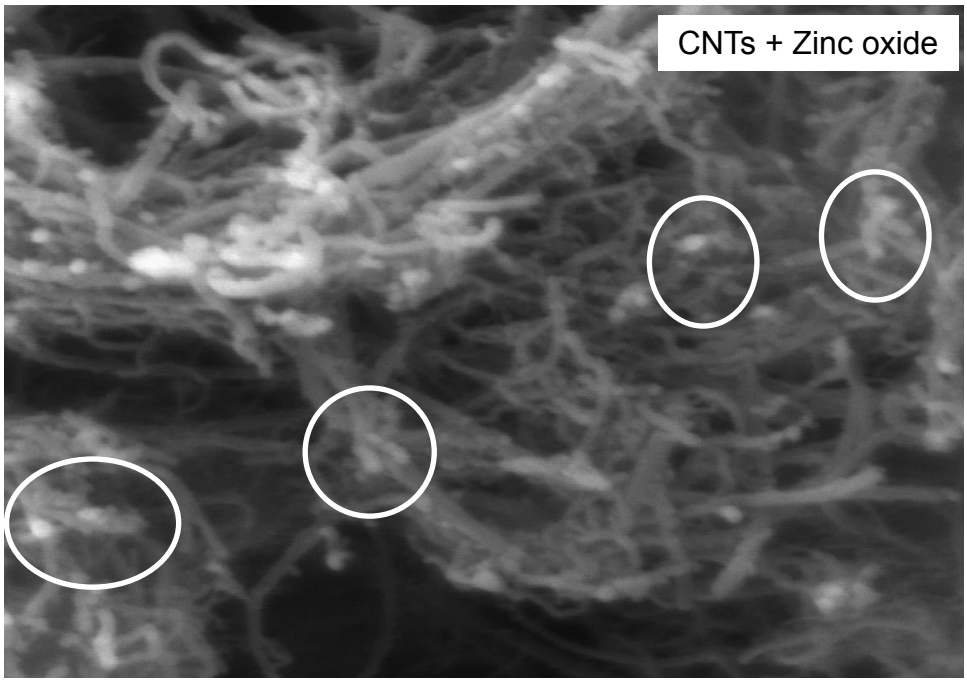

Figure 4-1: SEM images of raw CNTs and Zinc oxide impregnated CNTs

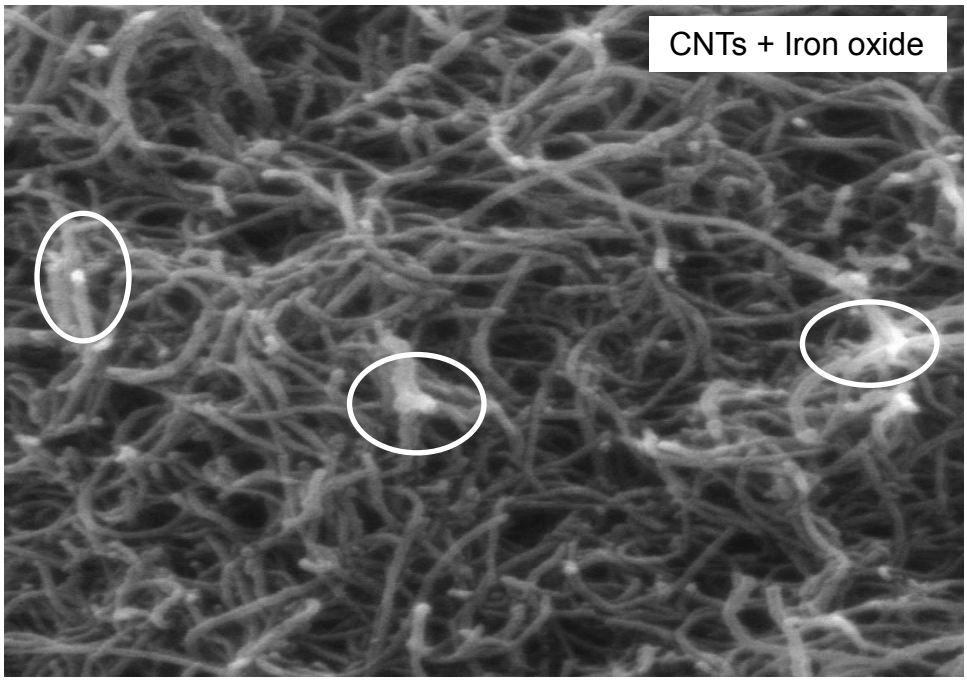

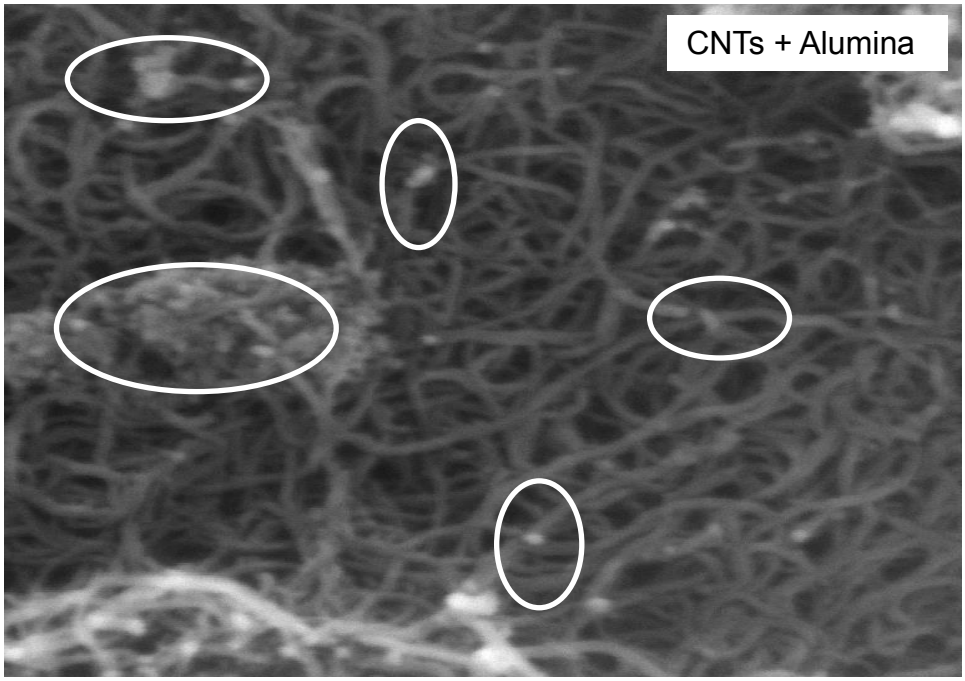

Figure 4-2: SEM images of Iron oxide impregnated CNTs and Aluminum oxide impregnated CNTs

4.1.2 Energy dispersive x-ray (EDX) analysis

EDX is one of qualitative technique which performs the spot analysis of a sample. This technique was used to confirm the presence of different elements in the samples. It is indicated in the Figure 4.3 that raw CNTs contains carbon as a major constitute and a little amount of nickel, which is indication of catalyst precursor used for growing CNTs. The presence of spectra for zinc and oxygen in zinc oxide impregnated CNTs along with carbon and nickel is provided in Figure 4.3.

Figure 4.4 also presented the spectrum of iron oxide impregnated CNTs, which indicates the presence of iron and oxygen along with carbon and nickel. Similarly, aluminum oxide impregnated CNTs contain aluminum and oxygen in addition to carbon and nickel as indicated in Figure 4.4.

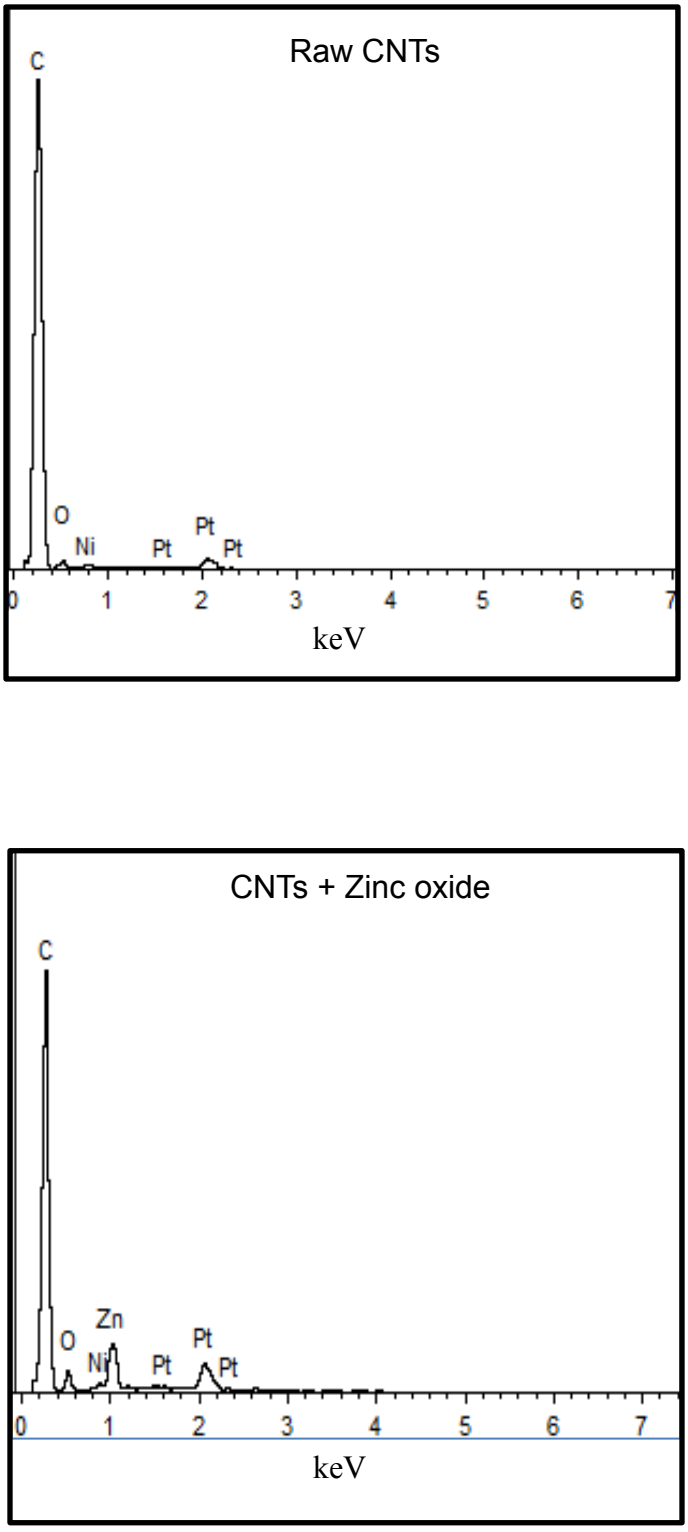

Figure 4-3: EDX Spectra for raw CNTs and zinc oxide impregnated CNTs

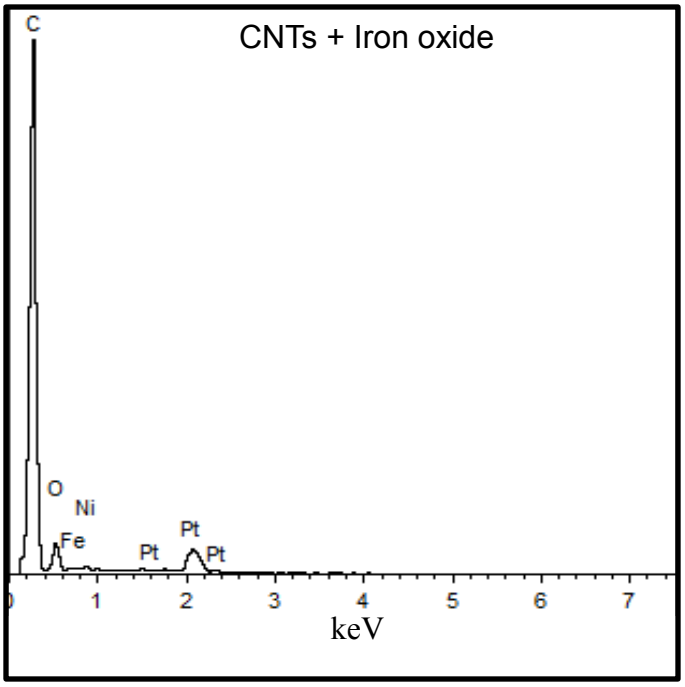

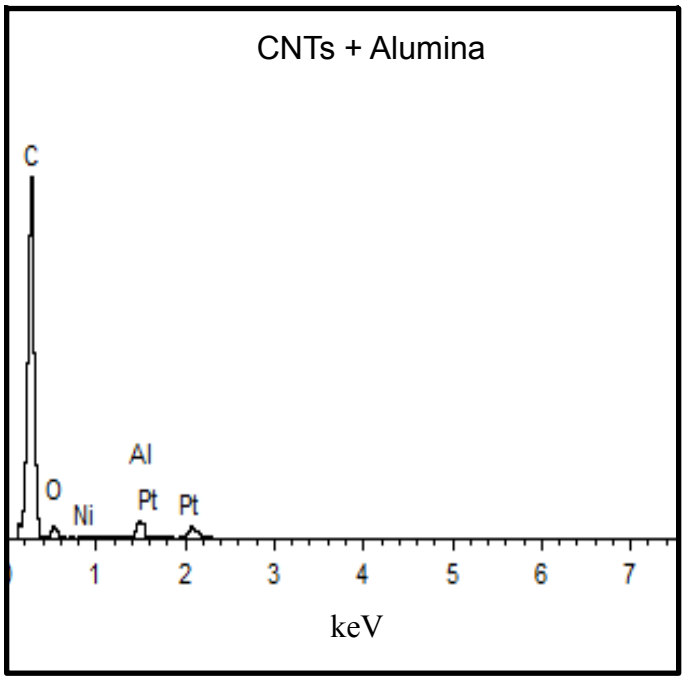

Figure 4-4: EDX Spectra for iron oxide impregnated CNTs and alumina impregnated CNTs

4.1.3 Thermogravimetric analysis (TGA)

Thermogravimetric analysis was carried out to study the thermal degradation temperature and purity of materials. Figure 4.5 demonstrates the thermogravimetric behavior of both raw and metal oxide nanoparticles impregnated CNTs. It can be observed that the raw CNTs are more stable and thermal degradation takes places in a relative narrow range of temperature 500 to 550 ^{o}C. Impregnation of CNTs with iron oxide nanoparticles and zinc oxide nanoparticles increased the destabilization in CNTs and degradation started at lower temperature 450 ^{o}C, while aluminum oxide impregnation does not affect the degradation temperature of CNTs because aluminum oxide has very low thermal conductivity. The mass left over the pan after burning of raw CNTs represents the catalyst particles, which was found to be nickel as confirmed from EDX analysis. It is also observed that the residual mass increased as we moved from raw to metal oxide impregnated CNTs. The higher residue mass (about 7%) left over for metal oxide impregnated CNTs indicates iron oxide, aluminum oxide and zinc oxide in different samples. Similar trends were observed in these studies [70,71].

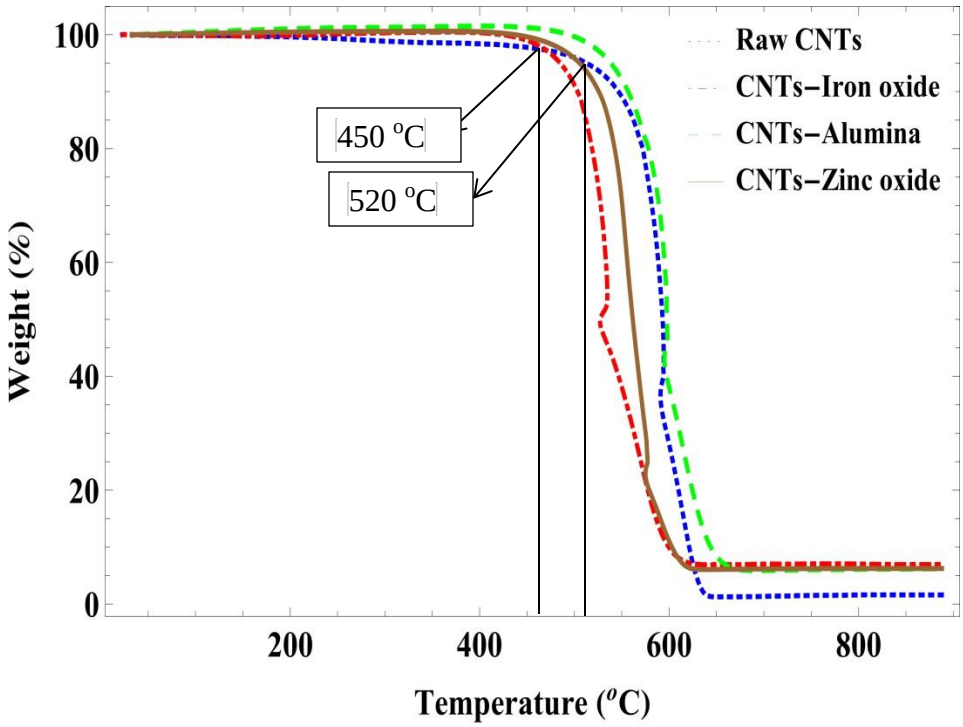

Figure 4-5: Thermogravimetric curves for raw and metal oxide impregnated CNTs

4.1.4 X-ray diffraction (XRD) analysis

XRD analysis was performed to analyze the phase structure of both CNTs and metallic oxide nanoparticles. The analysis was carried out at 2-theta range of 10^o to 100^o with step of 0.02^o and step time of 1 second. It is demonstrated in Figures 4.6 and 4.7 that the characteristics peaks corresponding to graphitic structure of CNTs exists at 2-theta value of 26^o and 43^o [58,62] in all samples. The peaks indicating the presence of zinc oxide are also visible from Figure 4.6 at 2-theta values of 35^o [72,73]. The peak corresponding to iron oxide exists at 2-theta value of 43^o [74,75] overlapped with CNTs peak. Similarly, the analysis of data for aluminum oxide impregnated CNTs shown in Figure 4.7 indicates the presence of aluminum oxide characterization peak at 2-theta value of 20^o [76]. The representative peak of nickel catalyst particles in all samples was overlapped with CNTs peak on 43^o [77].

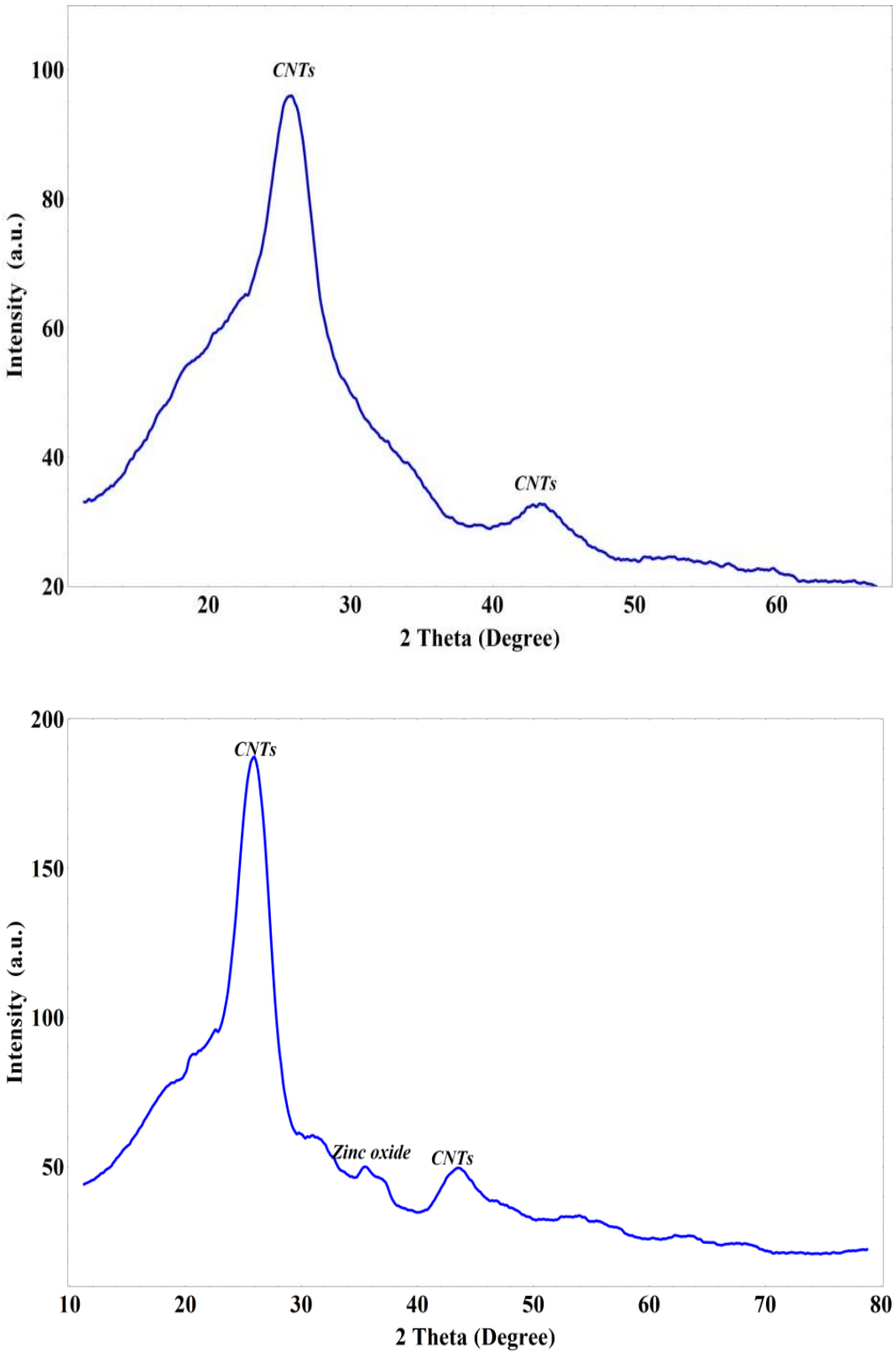

Figure 4-6: XRD pattern for raw CNT zinc oxide impregnated CNTs

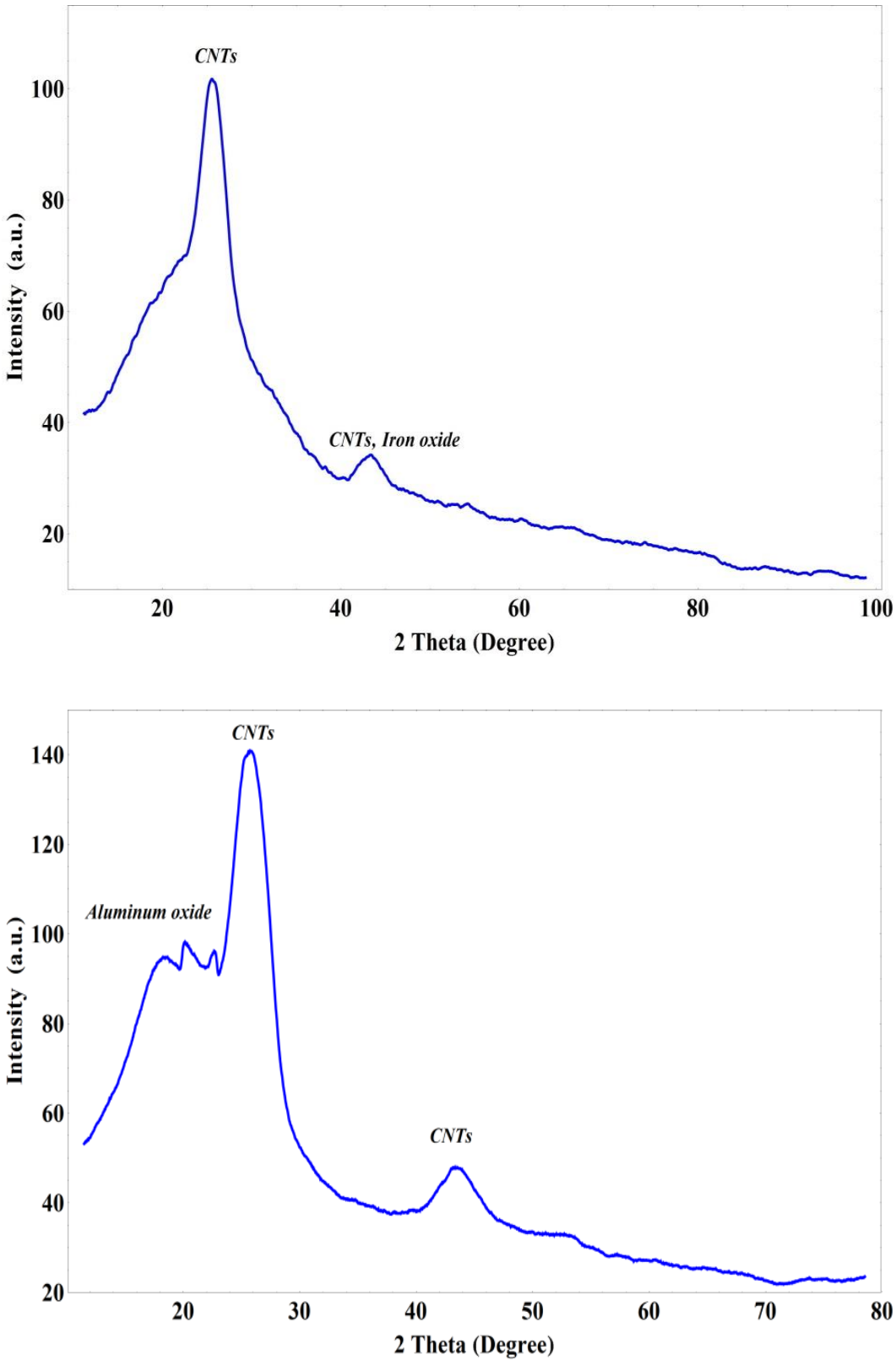

Figure 4-7: XRD pattern of iron oxide impregnated CNTs and aluminum oxide impregnated CNTs

4.1.5 Nitrogen isotherms and surface area analysis

Figures 4.8 and 4.9 demonstrate the nitrogen adsorption desorption isotherms for raw and metal oxide impregnated CNTs. Nitrogen adsorption isotherms were measured over a relative pressure (p/p_o) range of 0.01 to 0.989. These isotherms represent the monolayer adsorption and are of type (iii) according to classification of IUPAC (International Union of Pure and Applied Chemistry). The hysteresis loop is of type H3 in each curve and hysteresis occurs due to capillary condensation [78]. Surface area analysis is important in order to get information about adsorption sites of adsorbents. BET surface area was determined using standard BET equation and was found to be 138 m^2/g for raw CNTs, 195 m^2/g for zinc oxide impregnated CNTs, 216 m^2/g for iron oxide impregnated CNTs and 205 m^2/g for aluminum oxide impregnated CNTs. This indicated that after impregnation, surface area of CNTs increased due to metal oxide nanoparticles attachment on the surface of CNTs. This increase in surface area can provide more active sites for adsorption of pollutants.

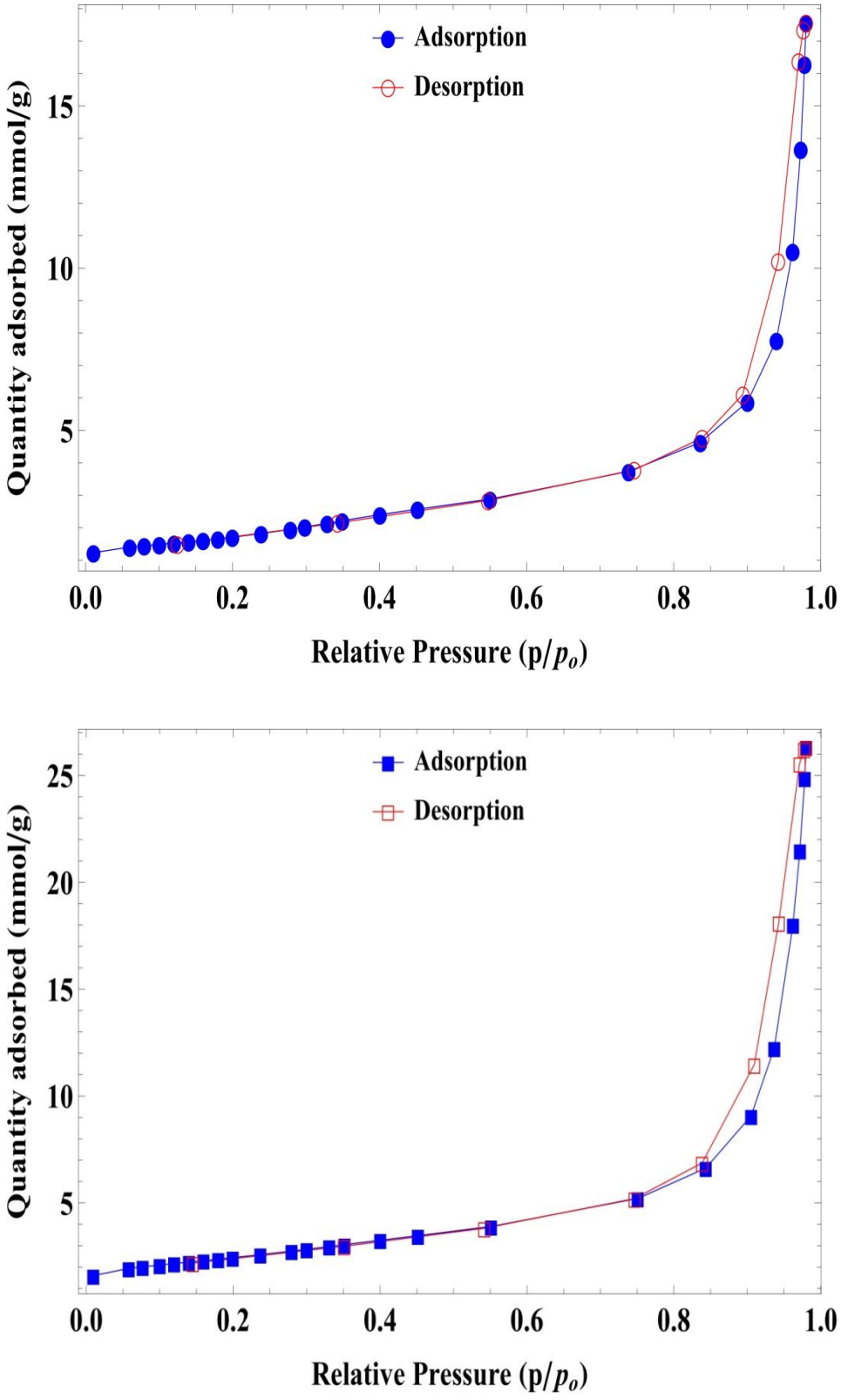

Figure 4-8: Adsorption desorption plot for raw CNT (upper) and zinc oxide impregnated CNTs (lower)

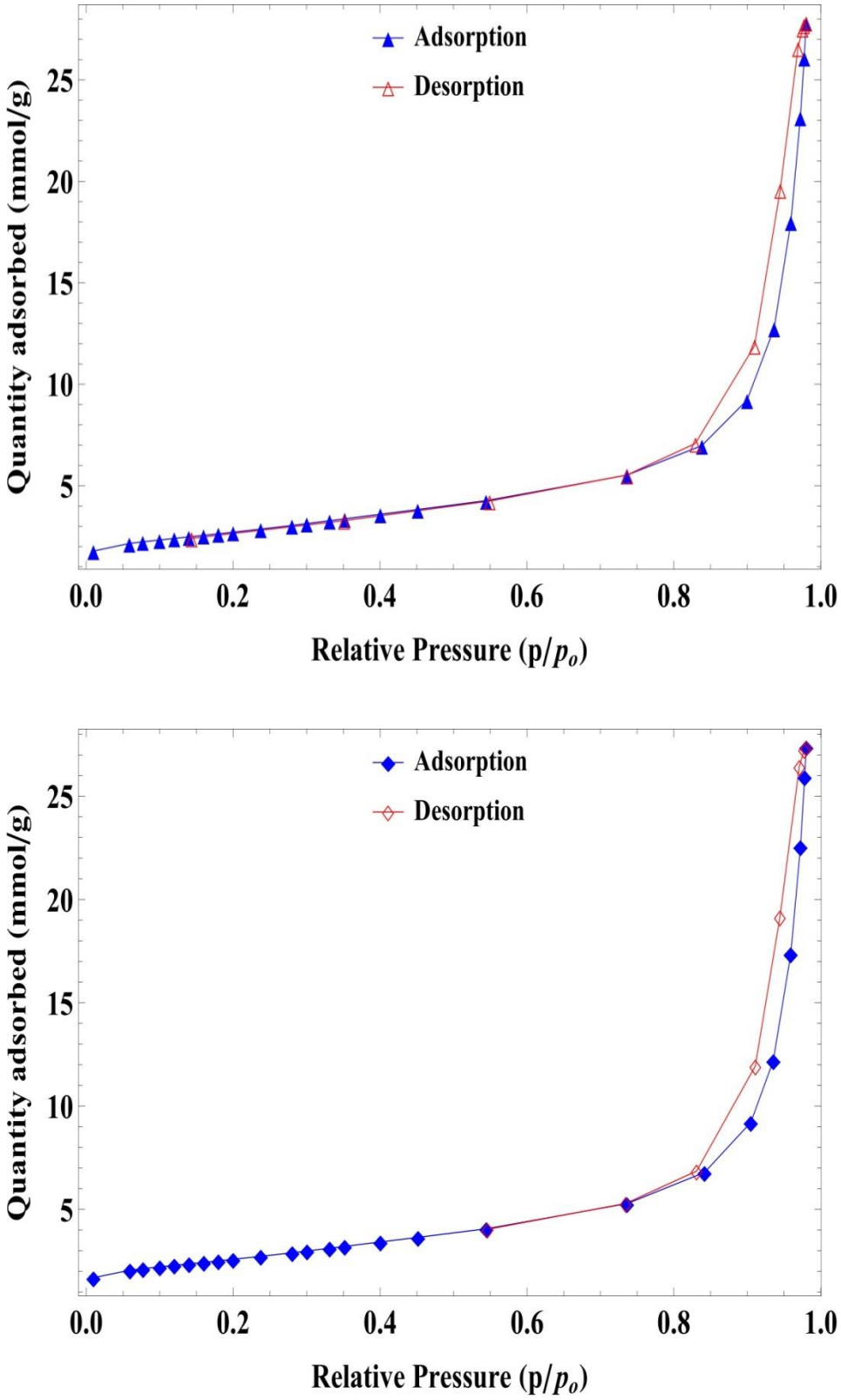

Figure 4-9: Adsorption desorption plot for zinc oxide (upper) and aluminum oxide impregnated CNTs (lower)

4.2 Adsorption Experimentation

In the following section, different parameters affecting the adsorption of benzene, toluene and xylene on the surface of adsorbents will be discussed. It is reported that various factors affecting the adsorption of different contaminates from water include contact time of adsorbent with adsorbate solution, dosage of adsorbent, initial pH of solution, initial concentration of adsorbate in solution [60,79].

Here, the effect of these parameters on adsorption of each contaminant is discussed in detail.

4.3 Factors Affecting the Adsorption of Benzene

The effect of contact time, adsorbent dosage and solution pH on removal of benzene using raw CNTs and metal oxide impregnated CNTs will be discussed in the following section.

4.3.1 Effect of contact time

The effect of contact time on benzene adsorption values and removal was carried out by varying the time from 60 minutes to 240 minutes. Initial concentration of benzene solution was 1 ppm, adsorbent dosage was 50 mg, shaking speed was 200 rpm and initial pH of solution was 6 for all samples. Figure 4.10 reveals the effect of contact time on removal efficiency of raw CNTs and metal oxide nanoparticles impregnated CNTs. Maximum removal achieved was 51% while maximum adsorption capacity was 1.14 mg/g with raw CNTs. By impregnating CNTs with metal oxide nanoparticles removal

efficiency and adsorption capacity both increased. Maximum removal was 70% and adsorption capacity was enhanced to 1.53 mg/g for iron oxide NPs impregnated CNTs. Similarly, removal efficiency of aluminum oxide impregnated CNTs was 71% removal and adsorption capacity was 1.56 mg/g. Zinc oxide impregnated CNTs provided 58% removal and adsorption capacity of 1.27 mg/g. The enhancement in removal efficiency of impregnated CNTs was due to higher surface area as observed in BET surface area analysis. More active sites were available for benzene molecules to be adsorbed on the surface of metal oxide impregnated CNTs, hence increasing the removal efficiency. It can also be observed from Figure 4.10 that by increasing the time provided for adsorption, adsorption capacity and percentage removal increased due to more time available for π-π bonding of benzene molecules with π bonds on CNTs surface. No change in pH was observed at the end of experiment.

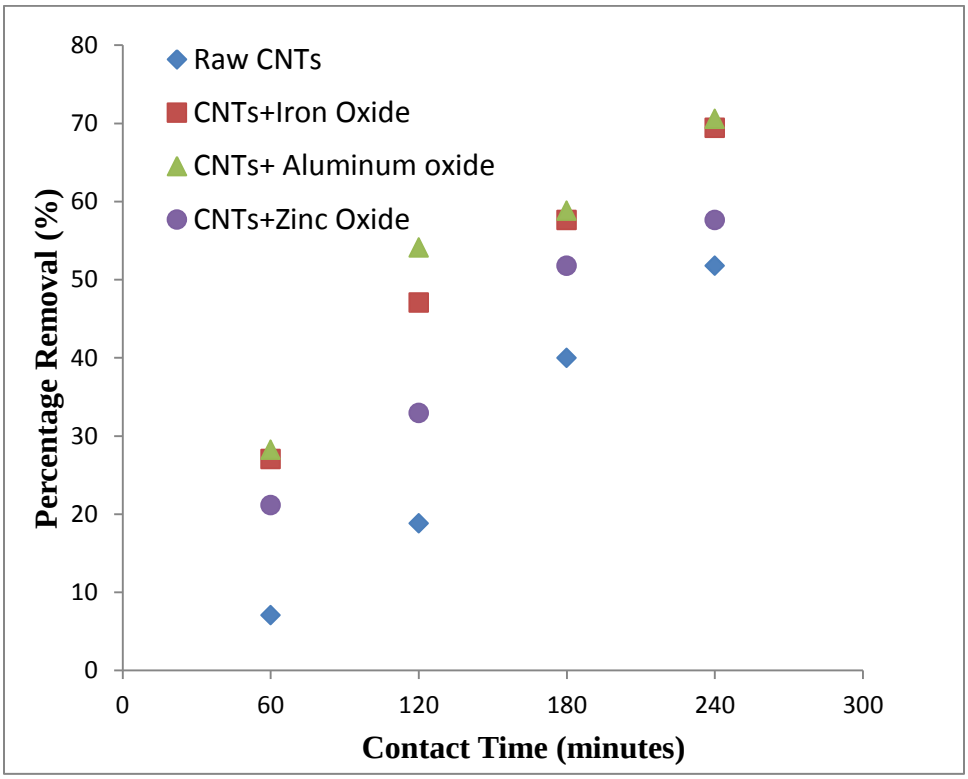

Figure 4-10: Effect of contact time on removal of benzene from water using raw and metal oxide NPs impregnated CNTs (Co= 1ppm, pH=6.0, shaking rpm= 200, dosage= 50mg, room temperature)

4.3.2 Effect of adsorbent dosage

The impact of adsorbent dosage on adsorption capacity and percentage removal was analyzed by using different amount of adsorbents which were 25, 50, 75 and 100 mg. Initial concentration of benzene solution used was 1 ppm while shaking rpm was 200, initial pH was 6 and contact time was 120 minutes for all samples. Figure 4.11 represents the effect of adsorbent dosage on removal efficiency of raw CNTs and various metal oxide nanoparticles impregnated CNTs. It is evident that by increasing the amount of adsorbent; percentage removal enhanced for all samples. By using raw CNTs initially with dosage of 25 mg, only 9.45% benzene was removed. However, removal efficiency was enhanced to 53% when dosage was increased from 25 to 100 mg. Iron oxide nanoparticles impregnated CNTs have initially 22% removal with 25 mg dosage while it was accelerated to 61% finally when dosage was 100 mg. For aluminum oxide impregnated CNTs, initial removal was 32% with 25 mg dosage and it was enhanced to 54% with 100 mg dosage. The possible reasons behind this enhancement in benzene adsorption are; by increasing the dosage of adsorbent, more active sites are provided hence increasing the chance for attachment of benzene molecules with CNTs surface. By increasing the amount of the adsorbent, removal does not increased at same ratio for all adsorbent, the possible reason here may be accumulation and agglomeration of CNTs with each other hence reducing the chance for attachment of more molecules.

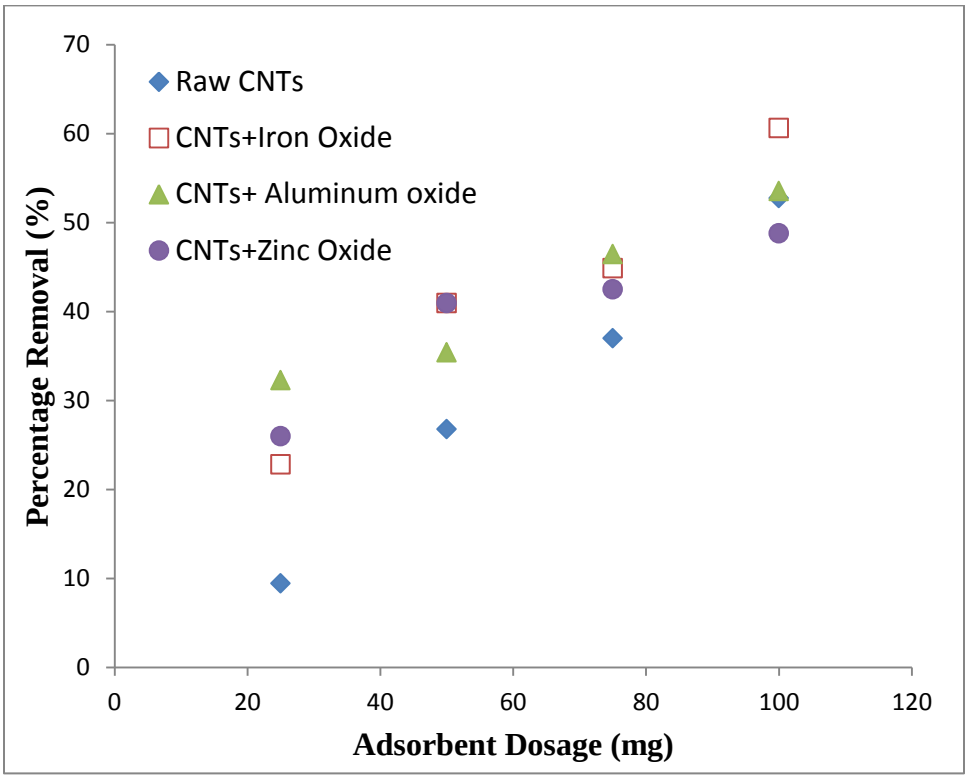

Figure 4-11: Effect of adsorbent dosage on removal of benzene from water using raw and metal oxide NPs impregnated CNTs (Co= 1 ppm, pH=6.0, rpm= 200, time= 2 hr., room temperature)

4.3.3 Effect of initial pH of solution

Figure 4.12 represents the pH effect on removal efficiency of raw and metal oxide nanoparticles impregnated CNTs. Significant improvement was observed for all adsorbents when pH was increased from 3 to 4. On the other hand, no significant improvement was noticed by increasing the initial pH of solution from 4 to 6. Increasing the initial pH from 6 to 8 reduced the removal for raw CNTs while there was no significant change for metal oxide impregnated CNTs. Benzene exists in the molecular form at whole range of pH. So in this case, dispersive interactions due to л-л bonding, electrostatic interaction between CNTs surface, metal oxide nanoparticles and benzene molecules were dominant in the removal of benzene from water. Similar findings were reported in literature [44].

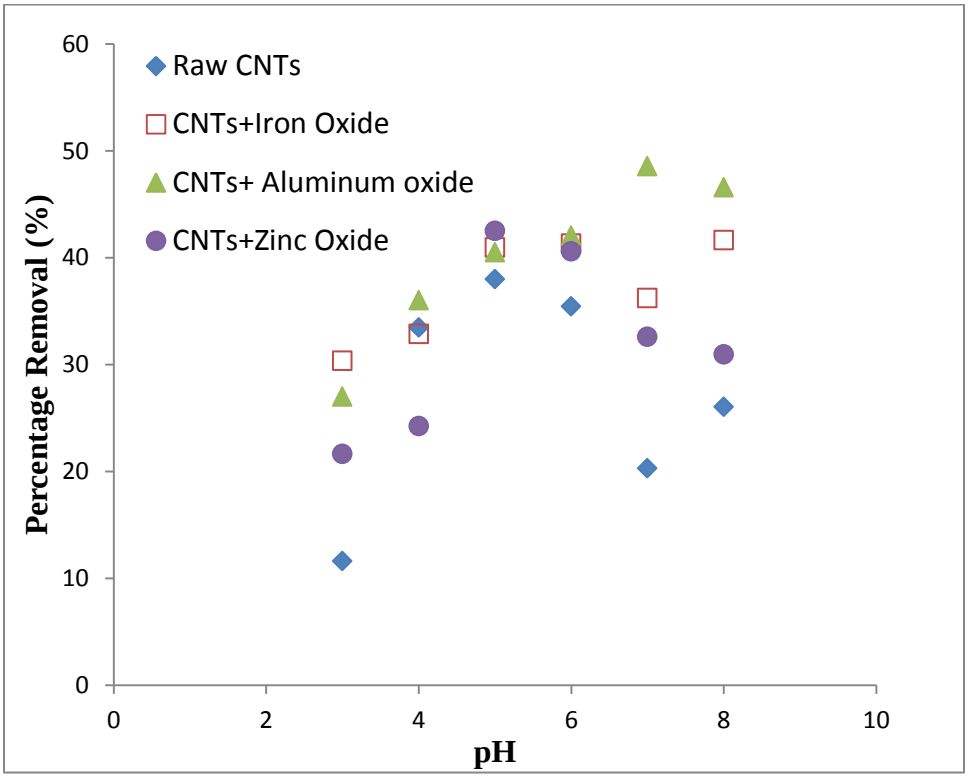

Figure 4-12: Effect of solution pH on removal of benzene from water using raw and metal oxide NPs impregnated CNTs (Co= 1ppm, rpm= 200, dosage= 50mg time= 2 hr., room temperature)

4.4 Factors Affecting the Adsorption of Toluene

Three factors were investigated for adsorption of toluene on the surface of adsorbents. Factors studied for removal of toluene from water include contact time, adsorbent dosage and initial concentration of adsorbate.

4.4.1 Effect of contact time

The effect of contact time on removal of toluene was studied by varying the contact time from 120 minutes to 360 minutes. It is observed from the Figure 4.13 that by increasing the contact time, removal was found to be enhanced. Initially, higher rate of removal can be observed for all adsorbents. As time passed, rate of removal slowed down and finally reached to almost equilibrium for all adsorbents. With the passing of time, removal efficiency slowed down because almost all available sites were occupied and there was repulsion between toluene molecules to occupy the remaining sites. Removal was 45 % for raw CNTs at the end of 120 minutes which was found to be enhanced to 63 % at the end of 360 minutes. Percentage removal increased uniformly for raw and zinc oxide impregnated CNTs while for iron oxide and aluminum oxide impregnated CNTs, it was less at the start but finally reached to 66% at the end of 360 minutes.

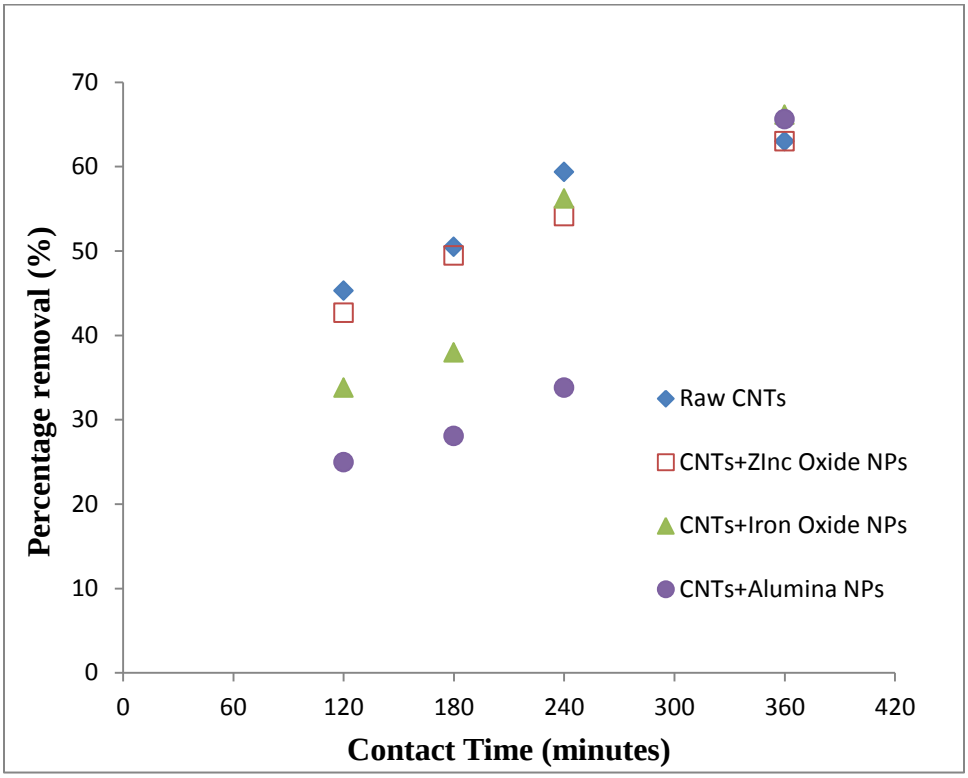

Figure 4-13: Effect of contact time on removal of toluene from water using raw and metal oxide NPs impregnated CNTs (Co= 100 ppm, pH=6.0, rpm= 200, dosage= 50 mg, room temperature)

4.4.2 Effect of adsorbent dosage

Figure 4.14 shows the impact on removal of toluene from water by changing the amount of adsorbents. It is evident form Figure 4.14 that the removal enhanced with increasing the adsorbent dosage for all adsorbents. The reason behind this increase in the removal was the addition in number of active sites available for adsorption with the increase of the adsorbent dosage. For raw CNTs, when the amount of adsorbent was increased from 25 mg to 50 mg, the removal was enhanced from 22% to 28%. Adsorption was not doubled here, which may be due to agglomeration of CNTs hence reducing the available active sites. Increase in adsorbent dosage upto 100 mg improved the removal to 48% and then almost constant with further addition of CNTs upto 150 mg. The percentage removal of toluene enhanced uniformly for zinc oxide impregnated CNTs as it was almost 11% with 25 mg of adsorbent and 22% using 50 mg of adsorbent, then with 100 mg, removal was about 48% while further increase in dosage did not improve removal and it was almost 51% with 150 mg dosage. Iron oxide nanoparticle impregnated CNTs also provided uniform removal efficiency in the start with 17% removal using 25 mg dosage and 32% with 50 mg dosage, but it increased to 52% with dosage of 100 mg and finally was almost 54% using 150 mg of the iron oxide impregnated CNTs. Finally, for the aluminum oxide impregnated CNTs, the removal percentage was found to be 17%, 22%, 44% and 54% for 25 mg, 50 mg, 100 mg and 150 mg dosage, respectively. Initially, increase in adsorption by increasing the amount of adsorbents for all materials was due to availability of more sites hence improving the removal but later it retarded or slowed down because of agglomeration of material with each other on further increase in adsorbent amount hence reducing the removal efficiency. Other possible reason may be

due to achievement of equilibrium between adsorption and desorption of toluene molecules, no further improvement in removal was noticed with increasing active sites.

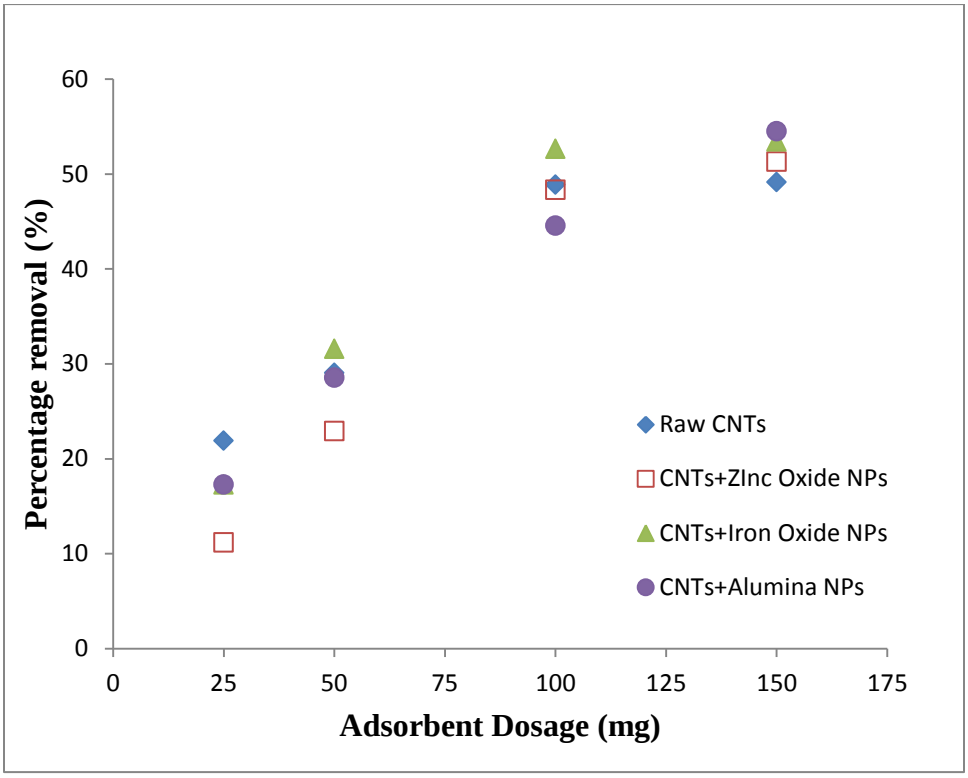

Figure 4-14: Effect of adsorbent dosage on removal of toluene from water using raw and metal oxide NPs impregnated CNTs (Co= 100 ppm, pH= 6.0, rpm= 200, time= 2 hr., room temperature)

4.4.3 Effect of initial concentration of adsorbate

Figure 4.15 illustrates the effect of toluene initial concentration on its removal from water. Increasing the initial concentration of toluene increased the removal efficiency for all adsorbents. The possible reasons behind this increment; may be due to higher concentration gradient removal increased, secondly, may be due to competition between the more molecules even low energy sites were also occupied hence leading to better removal efficiency.

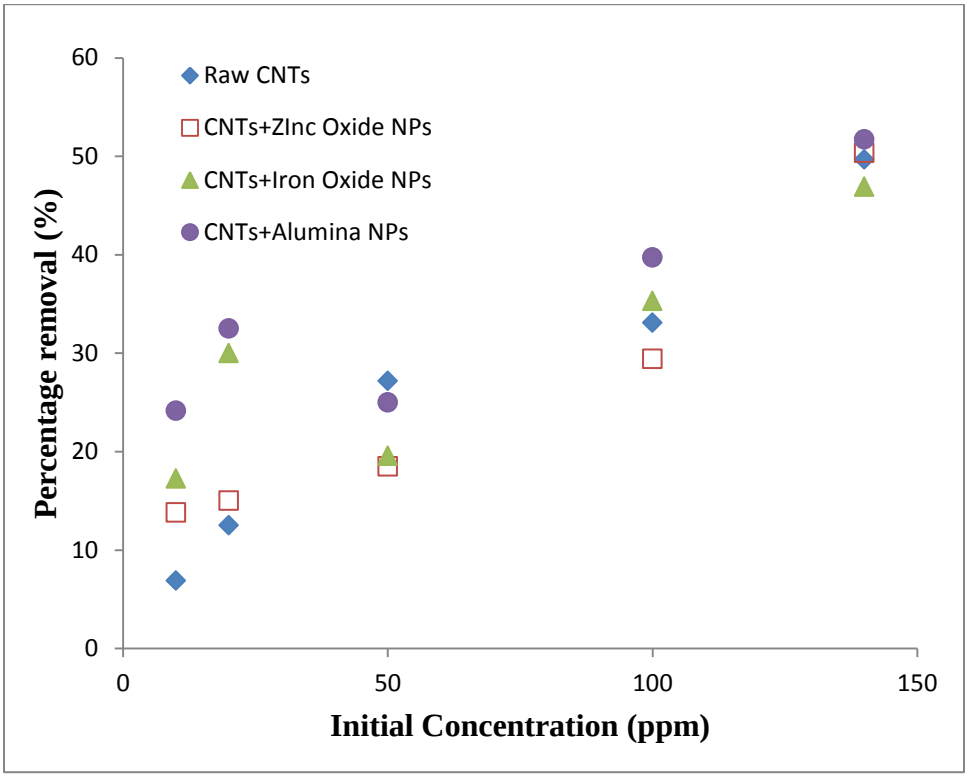

Figure 4-15: Effect of initial concentration on removal of toluene from water using raw and metal oxide NPs impregnated CNTs (Dosage= 50mg, pH= 6.0, rpm= 200, time= 2 hr., room temperature)

4.5 Factors Affecting the Adsorption of p-Xylene

Effect of variation of contact time, adsorbent dosage and initial adsorbate concentration on removal efficiency of p-xylene from water was studied and each effect is discussed in detail in the following section.

4.5.1 Effect of contact time

In order to study the effect of contact time on adsorption of p-xylene from water using different adsorbents, time was varied form 60 minutes to 480 minutes. All other factors which include adsorbent dosage of 50 mg, shaking speed of 200 rpm, pH of 6.0 and initial concentration of 100 ppm were held constant for all adsorbents. The results presented in Figure 4.16 demonstrate that adsorption of p-xylene from water was increased with time for all adsorbents. For raw CNTs, almost 60% removal was achieved in first 60 minute duration while later it increased to 75% in next 60 minutes. After 120 minutes contact time, removal rate became slow and final removal of 89% was achieved at the end of 480 minutes. CNTs impregnated with zinc oxide nanoparticles showed highest removal of 73% among all adsorbents in first 60 minutes and then slowly reached to final value of 87% removal in 480 minutes. CNTs impregnated with iron oxide nanoparticles showed 60% removal in first 60 minutes and then gradual increase of almost 5-6% was observed in removal with each passing hour and finally it was 86% after 480 minutes. Aluminum oxide impregnated CNTs provided second highest removal of 69% in first 60 minutes and then with slow increase touched 89% removal at the end of 480 minutes. In the start, highest rate of removal for all adsorbents was perhaps due to availability of a large number of vacant adsorption sites. Later, it was reduced because it

was difficult to occupy remaining sites due to repulsive forces between p-xylene molecules. Second reason may be in the start, rate of adsorption was higher than desorption hence providing higher removal, then it moved towards equilibrium hence balancing the adsorption and desorption rates and decrease in removal.

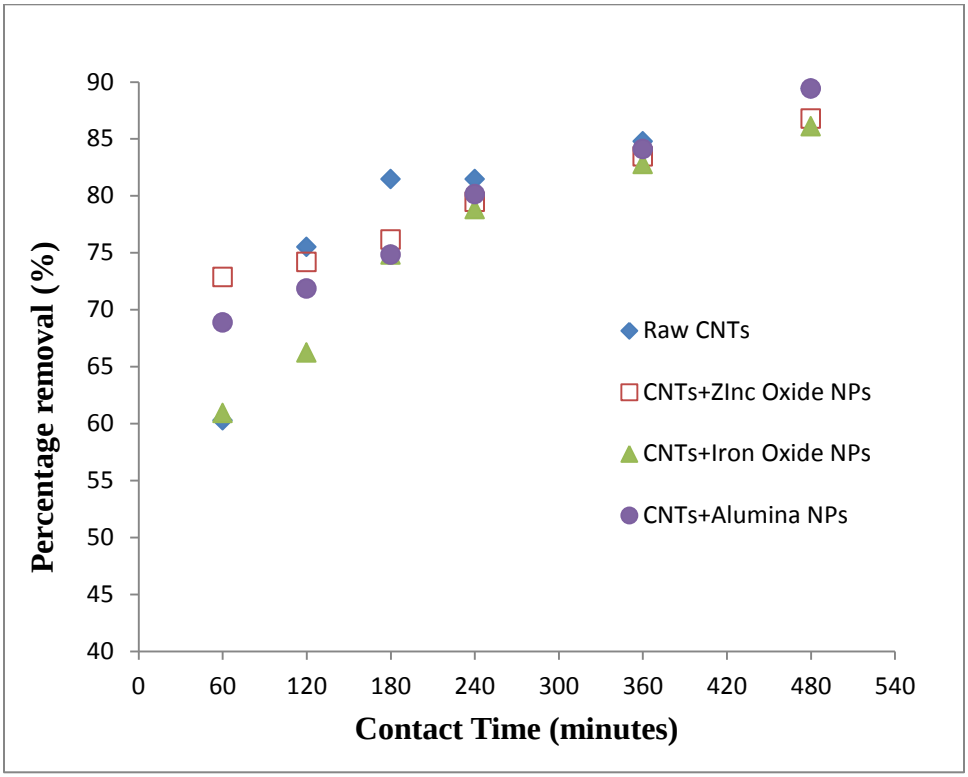

Figure 4-16: Effect of contact time on removal of p-xylene from water using raw and metal oxide NPs impregnated CNTs (Co= 100 ppm, pH=6.0, rpm= 200, dosage= 50 mg, room temperature)

4.5.2 Effect of adsorbent dosage

In order to study, the effect of adsorbent dosage on removal of p-xylene from water, amount of adsorbents was varied form 25 mg (adsorbent)/100 ml (solution) to 100 mg/100 ml. For all experiments contact time, pH, shaking speed, initial concentration and temperature were 2 hours, 6, 200 rpm, 100 ppm and 25 ^{o}C, respectively. It is demonstrated from Figure 4.17 that removal efficiency of p-xylene increased with increasing the dosage of adsorbents. Raw CNTs showed 67% removal using 25 mg dosage, which was increased to 80% with dosage of 50 mg, then with a slight increase was constant around 84% by increasing dosage upto 100 mg. Zinc oxide impregnated CNTs had highest removal of 77% as compared to other adsorbents with dosage of 25 mg, and it showed slight enhancement in removal reaching 84% with increasing the dosage upto 100 mg. Iron oxide impregnated CNTs have initially 68% removal leading to final value of 83% with a dosage of 100 mg. Aluminum oxide impregnated CNTs gave removal efficiency of 75% with dosage of 25 mg, while it was increased to 84% with dosage of 100 mg. Finally, it is observed that raw CNTs and iron oxide impregnated CNTs had significant increase in removal with higher adsorbent's dosage while very small increase in removal of p-xylene was obtained by increasing the amount of zinc oxide and aluminum oxide impregnated CNTs. The reason may be, by increasing the dosage of adsorbent, number of active adsorption sites increased hence leading to enhancement in removal efficiency. In case of zinc oxide and aluminum oxide impregnated CNTs, initially available sites (using dosage of 25 mg) were enough to accommodate the highest number of p-xylene molecules hence addition of more material does not provide any significant change in removal.

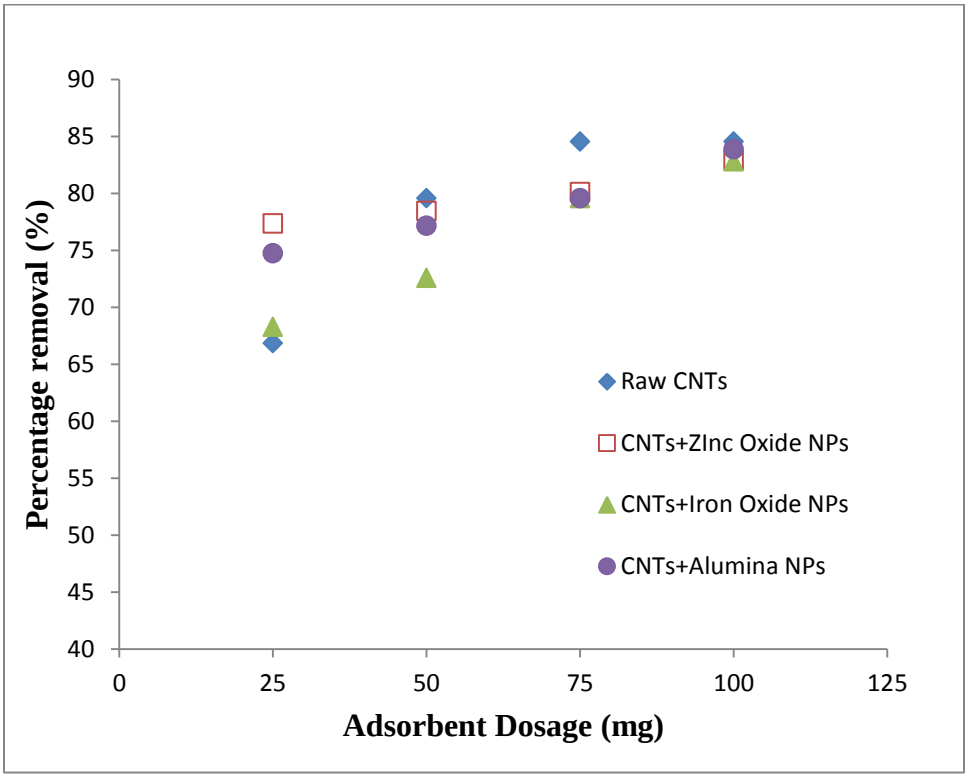

Figure 4-17: Effect of adsorbent dosage on removal of p-xylene from water using raw and metal oxide NPs impregnated CNTs (Co= 100 ppm, pH= 6.0, rpm= 200, time= 2 hr., room temperature)

4.5.3 Effect of initial concentration of adsorbate

Initial concentration of pollutant has important effect in adsorption. P-xylene initial concentration was varied from 20 ppm to 100 ppm to study the effect on removal efficiency, by keeping all other factors constant, as shown in Figure 4.18. Contact time of 2 hours, pH of 6.0, shaking speed of 200 rpm, room temperature and adsorbent dosage of 50 mg were used for all experiments. It was noted that the removal was decreased by increasing the initial concentration for all materials. The possible reason behind this phenomena may be due increase in concentration, no more sites were available to accommodate extra molecules and hence decreasing overall efficiency of removal.

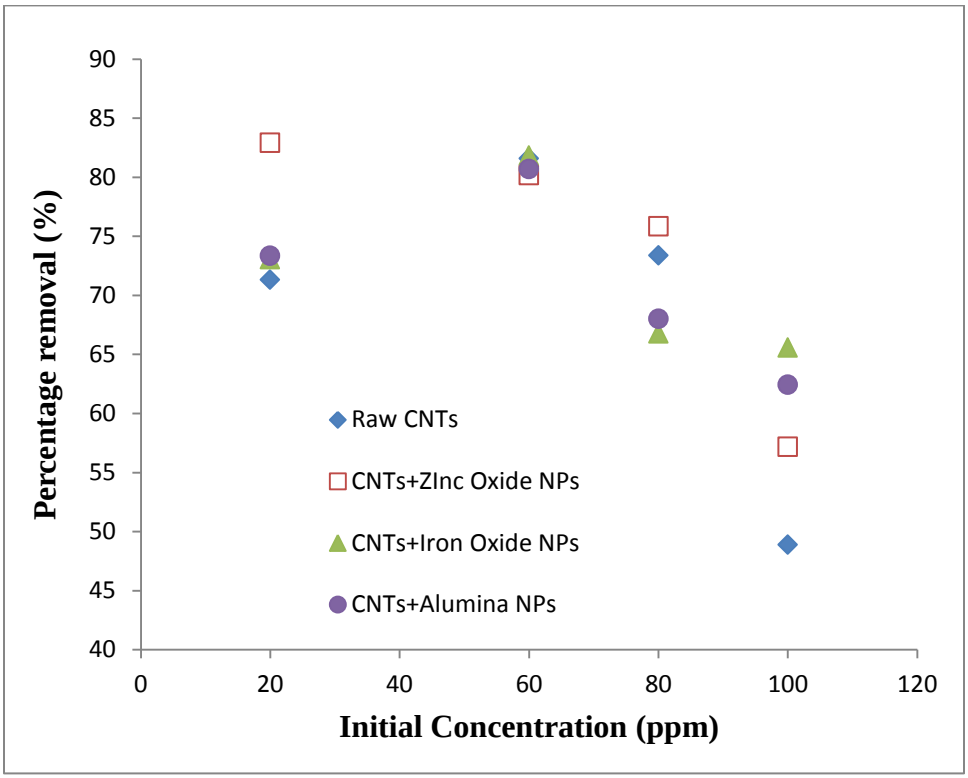

Figure 4-18: Effect of initial concentration on removal of p-xylene from water using raw and metal oxide NPs impregnated CNTs (Dosage= 50mg, pH= 6.0, rpm= 200, time= 2 hr., room temperature)

CHAPTER 5

RESULTS AND DISCUSSION

KINETIC AND ISOTHERM MODELS

This chapter deals with further extension of results for different adsorbents analyzed using kinetics and isotherms models. First part deals with fitting of BTX adsorption data using pseudo first order, pseudo second order and intraparticle diffusion models. Second part discusses the fitting of data using Langmuir and Freundlich isotherm models for further investigation of adsorption phenomena.

5.1 Kinetic Models Fitting

Most widely used kinetic models; pseudo first order (Lagergren's), pseudo second order (Ho's) and intraparticle diffusion (Weber's) models were applied to investigate the kinetics adsorption behavior of BTX on raw and impregnated CNTs.

Here, fitting of these models with experimental data is discussed in detail.

5.1.1 Benzene kinetic models fit

Figures 5.1, 5.2 and 5.3 show the fitting of benzene adsorption data on raw CNTs and metal oxide nanoparticles impregnated CNTs using pseudo first order, pseudo second order and intraparticle diffusion models. Table 5.1 represents the values of determination coefficients (R^2) and characteristics parameters calculated for benzene adsorption on all adsorbents.

Figure 5.1 represents the fitting of data with pseudo first order model and it shows a good fitting for all adsorbents and values of R^2 vary from 90% to 100% for different adsorbents. Iron oxide impregnated CNTs have best fitting with 100% regression coefficient value. From Figure 5.2, it is demonstrated that pseudo second order model also fits good for zinc oxide and iron oxide impregnated CNTs with R^2 value of 99% and 90%, respectively, but for raw CNTs and aluminum oxide impregnated CNTs, it shows poor fitting with R^2 of 86% and 81%, respectively. Figure 5.3 provides fitting of adsorption data with intraparticle model and shows best fit using all adsorbents with R^2 ranging from 94% to 99.5%.

Based on data fitting results, intraparticle diffusion model seems to represent best the data but curves does not pass through origin so, intraparticle diffusion has some effect on adsorption but it is not a complete controlling step in adsorption of benzene. Pseudo first order model showed best fitting after intraparticle model for all adsorbents. It is also clear from Table 5.1 that the values of $q_{e.calculated}$ by pseudo first order model are more close to experimental values, so this model is empirically best suitable model to represent the benzene adsorption data. Values of rate constant of first order model (k_1) are in order of zinc oxide impregnated CNTs > raw CNTs > aluminum oxide impregnated CNTs > iron oxide impregnated CNTs. It indicates zinc oxide impregnated CNTs reaches to equilibrium faster followed by raw CNTs and then aluminum oxide and iron oxide impregnated CNTs.

Finally, pseudo first order model was found best to describe the adsorption of benzene from water using raw and impregnated CNTs.

Pseudo first order model fit for benzene

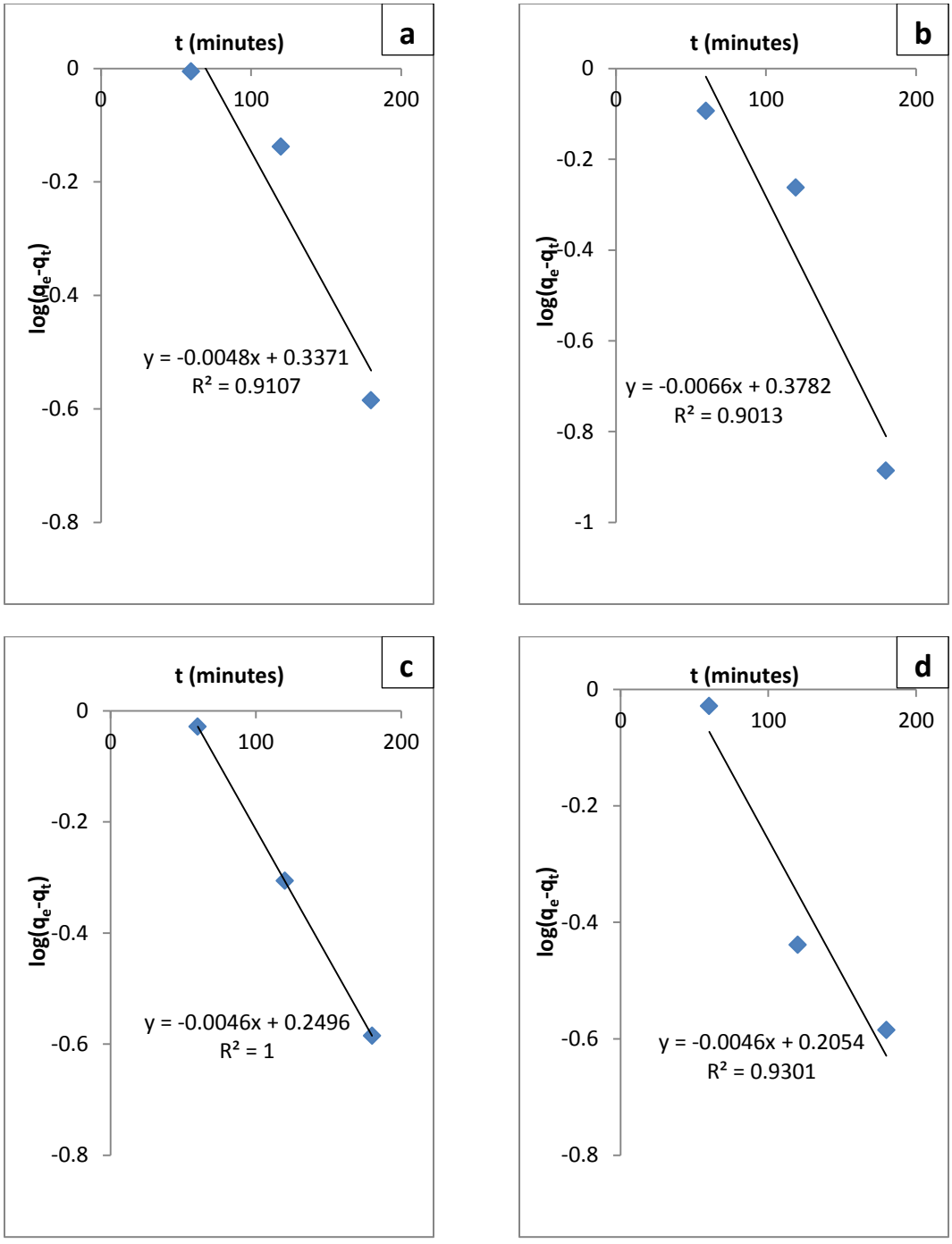

Figure 5-1: Pseudo first order model for fitting benzene adsorption using a) raw CNTs b) zinc oxide impregnated CNTs c) iron oxide impregnated CNTs d) alumina impregnated CNTs

Pseudo second order model fit for benzene

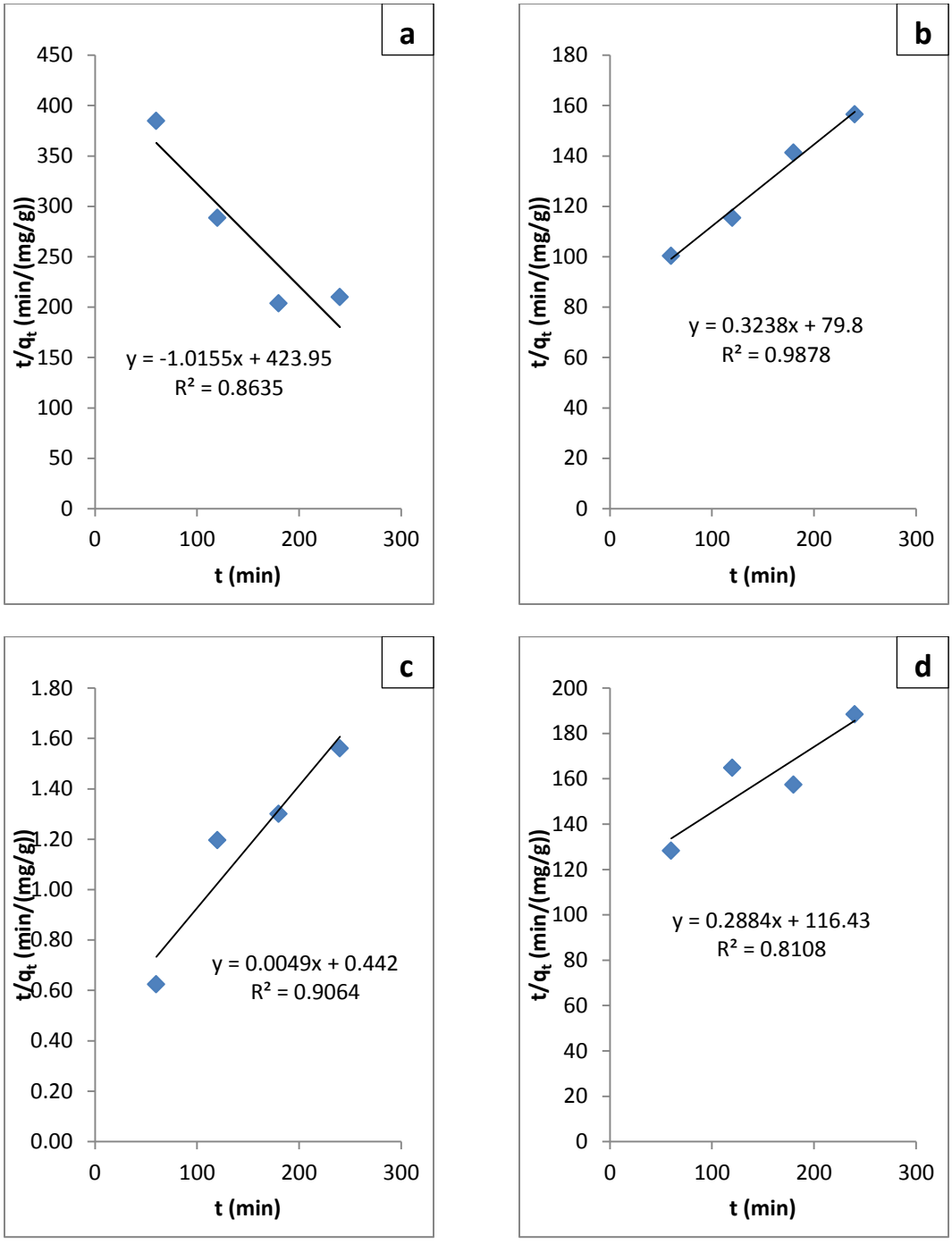

Figure 5-2: Pseudo second order model fitting for benzene adsorption using a) raw CNTs b) zinc oxide impregnated CNTs c) iron oxide impregnated CNTs d) alumina impregnated CNTs

Intraparticle diffusion model fit for benzene

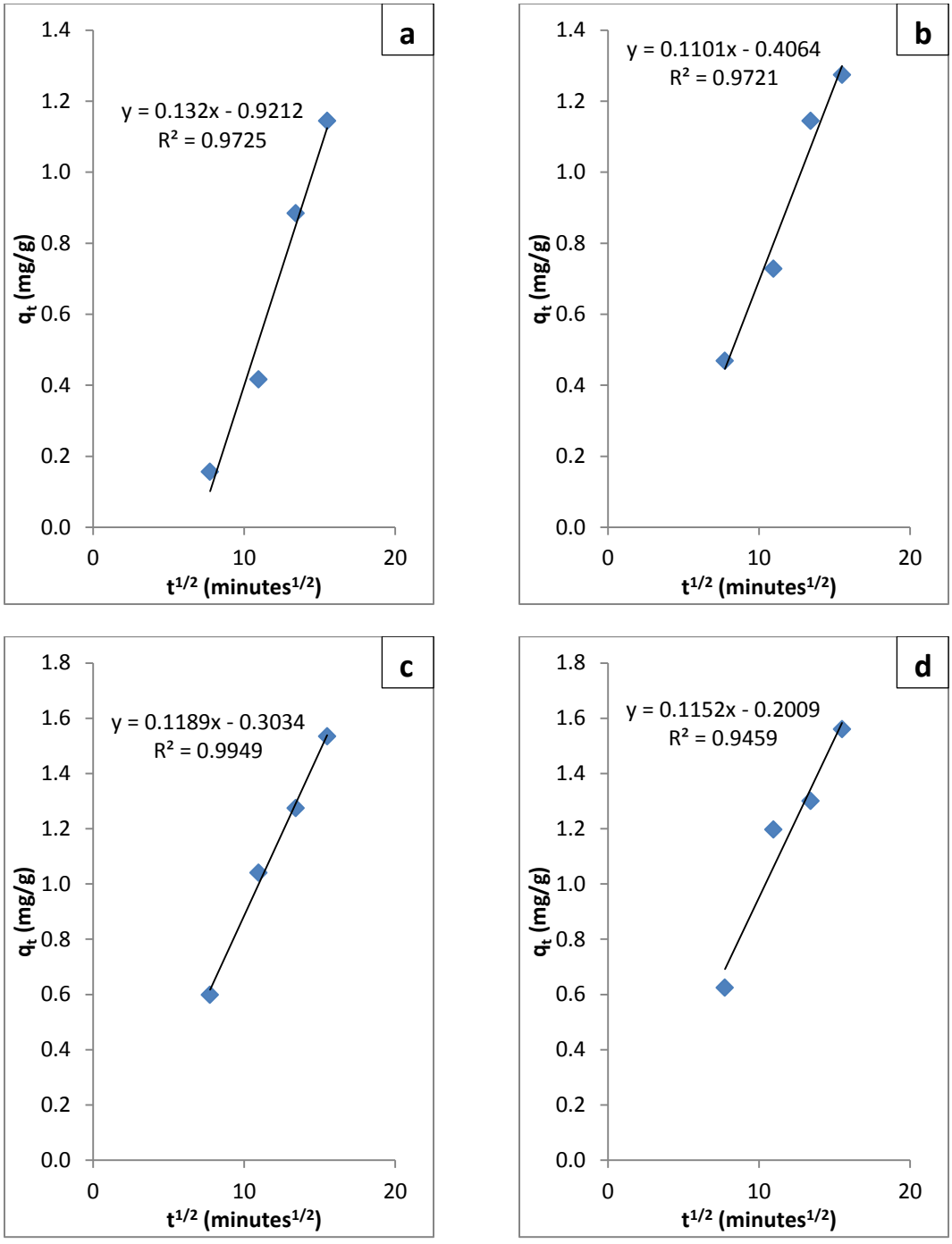

Figure 5-3: Intraparticle diffusion model fitting for benzene adsorption using a) raw CNTs b) zinc oxide impregnated CNTs c) iron oxide impregnated CNTs d) alumina impregnated CNTs

Table 5-1: Kinetic parameters of benzene absorbed on raw and impregnated CNTs

Adsorbents	Model	Parameters	Adsorbate
Raw CNTs	**Pseudo first order**	$k_1(min^{-1})$	4.800E-03
		$q_{e,calculated}$ (mg/g)	2.173
		R^2	0.911
	Pseudo second order	k_2 (g mg^{-1} min^{-1})	2.854E-07
		$q_{e,calculated}$ (mg/g)	90.909
		R^2	0.864
	Intraparticle diffusion	k_{id} (g mg^{-1} $min^{-0.5}$)	0.132
		C	-0.921
		R^2	0.973
Zinc oxide impregnated CNTs	**Pseudo first order**	$k_1(min^{-1})$	6.600E-03
		$q_{e,calculated}$ (mg/g)	2.389
		R^2	0.901
	Pseudo second order	k_2 (g mg^{-1} min^{-1})	7.144E-04
		$q_{e,calculated}$ (mg/g)	3.467
		R^2	0.811
	Intraparticle diffusion	k_{id} (g mg^{-1} $min^{-0.5}$)	0.110
		C	-0.406
		R^2	0.972

Iron oxide impregnated CNTs	**Pseudo first order**	$k_1(min^{-1})$	4.600E-03
		$q_{e,calculated}$ (mg/g)	1.777
		R^2	1.000
	Pseudo second order	k_2 (g mg^{-1} min^{-1})	1.314E-03
		$q_{e,calculated}$ (mg/g)	3.088
		R^2	0.988
	Intraparticle diffusion	k_{id} (g mg^{-1} $min^{-0.5}$)	0.120
		C	-0.303
		R^2	0.995
Aluminum oxide impregnated CNTs	**Pseudo first order**	$k_1(min^{-1})$	4.600E-03
		$q_{e,calculated}$ (mg/g)	1.605
		R^2	0.930
	Pseudo second order	k_2 (g mg^{-1} min^{-1})	1.785E-03
		$q_{e,calculated}$ (mg/g)	2.841
		R^2	0.921
	Intraparticle diffusion	k_{id} (g mg^{-1} $min^{-0.5}$)	0.115
		C	-0.201
		R^2	0.946

5.1.2 Toluene kinetic models fit

Toluene adsorption data fit is shown in Figures 5.4, 5.5 and 5.6. Determination co-efficient (R^2), first and second order model constants and adsorption capacity calculated are provided in Table 5.2.

Figure 5.4 shows that pseudo first order model has good fit for adsorption data of toluene using all adsorbents with R^2 ranging from 83% for iron oxide impregnated CNTs followed by 91% for zinc oxide impregnated CNTs then 95% for raw CNTs and 96% for aluminum oxide impregnated CNTs. Pseudo second order model has best fitting with data as it is clear from Figure 5.5 that iron oxide impregnated CNTs have R^2 as 87% being lowest one while it was 90%, 97% and 98% for aluminum oxide impregnated CNTs, zinc oxide impregnated CNTs and raw CNTs respectively. Figure 5.6 indicates that raw CNTs and zinc oxide impregnated CNTs have good fitting with intraparticle diffusion model for adsorption of toluene with R^2 as 91% and 94%, respectively,. Iron oxide impregnated CNTs and aluminum oxide impregnated CNTs have very poor fitting with this model. R^2 was only 61% and 35% for iron and aluminum oxide impregnated CNTs, respectively.

According to analysis of data fitting with three models, it is clear from values of regression coefficient that pseudo second order model is only best empirical representative model for adsorption of toluene on provided adsorbents. It can also be noticed form Table 5.2 that values of adsorption capacity calculated using this model ($q_{e,calculated}$) are more close to experimentally calculated values of adsorption capacity ($q_{e,exp}$). Values of rate constant of pseudo second order model followed the trend as aluminum oxide impregnated CNTs > zinc oxide impregnated CNTs > iron oxide

impregnated CNTs > raw CNTs. It is known that higher the value of the constant, the equilibrium will be achieved faster. It indicates that aluminum oxide impregnated CNTs achieved fastest equilibrium followed by zinc oxide impregnated CNTs, iron oxide impregnated CNTs and then finally raw CNTs.

Intraparticle diffusion model was found to have a good fit for raw CNTs and zinc oxide impregnated CNTs but it does not pass through origin so, intraparticle diffusion cannot be predicted as a sole representative to control the adsorption of toluene molecules.

Pseudo first order model fit for toluene

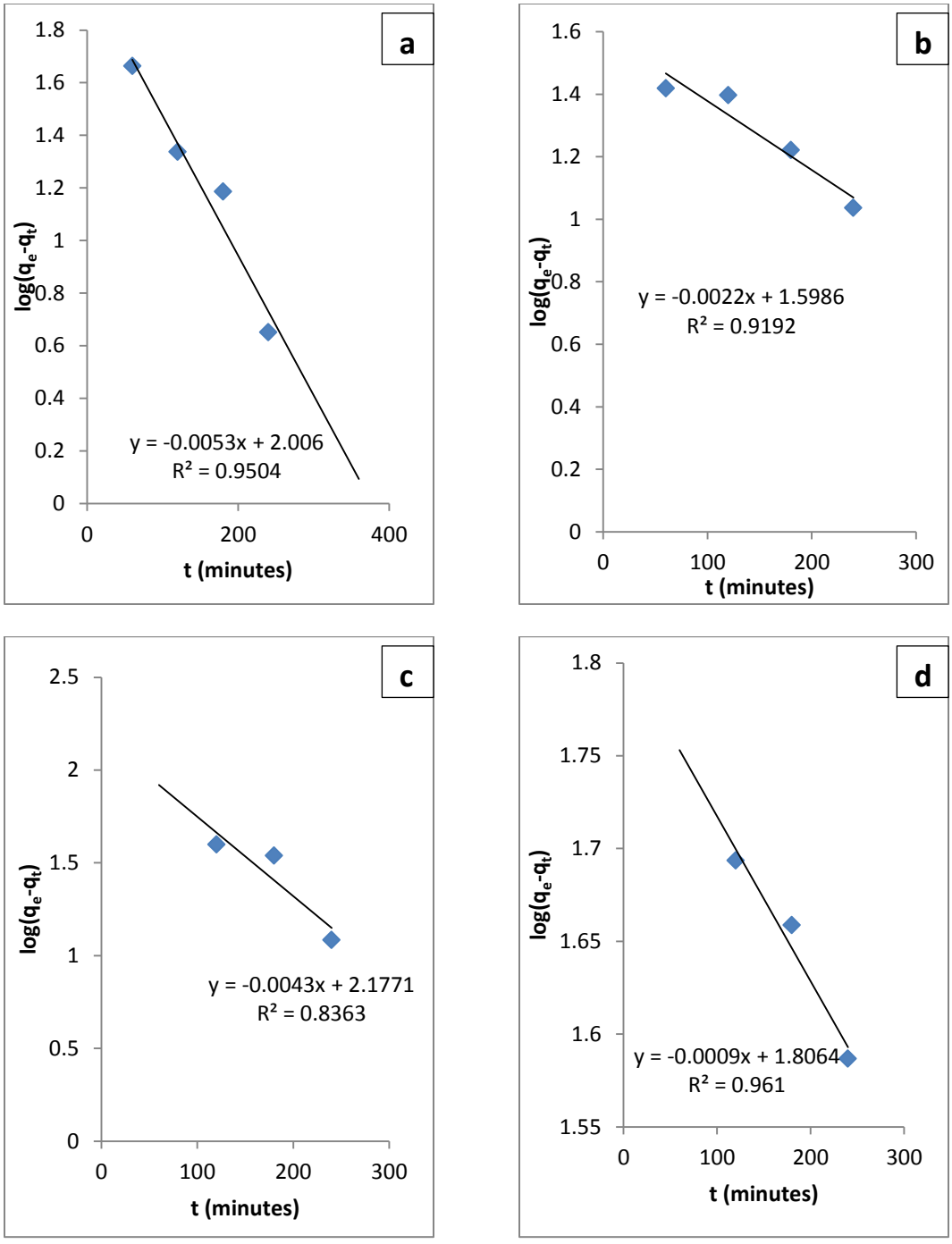

Figure 5-4: Pseudo first order model fitting for toluene adsorption using a) raw CNTs b) zinc oxide impregnated CNTs c) iron oxide impregnated CNTs d) alumina impregnated CNTs

Pseudo second order model fit for toluene

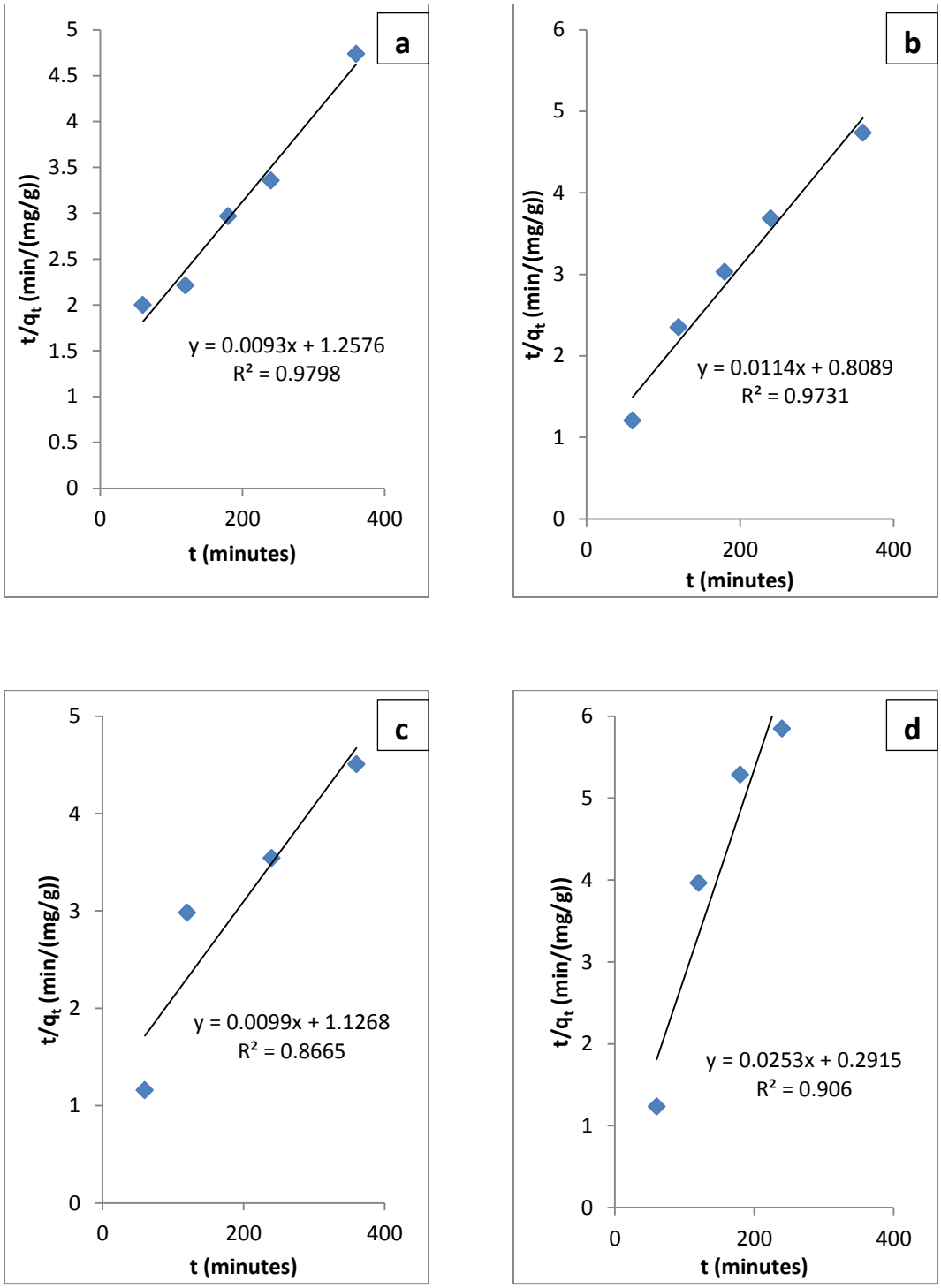

Figure 5-5: Pseudo second order model fitting for toluene adsorption using a) raw CNTs b) zinc oxide impregnated CNTs c) iron oxide impregnated CNTs d) alumina impregnated CNTs

Intraparticle diffusion model fit for toluene

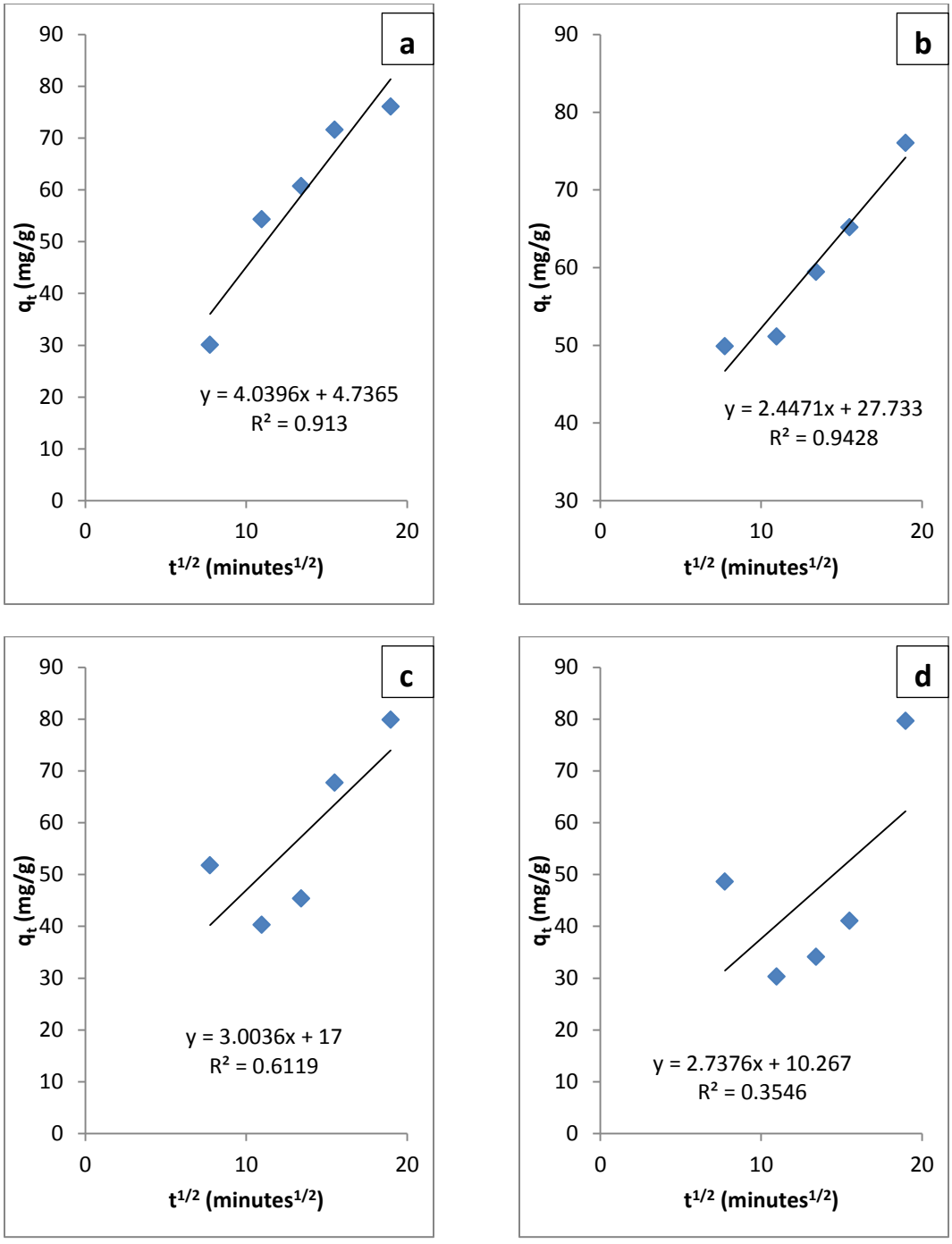

Figure 5-6: Intraparticle diffusion model fitting for toluene adsorption using a) raw CNTs b) zinc oxide impregnated CNTs c) iron oxide impregnated CNTs d) alumina impregnated CNTs

Table 5-2: Kinetic parameters of toluene absorbed on raw and impregnated CNTs

Adsorbents	Model	Parameters	Adsorbate
Raw CNTs	**Pseudo first order**	$k_1(min^{-1})$	5.300E-03
		$q_{e,calculated}$ (mg/g)	101.391
		R^2	0.950
	Pseudo second order	k_2 (g mg^{-1} min^{-1})	6.877E-05
		$q_{e,calculated}$ (mg/g)	107.527
		R^2	0.980
	Intraparticle diffusion	k_{id} (g mg^{-1} $min^{-0.5}$)	4.040
		C	4.737
		R^2	0.913
Zinc oxide impregnated CNTs	**Pseudo first order**	$k_1(min^{-1})$	2.200E-03
		$q_{e,calculated}$ (mg/g)	39.683
		R^2	0.919
	Pseudo second order	k_2 (g mg^{-1} min^{-1})	1.607E-04
		$q_{e,calculated}$ (mg/g)	87.719
		R^2	0.973
	Intraparticle diffusion	k_{id} (g mg^{-1} $min^{-0.5}$)	2.447
		C	27.733
		R^2	0.943

Iron oxide impregnated CNTs	**Pseudo first order**	$k_1(min^{-1})$	4.300E-03
		$q_{e,calculated}$ (mg/g)	150.349
		R^2	0.836
	Pseudo second order	k_2 (g mg^{-1} min^{-1})	8.698E-05
		$q_{e,calculated}$ (mg/g)	101.010
		R^2	0.867
	Intraparticle diffusion	k_{id} (g mg^{-1} $min^{-0.5}$)	3.004
		C	17.000
		R^2	0.612
Aluminum oxide impregnated CNTs	**Pseudo first order**	$k_1(min^{-1})$	9.000E-04
		$q_{e,calculated}$ (mg/g)	64.032
		R^2	0.961
	Pseudo second order	k_2 (g mg^{-1} min^{-1})	2.196E-03
		$q_{e,calculated}$ (mg/g)	39.526
		R^2	0.906
	Intraparticle diffusion	k_{id} (g mg^{-1} $min^{-0.5}$)	2.738
		C	10.267
		R^2	0.913

5.1.3 p-Xylene kinetic models fit

Figures 5.7, 5.8 and 5.9 demonstrate the fitting of experimental data with linearized form of pseudo first order, pseudo second order and intraparticle diffusion model for p-xylene using different adsorbents. Values of R^2 and other parameters calculated are presented in Table 5.3.

From Figure 5.7, it can be observed that all adsorbents have best fit using pseudo first order model with adsorption data of p-xylene. Value of R^2 was 94% for both raw and zinc oxide impregnated CNTs, while it was 97% for aluminum oxide impregnated CNTs and 99% for iron oxide impregnated CNTs. It was also seen from Figure 5.8 that all adsorbents have best fit using pseudo second order model for adsorption of p-xylene and values of R^2 were 99% to almost 100%. Adsorption data of p-xylene was also found to fit best with intraparticle diffusion model as seen in Figure 5.9 that R^2 was 88% for raw CNTs, 96% for iron oxide impregnated CNTs and 97% and 98% for zinc oxide impregnated CNTs and aluminum oxide impregnated CNTs, respectively.

It was found form fitting of data that all three models have good fit for adsorption of p-xylene on all adsorbents. Although, intraparticle diffusion model have best fit with experimental data but it does not passes through origin so, it can describe the adsorption behavior but does not completely control it. From pseudo first order and pseudo second order model, pseudo second order model showed highest R^2 values from 99.59 to 99.89%. It can also be seen form Table 5.3 that calculated adsorption capacity using second order model fit ($q_{e,calculated}$) was more close to experimental adsorption capacity ($q_{e,exp}$) for all adsorbents. The values of second order rate constant were in order of zinc oxide impregnated CNTs > raw CNTs > aluminum oxide impregnated CNTs > iron oxide

impregnated CNTs. Equilibrium will be achieved faster for an adsorbent with higher value of rate constant. Based on this rule, zinc oxide impregnated CNTs reached to equilibrium faster followed by raw CNTs and then aluminum oxide impregnated CNTs and at last iron oxide impregnated CNTs achieved equilibrium for adsorption of p-xylene.

Finally, although intraparticle diffusion was involved in adsorption but pseudo second order model was selected as best empirical model to describe the adsorption of p-xylene using all adsorbents.

Pseudo first order model fit for p-xylene

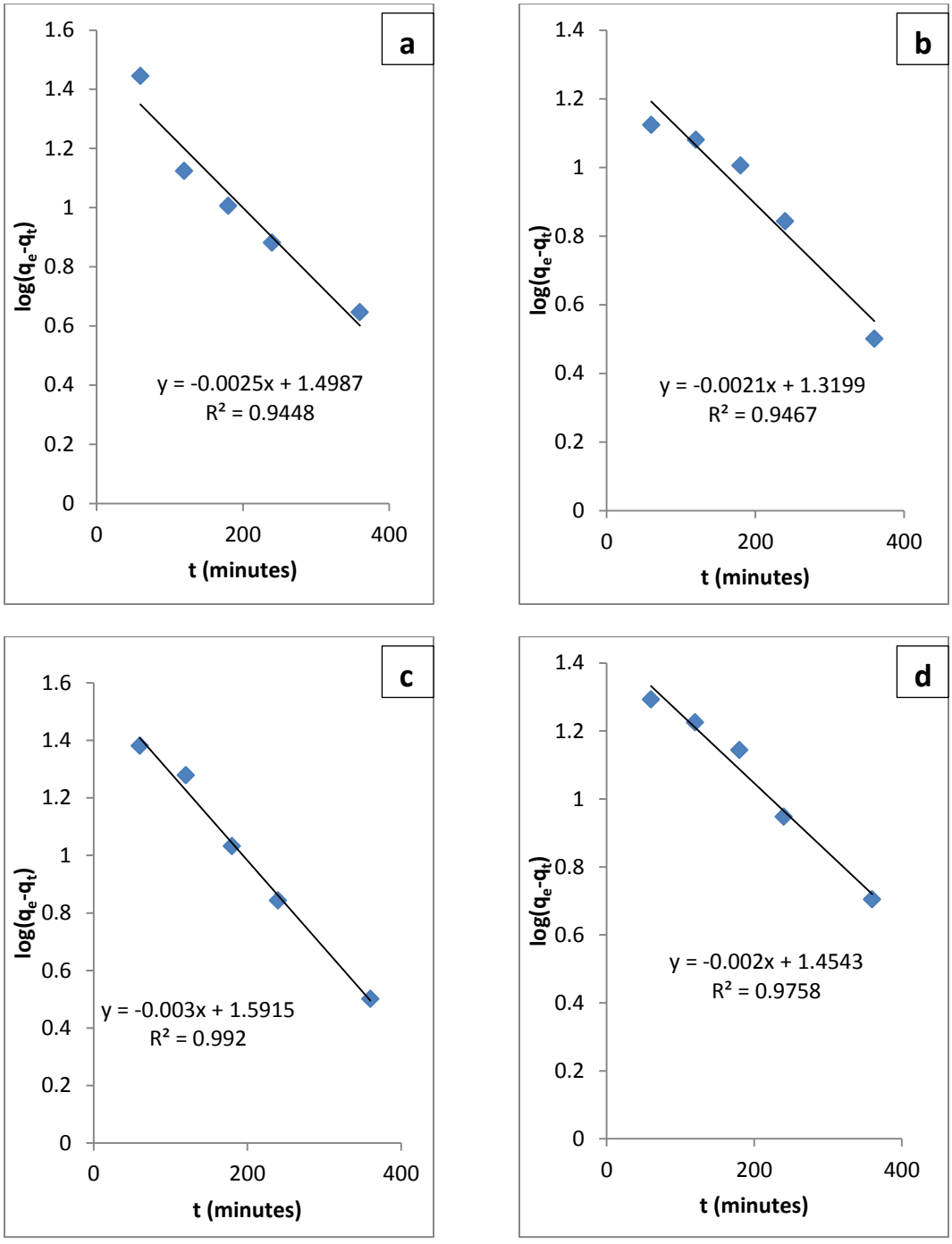

Figure 5-7: Pseudo first order model fitting for p-xylene adsorption using a) raw CNTs b) zinc oxide impregnated CNTs c) iron oxide impregnated CNTs d) alumina impregnated CNTs

Pseudo second order model fit for p-xylene

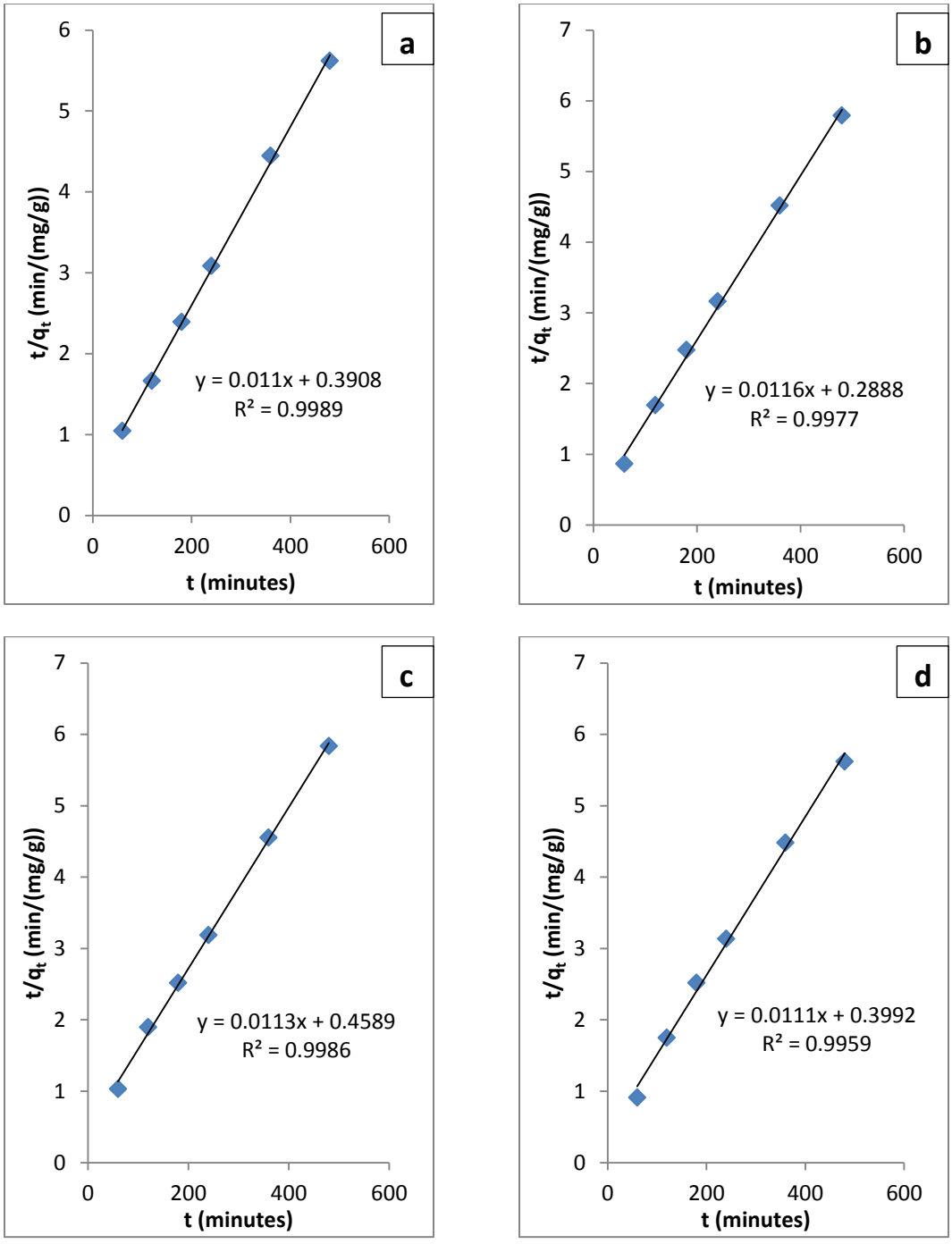

Figure 5-8: Pseudo second order model fitting for p-xylene adsorption using a) raw CNTs b) zinc oxide impregnated CNTs c) iron oxide impregnated CNTs d) alumina impregnated CNTs

Intraparticle diffusion model fit for p-xylene

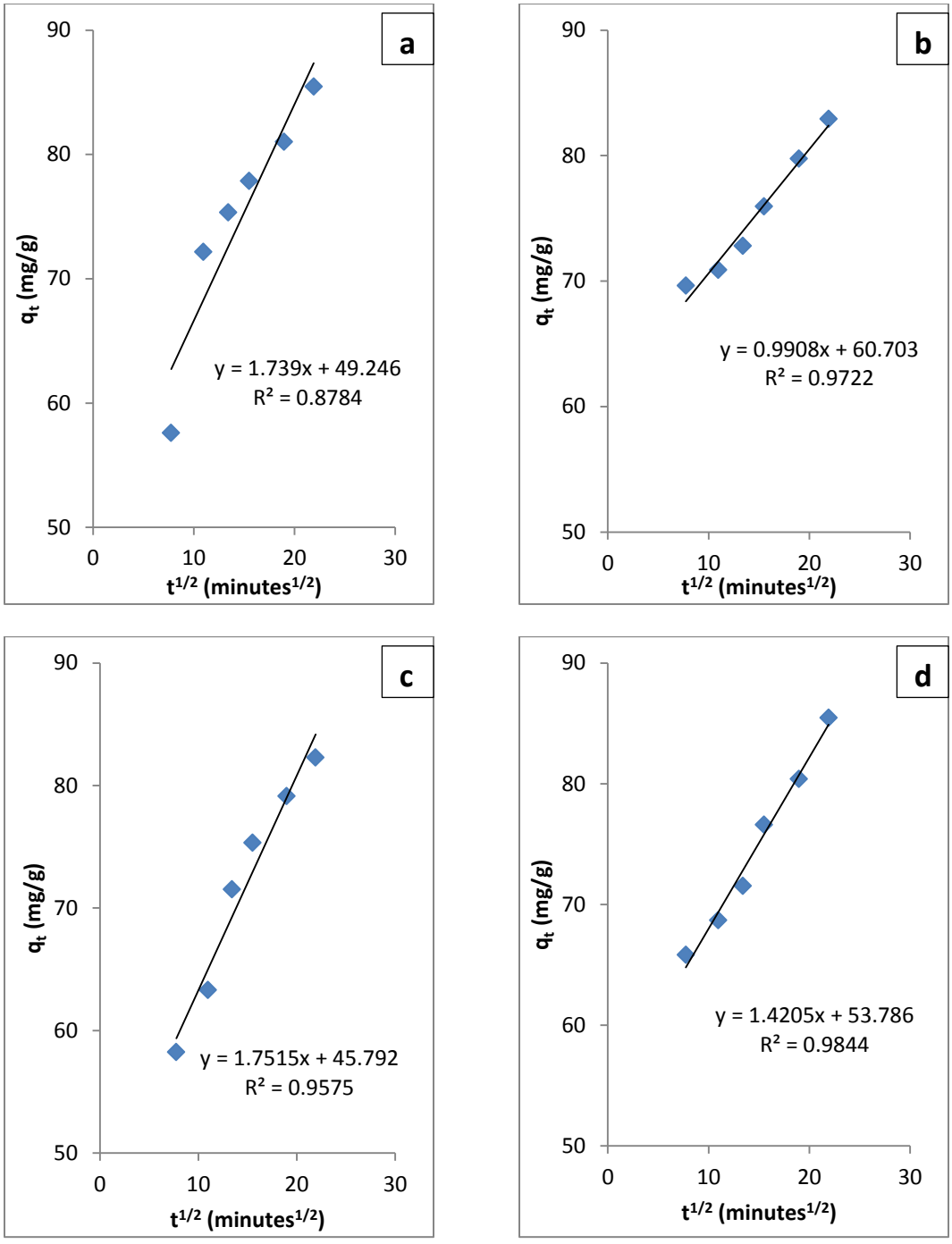

Figure 5-9: Intraparticle diffusion model fitting for p-xylene adsorption using a) raw CNTs b) zinc oxide impregnated CNTs c) iron oxide impregnated CNTs d) alumina impregnated CNTs

Table 5-3: Kinetic parameters of p-xylene absorbed on raw and impregnated CNTs

Adsorbents	Model	Parameters	Adsorbate
Raw CNTs	**Pseudo first order**	$k_1(min^{-1})$	2.500E-03
		$q_{e,calculated}$ (mg/g)	31.528
		R^2	0.945
	Pseudo second order	k_2 (g mg^{-1} min^{-1})	3.100E-04
		$q_{e,calculated}$ (mg/g)	90.909
		R^2	0.999
	Intraparticle diffusion	k_{id} (g mg^{-1} $min^{-0.5}$)	1.739
		C	49.246
		R^2	0.878
Zinc oxide impregnated CNTs	**Pseudo first order**	$k_1(min^{-1})$	2.100E-03
		$q_{e,calculated}$ (mg/g)	20.888
		R^2	0.947
	Pseudo second order	k_2 (g mg^{-1} min^{-1})	4.660E-04
		$q_{e,calculated}$ (mg/g)	86.207
		R^2	0.998
	Intraparticle diffusion	k_{id} (g mg^{-1} $min^{-0.5}$)	0.991
		C	60.703
		R^2	0.972

Iron oxide impregnated CNTs	**Pseudo first order**	$k_1(min^{-1})$	3.000E-03
		$q_{e,calculated}$ (mg/g)	39.039
		R^2	0.992
	Pseudo second order	k_2 (g mg^{-1} min^{-1})	2.780E-04
		$q_{e,calculated}$ (mg/g)	88.496
		R^2	0.999
	Intraparticle diffusion	k_{id} (g mg^{-1} $min^{-0.5}$)	1.752
		C	45.792
		R^2	0.958
Aluminum oxide impregnated CNTs	**Pseudo first order**	$k_1(min^{-1})$	2.000E-03
		$q_{e,calculated}$ (mg/g)	28.464
		R^2	0.976
	Pseudo second order	k_2 (g mg^{-1} min^{-1})	3.090E-04
		$q_{e,calculated}$ (mg/g)	90.090
		R^2	0.996
	Intraparticle diffusion	k_{id} (g mg^{-1} $min^{-0.5}$)	1.421
		C	53.786
		R^2	0.984

5.2 Isotherm Models Fitting

Isotherms model are most important in order to best understand the adsorption mechanism and to determine the amount of adsorbent required for adsorption of specific adsorbate. Langmuir and Freundlich isotherm models were used to fit the experimental data of BTX. In order to further explore the interactions involved in adsorption of BTX on surface of CNTs adsorption data was fitted with D-R model.

5.2.1 Isotherm models fitting for benzene

Figures 5.10, 5.11 and 5.12 show the fitting of benzene adsorption data with Langmuir, Freundlich and D-R models while Table 5.4 provides the values of regression constant and other factors calculated form fitting of data with models. All three models were found to provide good fitting with experimental data for all adsorbents.

Raw CNTs data showed good fitting with all three models. It was found that Langmuir isotherm model was best describing model for raw CNTs. With R^2 of 99.2%, maximum adsorption capacity was found to be 517 mg/g. Freundlich isotherm model heterogeneity parameter 'n' was 1.264 which indicates the favorable adsorption and value of energy calculated using D-R model was found as 0.027 kJ/mole which is indicative of physical adsorption of benzene on surface of CNTs.

Zinc oxide impregnated CNTs showed good fit using all three models with R^2 ranging from 89.2% to 99.9%. It was found that maximum adsorption capacity of benzene calculated using Langmuir model fit was 1215.64 mg/g, while value of Freundlich heterogeneity parameter 'n' was 1.101. For this adsorbent energy calculated was found to

be 0.026 kJ/mole hence providing evidence for physical adsorption of benzene on the surface of zinc oxide impregnated CNTs.

Adsorption experimental data of iron oxide impregnated CNTs was also seen to have a good fit with all three models and value of regression constant was found between 99.3-99.4%. It was observed that maximum adsorption capacity provided using Langmuir model fit was 987.584 mg/g. The value of 'n' using Freundlich isotherm model was 1.119. Adsorption energy calculated using D-R model was 0.025 kJ/mole, hence indicating physical adsorption.

Finally aluminum oxide impregnated CNTs adsorption data was found to fit best using all Langmuir, Freundlich and D-R isotherm models with R^2 of 98.2 and 99.9% respectively. The value of heterogeneity parameter was found as 0.943 that was close enough to 1 hence providing adsorption. The value of adsorption energy was calculated using D-R model fit and was indicating physical adsorption phenomena with a value 0.23 kJ/mole.

Values of constants for Langmuir (K_L) and Freundlich (K_F) models followed an order of raw CNTs > zinc oxide impregnated CNTs > iron oxide impregnated CNTs > aluminum oxide impregnated CNTs.

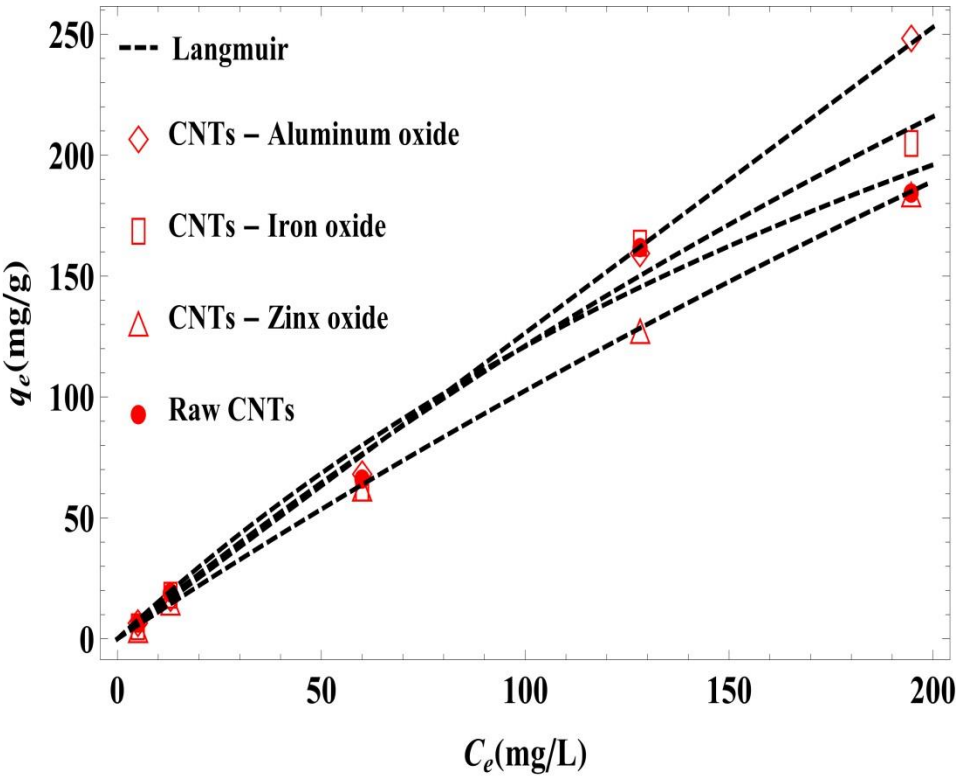

Figure 5-10: Isotherm model fit for benzene adsorption on raw and impregnated CNTs

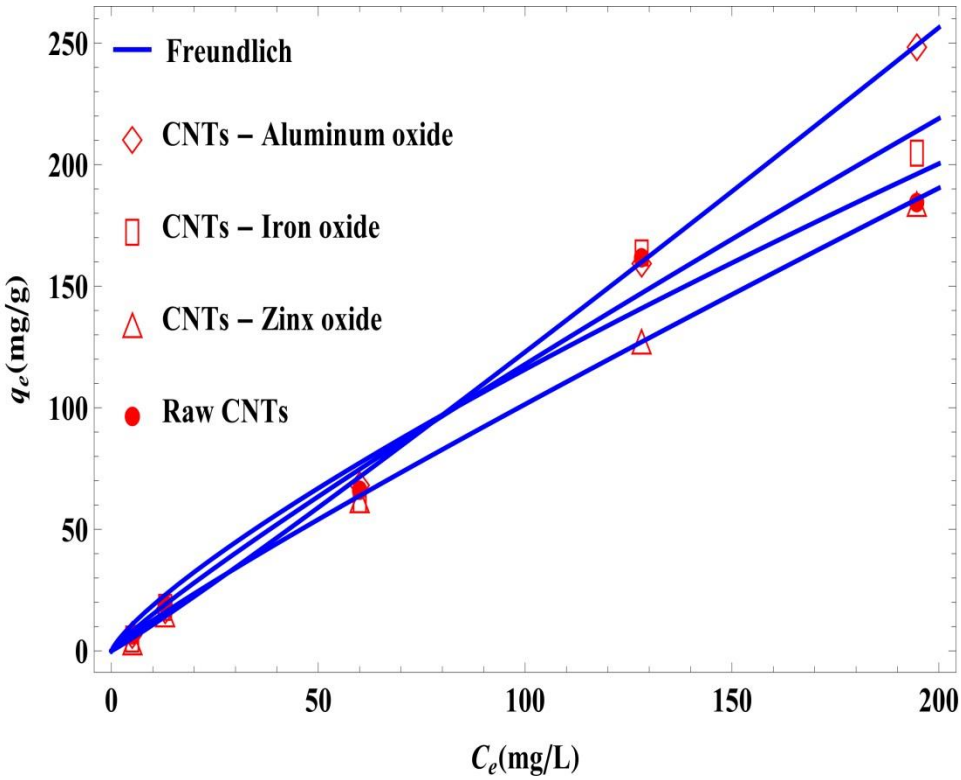

Figure 5-11: Freundlich isotherm model fit for benzene adsorption on raw and impregnated CNTs

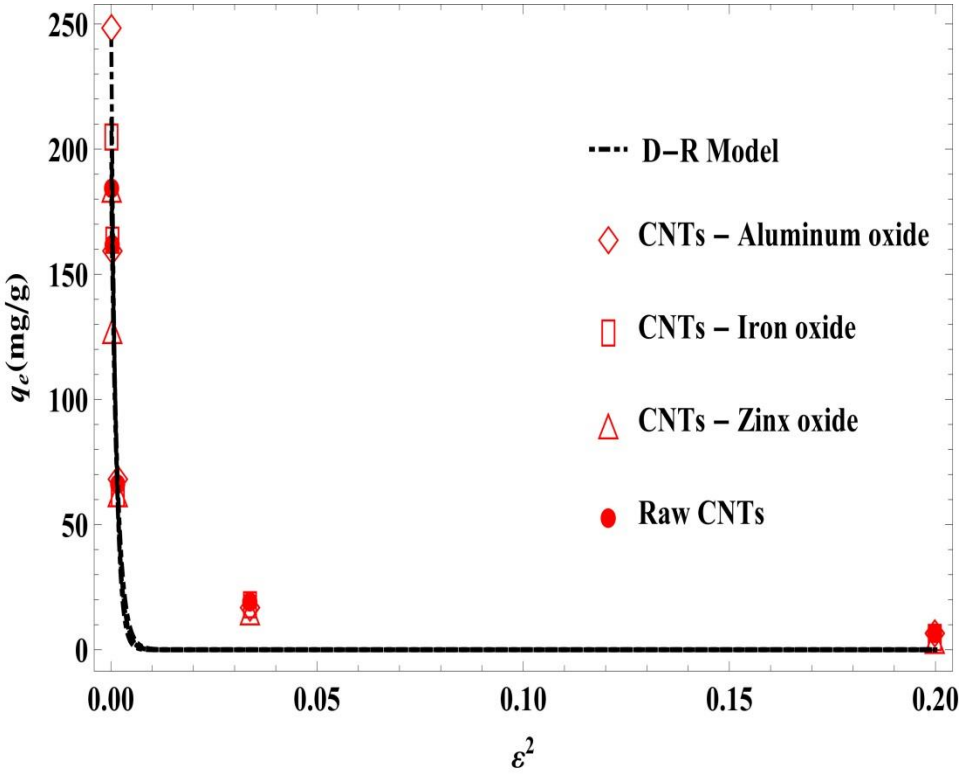

Figure 5-12: D-R isotherm model fit for benzene adsorption on raw and impregnated CNTs

Table 5-4: Isotherm models fitting parameters for adsorption of benzene using different adsorbents

Adsorbents	Model	Parameters	Values
Raw CNTs	**Langmuir**	K_L(L/mg)	0.003
		q_m (mg/g)	517.269
		R^2	0.992
	Freundlich	K_F (L/mg)	3.027
		n	1.264
		R^2	0.989
	Dubinin-Radushkevish (D-R)	q_m (mg/g)	207.209
		B ($mole^2/kJ^2$)	671.452
		E_a (kJ/mole)	0.027
		R^2	0.993
Zinc oxide impregnated CNTs	**Langmuir**	K_L(L/mg)	9.219E-04
		q_m (mg/g)	1215.640
		R^2	1.000
	Freundlich	K_F (L/mg)	1.548
		n	1.101
		R^2	1.000
	Dubinin-Radushkevish (D-R)	q_m (mg/g)	192.751
		B ($mole^2/kJ^2$)	731.321
		E_a (kJ/mole)	0.026
		R^2	0.984

Iron oxide impregnated CNTs	**Langmuir**	K_L (L/mg)	1.399E-03
		q_m (mg/g)	987.584
		R^2	0.994
	Freundlich	K_F (L/mg)	1.926
		n	1.119
		R^2	0.993
	Dubinin-Radushkevish (D-R)	q_m (mg/g)	228.718
		B ($mole^2/kJ^2$)	789.545
		E_a (kJ/mole)	0.025
		R^2	0.994
Aluminum oxide impregnated CNTs	**Langmuir**	K_L (L/mg)	4.830E-07
		q_m (mg/g)	2.619E+06
		R^2	0.999
	Freundlich	K_F (L/mg)	0.932
		n	0.943
		R^2	1.000
	Dubinin-Radushkevish (D-R)	q_m (mg/g)	266.510
		B ($mole^2/kJ^2$)	932.835
		E_a (kJ/mole)	0.232
		R^2	0.981

5.2.2 Isotherm models fitting for toluene

Figures 5.13, 5.14 and 5.15 demonstrate the results for fitting of toluene adsorption data with Langmuir, Freundlich and D-R isotherm models. The results of determination co-efficient (R^2) and various parameters are tabulated in Table 5.5. It is observed that values of R^2 vary from 87.8% to 98.1% hence providing good fit with experimental data for various adsorbents.

Raw CNTs have good fit with all three models but Freundlich isotherm model best describe the adsorption of toluene on raw CNTs with R^2 of 97.7%. Value of heterogeneity parameter 'n' is 0.429, which indicates favorable adsorption. Furthermore, value of adsorption energy was calculated using D-R model fitting and was found to be 0.031 kJ/mole, hence providing evidence of physical adsorption of toluene on surface of CNTs.

Zinc oxide impregnated CNTs were found to have good fit with Freundlich and D-R model only with regression co-efficient of 96.5% and 96.4%, respectively. Heterogeneity parameter calculated using Freundlich isotherm model fit was indicative of favorable adsorption having a value of 0.244. D-R isotherm model fitting provided adsorption energy as 0.023 kJ/mole, hence indicating physical adsorption of toluene.

Toluene adsorption data using iron oxide impregnated CNTs as adsorbent, was also found to have good fit with Freundlich and D-R models only. Values of 'n' calculated from Freundlich model fit was 0.395 while 'E_a' calculated using D-R model was 0.027 kJ/mole. Value of 'n' presented the favorable adsorption of toluene while, value of 'E_a' provided the proof of physical adsorption.

Data of aluminum oxide impregnated CNTs also showed best fit with Freundlich and D-R model only. Heterogeneity parameter calculated from Freundlich isotherm model fitting was 0.478. This value of ‘n’ provided strong adsorption affinity of toluene towards used adsorbent. D-R model fit was also used to calculate energy for adsorption of one mole of toluene on aluminum oxide impregnated CNTs which was 0.029 kJ/mole. This value showed that only physical interactions were involved in adsorption of toluene.

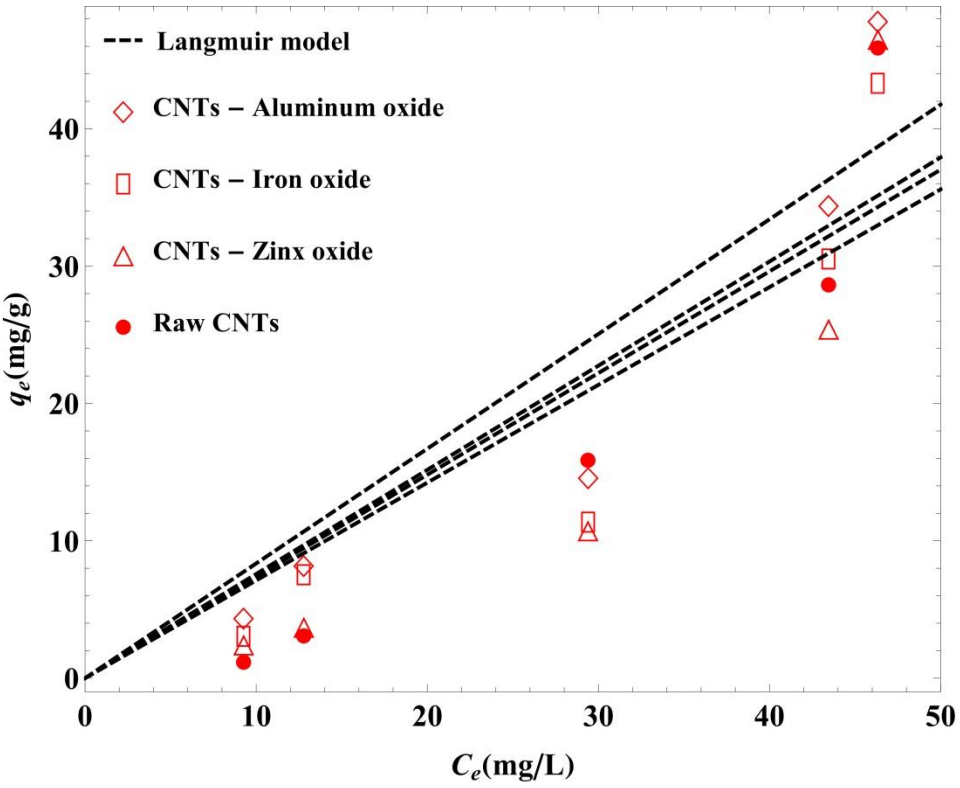

Figure 5-13: Langmuir isotherm model fitting for toluene using raw and impregnated CNTs

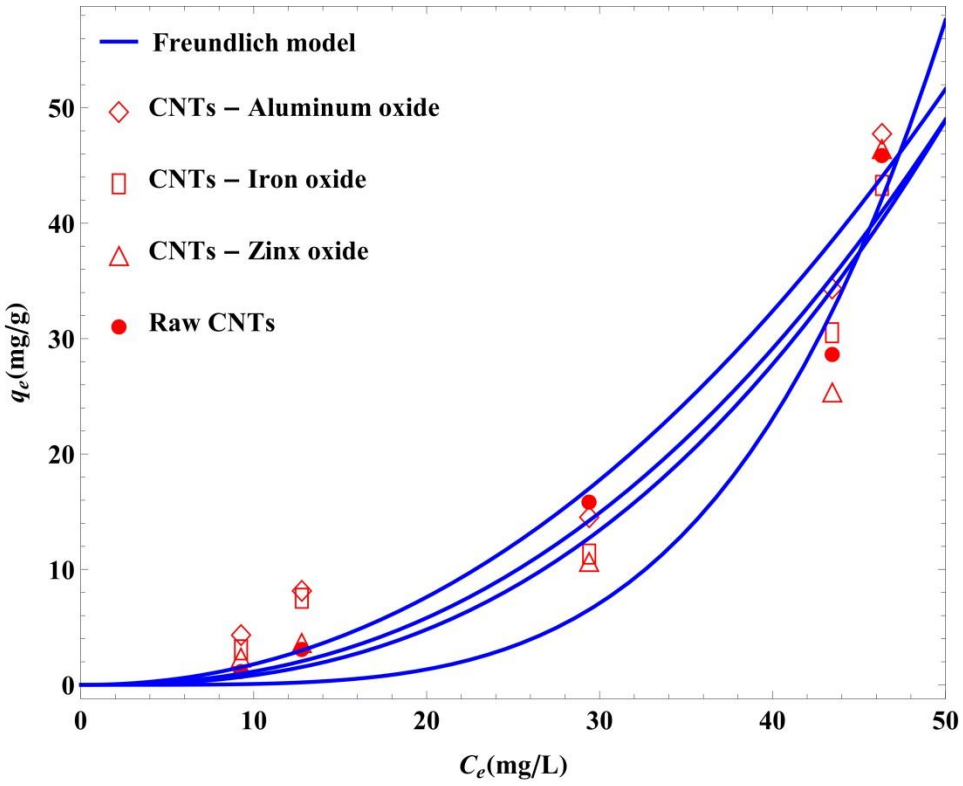

Figure 5-14: Freundlich isotherm model fitting for toluene using raw and impregnated CNTs

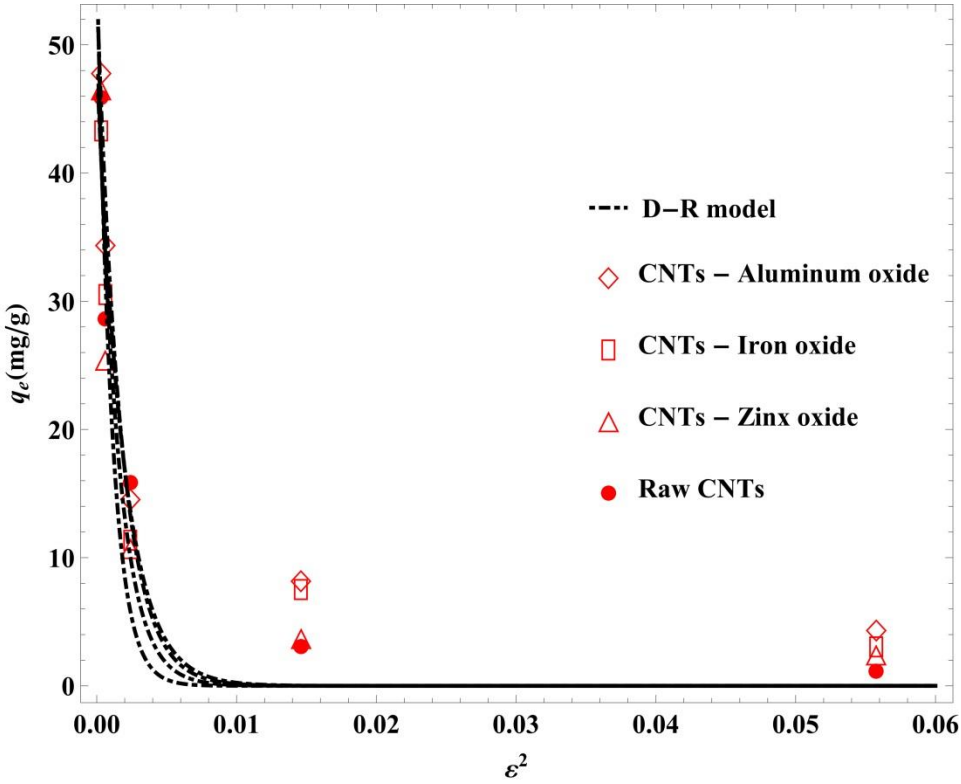

Figure 5-15: D-R isotherm model fitting for toluene using raw and impregnated CNTs

Table 5-5: Isotherm models fitting parameters for adsorption of toluene using different adsorbents

Adsorbents	Model	Parameters	Values
Raw CNTs	**Langmuir**	K_L (L/mg)	2.109E-10
		q_m (mg/g)	3.596E+09
		R^2	0.922
	Freundlich	K_F (L/mg)	5.410E-03
		n	0.429
		R^2	0.977
	Dubinin-Radushkevish (D-R)	q_m (mg/g)	48.587
		B ($mole^2/kJ^2$)	528.036
		E_a (kJ/mole)	0.031
		R^2	0.974
Zinc oxide impregnated CNTs	**Langmuir**	K_L (L/mg)	1.991E-07
		q_m (mg/g)	3.575E+06
		R^2	0.878
	Freundlich	K_F (L/mg)	6.089E-06
		n	0.244
		R^2	0.965
	Dubinin-Radushkevish (D-R)	q_m (mg/g)	57.024
		B ($mole^2/kJ^2$)	948.953
		E_a (kJ/mole)	0.023
		R^2	0.964

Iron oxide impregnated CNTs	**Langmuir**	K_L (L/mg)	2.501E-07
		qm (mg/g)	2.961E+06
		R^2	0.931
	Freundlich	K_F (L/mg)	2.415E-03
		n	0.395
		R^2	0.978
	Dubinin-Radushkevish (D-R)	q_m (mg/g)	50.895
		B ($mole^2/kJ^2$)	674.540
		E_a (kJ/mole)	0.027
		R^2	0.972
Aluminum oxide impregnated CNTs	**Langmuir**	K_L (L/mg)	2.690E-10
		q_m (mg/g)	3.105E+09
		R^2	0.947
	Freundlich	K_F (L/mg)	1.450E-02
		n	0.478
		R^2	0.981
	Dubinin-Radushkevish (D-R)	q_m (mg/g)	54.373
		B ($mole^2/kJ^2$)	585.477
		E_a (kJ/mole)	0.029
		R^2	0.971

5.2.3 Isotherm models fitting for p-xylene

Figures 5.16, 5.17 and 5.18 represent the fitting of p-xylene adsorption data with Langmuir, Freundlich and D-R isotherm models, respectively while Table 5.6 provides values for regression co-efficient of fitting and other parameters obtained from fitting.

Raw CNTs were proved to have a good efficiency for adsorption of p-xylene and it can be seen that data of p-xylene adsorption best fits with two models; Freundlich and D-R. Although Langmuir was also found to give a good fit but parameters calculated are not fine. So, Freundlich model was considered to best describe the data and value of heterogeneity parameter 'n' was found to be 0.975 which is close to unity hence indicating favorable adsorption of p-xylene on a homogenous surface. D-R model fit provided the value of adsorption energy 'E_a' was 0.037 kJ/mole, hence indicating physical adsorption of p-xylene molecules on the surface of CNTs.

Zinc oxide impregnated CNTs data fit provided good fit with all three models but best results were obtained with Freundlich isotherm model with R^2 of 99.9%. Heterogeneity parameter 'n' was found as 0.958, again indicating favorable and homogenous adsorption of p-xylene molecules. E_a calculated from D-R model fit was 0.036 kJ/mole, which showed physical adsorption of p-xylene.

Adsorption of p-xylene using iron oxide impregnated CNTs was also found to have a good fit using all three models. But best model fitting was obtained using Freundlich isotherm model. Heterogeneity parameter showed favorable adsorption with a value of 0.904. D-R model fit was also good to describe this phenomenon and value of 'E_a' was

0.034. So, it confirmed that physical adsorption of p-xylene took place on the surface of iron oxide impregnated CNTs.

Aluminum oxide impregnated CNTs were found to provide good fitting with all three models. It was realized that Freundlich model was best to describe the adsorption phenomenon with this adsorbent. Heterogeneity parameter indicated favorable adsorption with value of '0.949'. Adsorption energy for this phenomenon was obtained from fit of D-R model, with a value of 0.035 kJ/mole and it showed that physical adsorption took place here.

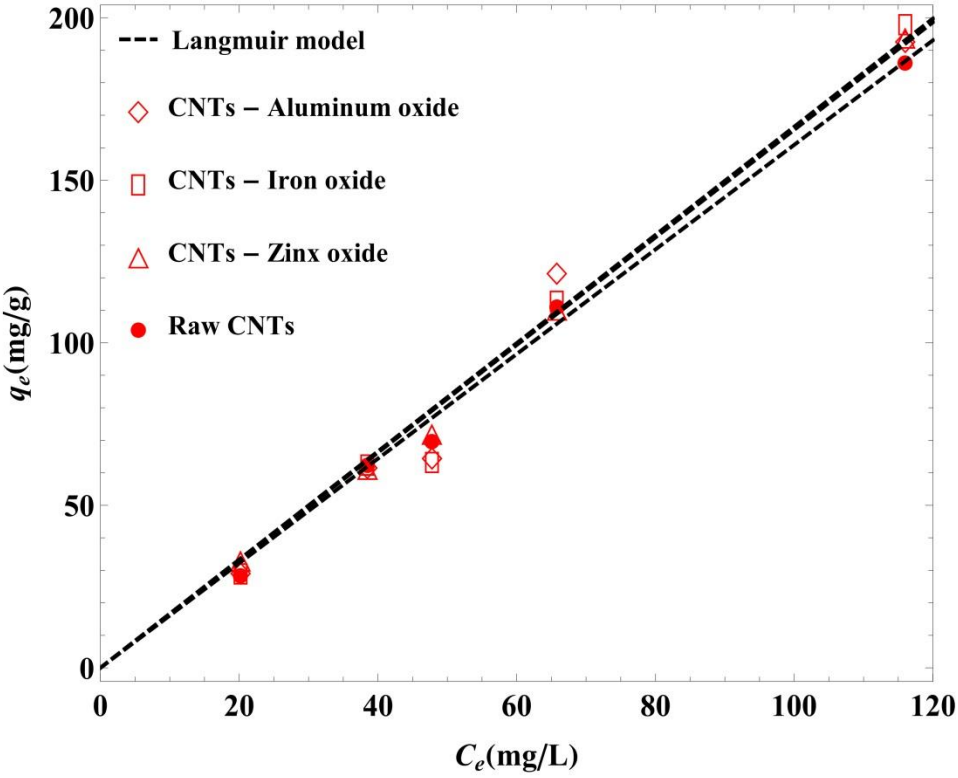

Figure 5-16: Langmuir isotherm model fitting for p-xylene using raw and impregnated CNTs

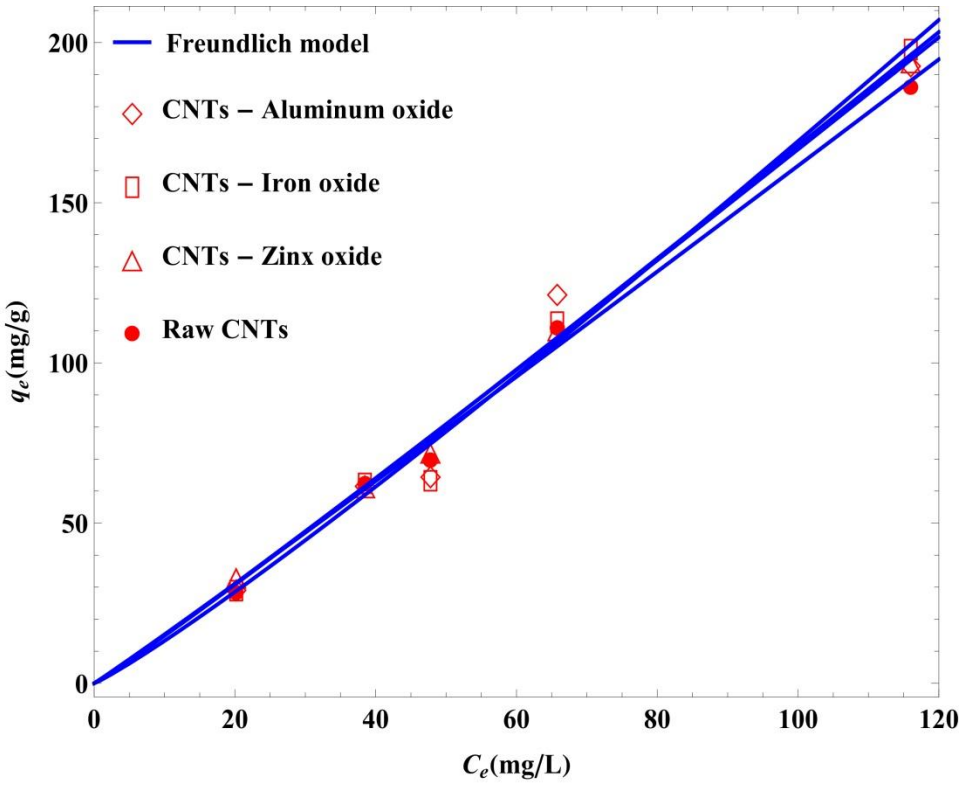

Figure 5-17: Freundlich isotherm model fitting for p-xylene using raw and impregnated CNTs

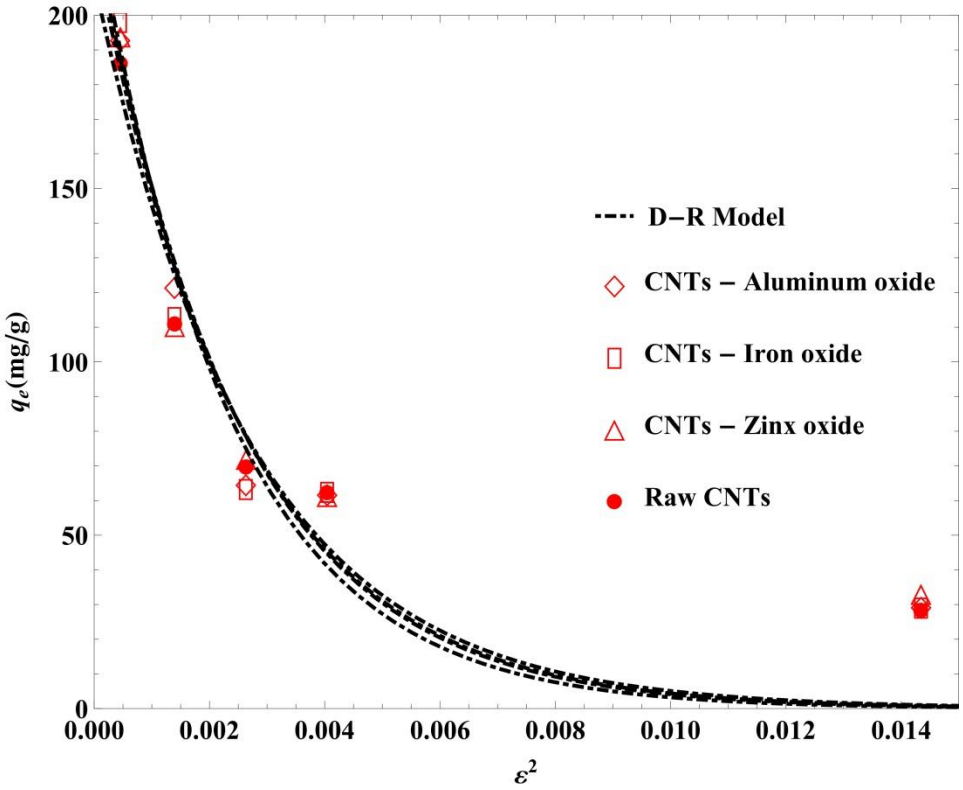

Figure 5-18: D-R isotherm model fitting for p-xylene using raw and impregnated CNTs

Table 5-6: Parameters of isotherm models for adsorption of p-xylene using different adsorbents

Adsorbents	Model	Parameters	Values
Raw CNTs	**Langmuir**	K_L (L/mg)	1.937E-09
		q_m (mg/g)	8.306E+08
		R^2	0.998
	Freundlich	K_F (L/mg)	1.438
		n	0.975
		R^2	0.999
	Dubinin-Radushkevish (D-R)	q_m (mg/g)	210.214
		B ($mole^2/kJ^2$)	372.539
		E_a (kJ/mole)	0.037
		R^2	0.976
Zinc oxide impregnated CNTs	**Langmuir**	K_L (L/mg)	7.408E-07
		q_m (mg/g)	2.234E+06
		R^2	0.999
	Freundlich	K_F (L/mg)	1.362
		n	0.958
		R^2	0.999
	Dubinin-Radushkevish (D-R)	q_m (mg/g)	220.178
		B ($mole^2/kJ^2$)	391.730
		E_a (kJ/mole)	0.036
		R^2	0.971

Iron oxide impregnated CNTs	**Langmuir**	K_L (L/mg)	3.338E-07
		q_m (mg/g)	4.988E+06
		R^2	0.995
	Freundlich	K_F (L/mg)	1.035
		n	0.904
		R^2	0.997
	Dubinin-Radushkevish (D-R)	q_m (mg/g)	230.295
		B ($mole^2/kJ^2$)	426.679
		E_a (kJ/mole)	0.034
		R^2	0.972
Aluminum oxide impregnated CNTs	**Langmuir**	K_L (L/mg)	8.367E-10
		q_m (mg/g)	1.988E+09
		R^2	0.994
	Freundlich	K_F (L/mg)	1.312
		n	0.949
		R^2	0.994
	Dubinin-Radushkevish (D-R)	q_m (mg/g)	224.465
		B ($mole^2/kJ^2$)	399.622
		E_a (kJ/mole)	0.035
		R^2	0.977

CHAPTER 6

CONCLUSION AND RECOMMENDATIONS

The following highlights the removal of BTX from aqueous solution using both raw and impregnated CNTs.

6.1 Conclusions

The following can be concluded form the work.

- Raw and metal (Zn, Fe, Al) oxide nanoparticles impregnated CNTs were applied for removal of BTX from water. Various parameters were optimized for the adsorption phenomena.
- Contact time and adsorbent dosage were found to increase the adsorption of all three components form water using both raw and impregnated CNTs.
- pH was observed to have no significant effect on removal efficiency of benzene in the range of 5 to 8.
- Maximum removal of benzene was achieved as 71% in 240 minutes using aluminum oxide impregnated CNTs while, benzene initial concentration was 1 ppm, pH was 6.0, shaking speed was 200 rpm and adsorbent dosage was 50 mg at room temperature for all samples.
- 63% removal of toluene was achieved in 360 minutes using both raw and impregnated CNTs while, initial concentration of toluene was 100 ppm, initial pH

of solution was 6.0, shaking speed was 200 rpm and adsorbent dosage was 50 mg for all samples at room temperature.

- Highest removal of p-xylene was 89% which has been achieved using raw CNTs and aluminum oxide impregnated CNTs as an adsorbent in 480 minutes. For all samples, initial concentration of p-xylene, pH, shaking speed and adsorbent dosage were 100 ppm, 6.0, 200 rpm and 50 mg for all samples at room temperature.
- Kinetics and isotherms model fitting was carried out to understand the phenomena of BTX adsorption on CNTs.
- Adsorption kinetic data was used to fit with kinetics models such as pseudo first order, pseudo second order and intraparticle diffusion model.
- The results indicated that pseudo first order model was best to describe the adsorption phenomena of benzene using raw and metal oxide impregnated CNTs.
- For toluene, pseudo first order and second order models had promising fit with adsorption data but determination co-efficient and kinetics parameters indicated that best match was acquired using pseudo second order model.
- In case of p-xylene, although all three models were found to fit good with experimental data but determination coefficient and other factors revealed that pseudo second order model was best for describing the adsorption phenomena of p-xylene.
- In order to further investigate the adsorption phenomena, adsorption capacity and adsorption energy data was fit with Langmuir, Freundlich and Dubinin-Radushkevich (D-R) isotherm models.

- Langmuir isotherm model was found to best describe the adsorption of benzene using both raw and impregnated CNTs with adsorption capacity of 517 mg/g for raw CNTs, for zinc oxide impregnated CNTs and for iron oxide impregnated CNTs calculated using Langmuir model fit.
- Toluene adsorption data was found to be best described using Freundlich and D-R isotherm models. Dimensionless parameter ‘n’ indicated favorable homogenous adsorption with a value of 0.429 for raw CNTs, 0.244 for zinc oxide impregnated CNTs, 0.395 for iron oxide impregnated CNTs and 0.478 for aluminum oxide impregnated CNTs.
- Freundlich and D-R isotherm models best described p-xylene adsorption and the values of adsorption energy calculated using D-R model fit required for adsorption of 1 mole of p-xylene on were 0.037 kJ/mole for raw CNTs, 0.036 kJ/mole for zinc oxide impregnated CNTs, 0.034 kJ/mole for iron oxide impregnated CNTs and finally 0.035 kJ/mole for aluminum oxide impregnated CNTs. These values indicated the physical adsorption of p-xylene on all adsorbents.

6.2 Recommendations

Some recommendations for future work are as follows.

- All adsorbents were used once in this study, material should be recycled and used again to check the stability.
- The materials used for adsorption of BTX in batch process were found to have good removal efficiency and adsorption capacity. These materials should be tested in continuous process.
- Carbon nanotubes were impregnated with different metal oxide nanoparticles in this study, it is recommended to use metal carbide and metal nitride impregnated CNTs.

References

[1] John J. McKetta Jr, Encyclopedia of Chemical Processing and Design: Volume 67 - Water and Wastewater Treatment: Protective Coating Systems to Zeolite, CRC Press, 1999. http://books.google.com/books?id=uDuCw37SaUMC&pgis=1 (accessed October 12, 2014).

[2] J.A. Kent, Kent and Riegel's Handbook of Industrial Chemistry and Biotechnology: Vol. 1, Springer Science & Business Media, 2010. http://books.google.com/books?id=AYjFoLCNHYUC&pgis=1 (accessed October 12, 2014).

[3] C. Kent, Basics of Toxicology, John Wiley & Sons, 1998. http://books.google.com/books?id=VEUlWz4vQssC&pgis=1 (accessed December 13, 2014).

[4] X. Qu, P.J.J. Alvarez, Q. Li, Applications of nanotechnology in water and wastewater treatment., Water Res. 47 (2013) 3931–3946. doi:10.1016/j.watres.2012.09.058.

[5] X. Liu, M. Wang, S. Zhang, B. Pan, Application potential of carbon nanotubes in water treatment: A review, J. Environ. Sci. 25 (2013) 1263–1280. doi:10.1016/S1001-0742(12)60161-2.

[6] O. US EPA, Drinking Water Contaminants, (n.d.). http://water.epa.gov/drink/contaminants/#Organic (accessed October 12, 2014).

[7] M. Farhadian, D. Duchez, C. Vachelard, C. Larroche, BTX removal from polluted water through bioleaching processes., Appl. Biochem. Biotechnol. 151 (2008) 295–306. doi:10.1007/s12010-008-8189-0.

[8] I. Ali, V.K. Gupta, Advances in water treatment by adsorption technology., Nat. Protoc. 1 (2006) 2661–7. doi:10.1038/nprot.2006.370.

[9] S. Iijima, Helical microtubules of graphitic carbon, Nature. 354 (1991) 56–58. doi:10.1038/354056a0.

[10] L. Woods, Ş. Bădescu, T. Reinecke, Adsorption of simple benzene derivatives on carbon nanotubes, Phys. Rev. B. 75 (2007) 155415. doi:10.1103/PhysRevB.75.155415.

[11] A. Star, T.-R. Han, J.-C.P. Gabriel, K. Bradley, G. Grüner, Interaction of Aromatic Compounds with Carbon Nanotubes: Correlation to the Hammett Parameter of the

Substituent and Measured Carbon Nanotube FET Response, Nano Lett. 3 (2003) 1421–1423. doi:10.1021/nl0346833.

[12] S. Agnihotri, J.P.B. Mota, M. Rostam-Abadi, M.J. Rood, Adsorption site analysis of impurity embedded single-walled carbon nanotube bundles, Carbon N. Y. 44 (2006) 2376–2383. doi:10.1016/j.carbon.2006.05.038.

[13] G.U. Sumanasekera, B.K. Pradhan, H.E. Romero, K.W. Adu, P.C. Eklund, Giant Thermopower Effects from Molecular Physisorption on Carbon Nanotubes, Phys. Rev. Lett. 89 (2002) 166801. doi:10.1103/PhysRevLett.89.166801.

[14] X. Ren, C. Chen, M. Nagatsu, X. Wang, Carbon nanotubes as adsorbents in environmental pollution management: A review, Chem. Eng. J. 170 (2011) 395–410. doi:10.1016/j.cej.2010.08.045.

[15] H.-H. Cho, B.A. Smith, J.D. Wnuk, D.H. Fairbrother, W.P. Ball, Influence of Surface Oxides on the Adsorption of Naphthalene onto Multiwalled Carbon Nanotubes, Environ. Sci. Technol. 42 (2008) 2899–2905. doi:10.1021/es702363e.

[16] C.-H. Wu, Studies of the equilibrium and thermodynamics of the adsorption of Cu(2+) onto as-produced and modified carbon nanotubes., J. Colloid Interface Sci. 311 (2007) 338–46. doi:10.1016/j.jcis.2007.02.077.

[17] F. Yu, J. Ma, Y. Wu, Adsorption of toluene, ethylbenzene and xylene isomers on multi-walled carbon nanotubes oxidized by different concentration of NaOCl, Front. Environ. Sci. Eng. China. 6 (2011) 320–329. doi:10.1007/s11783-011-0340-4.

[18] O.G. Apul, T. Karanfil, Adsorption of Synthetic Organic Contaminants by Carbon Nanotubes: A Critical Review, Water Res. 68 (2014) 34–55. doi:10.1016/j.watres.2014.09.032.

[19] Y. Liu, J. Zhang, X. Chen, J. Zheng, G. Wang, G. Liang, Insights into the adsorption of simple benzene derivatives on carbon nanotubes, RSC Adv. 4 (2014) 58036–58046. doi:10.1039/C4RA10195B.

[20] W. Chen, L. Duan, L. Wang, D. Zhu, Adsorption of Hydroxyl- and Amino-Substituted Aromatics to Carbon Nanotubes, Environ. Sci. Technol. 42 (2008) 6862–6868. doi:10.1021/es8013612.

[21] K. Yang, W. Wu, Q. Jing, L. Zhu, Aqueous Adsorption of Aniline, Phenol, and their Substitutes by Multi-Walled Carbon Nanotubes, Environ. Sci. Technol. 42 (2008) 7931–7936. doi:10.1021/es801463v.

[22] S. Zhang, T. Shao, S.S.K. Bekaroglu, T. Karanfil, Adsorption of synthetic organic chemicals by carbon nanotubes: Effects of background solution chemistry., Water Res. 44 (2010) 2067–2074. doi:10.1016/j.watres.2009.12.017.

[23] B. Pan, B. Xing, Adsorption Mechanisms of Organic Chemicals on Carbon Nanotubes, Environ. Sci. Technol. 42 (2008) 9005–9013. doi:10.1021/es801777n.

[24] J. Chen, W. Chen, D. Zhu, Adsorption of Nonionic Aromatic Compounds to Single-Walled Carbon Nanotubes: Effects of Aqueous Solution Chemistry, Environ. Sci. Technol. 42 (2008) 7225–7230. doi:10.1021/es801412j.

[25] S. Zhang, T. Shao, S.S.K. Bekaroglu, T. Karanfil, The Impacts of Aggregation and Surface Chemistry of Carbon Nanotubes on the Adsorption of Synthetic Organic Compounds, Environ. Sci. Technol. 43 (2009) 5719–5725. doi:10.1021/es900453e.

[26] S. Zhang, T. Shao, H.S. Kose, T. Karanfil, Adsorption kinetics of aromatic compounds on carbon nanotubes and activated carbons., Environ. Toxicol. Chem. 31 (2012) 79–85. doi:10.1002/etc.724.

[27] B.A. Abussaud, N. Ulkem, D. Berk, G.J. Kubes, Wet Air Oxidation of Benzene, Ind. Eng. Chem. Res. 47 (2008) 4325–4331.

[28] H. Shim, W. Ma, A. Lin, K. Chan, Bio-removal of mixture of benzene, toluene, ethylbenzene, and xylenes/total petroleum hydrocarbons/trichloroethylene from contaminated water, J. Environ. Sci. 21 (2009) 758–763. doi:10.1016/S1001-0742(08)62337-2.

[29] I. Oller, S. Malato, J. a Sánchez-Pérez, Combination of Advanced Oxidation Processes and biological treatments for wastewater decontamination--a review., Sci. Total Environ. 409 (2011) 4141–66. doi:10.1016/j.scitotenv.2010.08.061.

[30] M. Bahmani, V. Bitarafhaghighi, K. Badr, P. Keshavarz, D. Mowla, The photocatalytic degradation and kinetic analysis of BTEX components in polluted wastewater by UV/H 2 O 2 -based advanced oxidation, Desalin. Water Treat. 52 (2013) 3054–3062. doi:10.1080/19443994.2013.797369.

[31] K. Kabra, R. Chaudhary, R.L. Sawhney, Treatment of Hazardous Organic and Inorganic Compounds through Aqueous-Phase Photocatalysis: A Review, Ind. Eng. Chem. Res. 43 (2004) 7683–7696. doi:10.1021/ie0498551.

[32] M.N. Chong, B. Jin, C.W.K. Chow, C. Saint, Recent developments in photocatalytic water treatment technology: a review., Water Res. 44 (2010) 2997–3027. doi:10.1016/j.watres.2010.02.039.

[33] L. Ai, H. Huang, Z. Chen, X. Wei, J. Jiang, Activated carbon/CoFe2O4 composites: Facile synthesis, magnetic performance and their potential application for the removal of malachite green from water, Chem. Eng. J. 156 (2010) 243–249. doi:10.1016/j.cej.2009.08.028.

[34] P. Chingombe, B. Saha, R.J. Wakeman, Sorption of atrazine on conventional and surface modified activated carbons., J. Colloid Interface Sci. 302 (2006) 408–16. doi:10.1016/j.jcis.2006.06.065.

[35] C.R. Altare, R.S. Bowman, L.E. Katz, K. a. Kinney, E.J. Sullivan, Regeneration and long-term stability of surfactant-modified zeolite for removal of volatile organic compounds from produced water, Microporous Mesoporous Mater. 105 (2007) 305–316. doi:10.1016/j.micromeso.2007.04.001.

[36] S.S. Tahir, N. Rauf, Removal of a cationic dye from aqueous solutions by adsorption onto bentonite clay., Chemosphere. 63 (2006) 1842–8. doi:10.1016/j.chemosphere.2005.10.033.

[37] Y. Kalmykova, N. Moona, A.-M. Strömvall, K. Björklund, Sorption and degradation of petroleum hydrocarbons, polycyclic aromatic hydrocarbons, alkylphenols, bisphenol A and phthalates in landfill leachate using sand, activated carbon and peat filters., Water Res. 56 (2014) 246–57. doi:10.1016/j.watres.2014.03.011.

[38] M.A. Atieh, Removal of Chromium (VI) from polluted water using carbon nanotubes supported with activated carbon, Procedia Environ. Sci. 4 (2011) 281–293. doi:10.1016/j.proenv.2011.03.033.

[39] F. Wang, W. Sun, W. Pan, N. Xu, Adsorption of sulfamethoxazole and 17β-estradiol by carbon nanotubes/CoFe2O4 composites, Chem. Eng. J. 274 (2015) 17–29. doi:10.1016/j.cej.2015.03.113.

[40] P. Hadi, K.Y. Yeung, J. Barford, K.J. An, G. McKay, Significance of microporosity on the interaction of phenol with porous graphitic carbon, Chem. Eng. J. 269 (2015) 20–26. doi:10.1016/j.cej.2015.01.090.

[41] P. Weschayanwiwat, O. Kunanupap, J.F. Scamehorn, Benzene removal from waste water using aqueous surfactant two-phase extraction with cationic and anionic surfactant mixtures., Chemosphere. 72 (2008) 1043–8. doi:10.1016/j.chemosphere.2008.03.065.

[42] X. Peng, Y. Li, Z. Luan, Z. Di, H. Wang, B. Tian, et al., Adsorption of 1,2-dichlorobenzene from water to carbon nanotubes, Chem. Phys. Lett. 376 (2003) 154–158. doi:10.1016/S0009-2614(03)00960-6.

[43] O.G. Apul, Q. Wang, Y. Zhou, T. Karanfil, Adsorption of aromatic organic contaminants by graphene nanosheets: comparison with carbon nanotubes and activated carbon., Water Res. 47 (2013) 1648–54. doi:10.1016/j.watres.2012.12.031.

[44] N. Wibowo, L. Setyadhi, D. Wibowo, J. Setiawan, S. Ismadji, Adsorption of benzene and toluene from aqueous solutions onto activated carbon and its acid and heat treated forms: influence of surface chemistry on adsorption., J. Hazard. Mater. 146 (2007) 237–42. doi:10.1016/j.jhazmat.2006.12.011.

[45] C.S. Chuang, M.-K. Wang, C.-H. Ko, C.-C. Ou, C.-H. Wu, Removal of benzene and toluene by carbonized bamboo materials modified with TiO2., Bioresour. Technol. 99 (2008) 954–8. doi:10.1016/j.biortech.2007.03.003.

[46] C.L. Mangun, Z. Yue, J. Economy, S. Maloney, P. Kemme, D. Cropek, Adsorption of Organic Contaminants from Water Using Tailored ACFs, (2001) 2356–2360.

[47] P. a. Gauden, A.P. Terzyk, G. Rychlicki, P. Kowalczyk, K. Lota, E. Raymundo-Pinero, et al., Thermodynamic properties of benzene adsorbed in activated carbons and multi-walled carbon nanotubes, Chem. Phys. Lett. 421 (2006) 409–414. doi:10.1016/j.cplett.2006.02.003.

[48] F. Su, C. Lu, S. Hu, Adsorption of benzene, toluene, ethylbenzene and p-xylene by NaOCl-oxidized carbon nanotubes, Colloids Surfaces A Physicochem. Eng. Asp. 353 (2010) 83–91. doi:10.1016/j.colsurfa.2009.10.025.

[49] C.-J.M. Chin, M.-W. Shih, H.-J. Tsai, Adsorption of nonpolar benzene derivatives on single-walled carbon nanotubes, Appl. Surf. Sci. 256 (2010) 6035–6039. doi:10.1016/j.apsusc.2010.03.115.

[50] C.L. Mangun, Z. Yue, J. Economy, S. Maloney, P. Kemme, D. Cropek, Adsorption of Organic Contaminants from Water Using Tailored ACFs, (2001) 2356–2360.

[51] W. Chen, L. Duan, D. Zhu, Adsorption of Polar and Nonpolar Organic Chemicals to Carbon Nanotubes, Environ. Sci. Technol. 41 (2007) 8295–8300. doi:10.1021/es071230h.

[52] C.-J.M. Chin, L.-C. Shih, H.-J. Tsai, T.-K. Liu, Adsorption of o-xylene and p-xylene from water by SWCNTs, Carbon N. Y. 45 (2007) 1254–1260. doi:10.1016/j.carbon.2007.01.015.

[53] F. Su, C. Lu, S. Hu, Adsorption of benzene, toluene, ethylbenzene and p-xylene by NaOCl-oxidized carbon nanotubes, Colloids Surfaces A Physicochem. Eng. Asp. 353 (2010) 83–91. doi:10.1016/j.colsurfa.2009.10.025.

[54] F. Yu, Y. Wu, X. Li, J. Ma, Kinetic and thermodynamic studies of toluene, ethylbenzene, and m-xylene adsorption from aqueous solutions onto KOH-activated multiwalled carbon nanotubes., J. Agric. Food Chem. 60 (2012) 12245–53. doi:10.1021/jf304104z.

[55] C. Lu, Y.-L. Chung, K.-F. Chang, Adsorption of trihalomethanes from water with carbon nanotubes., Water Res. 39 (2005) 1183–9. doi:10.1016/j.watres.2004.12.033.

[56] F.A. Al-Khaldi, B. Abu-Sharkh, A.M. Abulkibash, M.A. Atieh, Cadmium removal by activated carbon, carbon nanotubes, carbon nanofibers, and carbon fly ash: a comparative study, Desalin. Water Treat. (2013) 1–13. doi:10.1080/19443994.2013.847805.

[57] M.A. Atieh, O.Y. Bakather, B.S. Tawabini, A. a. Bukhari, M. Khaled, M. Alharthi, et al., Removal of Chromium (III) from Water by Using Modified and Nonmodified Carbon Nanotubes, J. Nanomater. 2010 (2010) 1–9. doi:10.1155/2010/232378.

[58] C. Lu, F. Su, S. Hu, Surface modification of carbon nanotubes for enhancing BTEX adsorption from aqueous solutions, Appl. Surf. Sci. 254 (2008) 7035–7041. doi:10.1016/j.apsusc.2008.05.282.

[59] V.K. Gupta, S. Agarwal, T. a Saleh, Chromium removal by combining the magnetic properties of iron oxide with adsorption properties of carbon nanotubes., Water Res. 45 (2011) 2207–12. doi:10.1016/j.watres.2011.01.012.

[60] A. Zeino, A. Abulkibash, M. Khaled, M. Atieh, Bromate Removal from Water Using Doped Iron Nanoparticles on Multiwalled Carbon Nanotubes (CNTS), J. Nanomater. 2014 (2014) 1–9. doi:10.1155/2014/561920.

[61] B.S. Tawabini, S.F. Al-Khaldi, M.M. Khaled, M. a Atieh, Removal of arsenic from water by iron oxide nanoparticles impregnated on carbon nanotubes., J. Environ. Sci. Health. A. Tox. Hazard. Subst. Environ. Eng. 46 (2011) 215–23. doi:10.1080/10934529.2011.535389.

[62] Vinod Gupta and Tawfik A. Saleh, Synthesis of Carbon Nanotube-Metal Oxides Composites ; Adsorption, in: D.S. Bianco (Ed.), Carbon Nanotub. - From Res. to Appl., InTech, 2011: pp. 295–312. http://www.intechopen.com/books/carbon-nanotubesfrom-.

[63] N. Chaudhary, C. Balomajumder, B. Agrawal, V.S. Jagati, Removal of Phenol Using Fly Ash and Impregnated Fly Ash: An Approach to Equilibrium, Kinetic, and Thermodynamic Study, Sep. Sci. Technol. 50 (2014) 690–699. doi:10.1080/01496395.2014.958170.

[64] S. Azizian, Kinetic models of sorption: a theoretical analysis., J. Colloid Interface Sci. 276 (2004) 47–52. doi:10.1016/j.jcis.2004.03.048.

[65] N. Samadi, R. Hasanzadeh, M. Rasad, Adsorption isotherms, kinetic, and desorption studies on removal of toxic metal ions from aqueous solutions by polymeric adsorbent, J. Appl. Polym. Sci. (2014) n/a–n/a. doi:10.1002/app.41642.

[66] K.Y. Foo, B.H. Hameed, Insights into the modeling of adsorption isotherm systems, Chem. Eng. J. 156 (2010) 2–10. doi:10.1016/j.cej.2009.09.013.

[67] K. Vijayaraghavan, T.V.N. Padmesh, K. Palanivelu, M. Velan, Biosorption of nickel(II) ions onto Sargassum wightii: application of two-parameter and three-parameter isotherm models., J. Hazard. Mater. 133 (2006) 304–8. doi:10.1016/j.jhazmat.2005.10.016.

[68] M.S. Onyango, Y. Kojima, O. Aoyi, E.C. Bernardo, H. Matsuda, Adsorption equilibrium modeling and solution chemistry dependence of fluoride removal from water by trivalent-cation-exchanged zeolite F-9., J. Colloid Interface Sci. 279 (2004) 341–50. doi:10.1016/j.jcis.2004.06.038.

[69] M.C. Ncibi, S. Gaspard, M. Sillanpää, As-synthesized multi-walled carbon nanotubes for the removal of ionic and non-ionic surfactants., J. Hazard. Mater. 286 (2015) 195–203. doi:10.1016/j.jhazmat.2014.12.039.

[70] E. Fortunati, F. D'Angelo, S. Martino, a. Orlacchio, J.M. Kenny, I. Armentano, Carbon nanotubes and silver nanoparticles for multifunctional conductive biopolymer composites, Carbon N. Y. 49 (2011) 2370–2379. doi:10.1016/j.carbon.2011.02.004.

[71] M. Naebe, J. Wang, A. Amini, H. Khayyam, N. Hameed, L.H. Li, et al., Mechanical property and structure of covalent functionalised graphene/epoxy nanocomposites., Sci. Rep. 4 (2014) 4375. doi:10.1038/srep04375.

[72] M.P. Reddy, I.G. Kim, D.S. Yoo, W. Madhuri, Characterization and Electromagnetic Studies on NiZn and NiCuZn Ferrites Prepared by Microwave Sintering Technique, 2012 (2012) 628–632.

[73] J. Qiu, M. Guo, X. Wang, Electrodeposition of hierarchical ZnO nanorod-nanosheet structures and their applications in dye-sensitized solar cells., ACS Appl. Mater. Interfaces. 3 (2011) 2358–67. doi:10.1021/am2002789.

[74] Z.-Z. Zhu, Z. Wang, H.-L. Li, Functional multi-walled carbon nanotube/polyaniline composite films as supports of platinum for formic acid electrooxidation, Appl. Surf. Sci. 254 (2008) 2934–2940. doi:10.1016/j.apsusc.2007.10.033.

[75] Z. Yong, Z. Zhu, Z. Wang, J. Hu, Q. Pan, One-dimensional carbon nanotube–Fe x C y nanocrystal composite, Nanotechnology. 18 (2007) 105602. doi:10.1088/0957-4484/18/10/105602.

[76] I. Ahmad, H. Cao, H. Chen, H. Zhao, A. Kennedy, Y.Q. Zhu, Carbon nanotube toughened aluminium oxide nanocomposite, J. Eur. Ceram. Soc. 30 (2010) 865–873. doi:10.1016/j.jeurceramsoc.2009.09.032.

[77] K. Wang, L. Li, H. Zhang, A novel synthesis of nickel oxide and its electrochemical performances, Int. J. Electrochem. Sci. 8 (2013) 4785–4791. http://www.electrochemsci.org/papers/vol8/80404785.pdf (accessed June 11, 2015).

[78] S.T. Sing K.S.W., Everett D.H., Haul R.A..W., Moscou L., Pierotti R.A., Rouquerol J., REPORTING PHYSISORPTION DATA FOR GAS / SOLID SYSTEMS with Special Reference to the Determination of Surface Area and Porosity, 57 (1985) 603–619.

[79] B. Tawabini, S. Al-Khaldi, M. Atieh, M. Khaled, Removal of mercury from water by multi-walled carbon nanotubes., Water Sci. Technol. 61 (2010) 591–8. doi:10.2166/wst.2010.897.

Appendices

Appendix A

Calculation of Percentage Removal and Adsorption Capacity

Percentage Removal

$$Removal\ (\%)\ = \frac{C_o - C}{C_o} * 100$$

While C_o is initial concentration, C is concentration at any time t.

For example, if C_o = 0.85 mg/L and C = 0.41 mg/L

Then,

Removal (%) = 51.76

Equilibrium adsorption capacity experimental ($q_{e,exp.}$)

Experimental equilibrium adsorption capacity was used for fitting of kinetics and isotherm models.

$$\text{Equilibrium a}dsorption\ capacity, experimental\ (qe, exp.)\ = \frac{(C_e - C_o) * V}{m}$$

For example, if C_o = 0.85 mg/L, C_e= 0.41 mg/L, V=130 ml, m=50 mg

$Q_{e,exp}$.= 1.14 mg/g

Equilibrium adsorption capacity calculated ($q_{e,calculated}$)

Equilibrium adsorption capacity calculated ($q_{e,calculated}$) was obtained from fitting of experimental data with kinetic models.

For example, in case of fitting of data using pseudo second order model

$$\frac{t}{q_t} = \frac{1}{k_2 q_e^2} + \frac{t}{q_e}$$

q_e is calculated from the slope of a plot of 't/q_t' vs. 't'. This q_e is called $q_{e,calculated}$. From Table 5.1, by fitting of data for raw CNTs $q_{e,calculated}$ was 2.173.

Appendix B

Calculation of COD

Theoretical chemical oxygen demand (COD) of toluene is calculated as follows,

$$C_7H_8 + 9\ O_2 \longrightarrow 7\ CO_2 + 4\ H_2O$$

Hence, nine moles of oxygen are required for complete oxidation of one mole of toluene.

Based on weight,

$$Amount\ of\ oxygen\ required\ = \frac{32 * \ Moles\ of\ Oxygen}{92 * Moles\ of\ Toluene}$$

$$Amount\ of\ oxygen\ required\ = \frac{32 * \ 9}{92 * 1} = \frac{3.13\ mg\ of\ O_2}{mg\ of\ Toluene}$$

Hence, 3.13 mg of oxygen is required for 1 mg of toluene.

So, based on concentration of toluene in a sample, COD can be calculated. For example, if concentration of toluene is 50 mg/L or 50 ppm,

$$COD\ = \ 3.13 * 50 = 156.5\ mg/L$$

Hence, generally COD is,

$$COD\ (mg/L)\ = \frac{mg\ of\ O_2}{mg\ of\ a\ component} * \text{ Concentration of a component } (mg/L)$$

Vitae

Name	Aamir Abbas
Nationality	Pakistani
Date of Birth	20th August, 1988
Email	abbas.aamir14@gmail.com
Address	Dera Muhammad wala P/O Utra Kalan, Tehsil and District Mianwali, 42200, Punjab, Pakistan
Academic Background	B.Sc. Chemical Engineering, 2012, University of the Punjab, Lahore, Pakistan

Publications

1 **Abbas A.**, Ihsanullah, Abussaud B.A., Al-Baghli N.A.H., Atieh M.A., Benzene removal from water using CNTs impregnated with iron oxide nanoparticles (Submitted)

2 Ihsanullah, **Abbas A.**, Atieh M.A, Laoui T., Synthesis and characterization of silver doped carbon nanotubes membrane using a novel technique, Poster presentation, AMPM Research Conference, KAUST Jeddah, Saudi Arabia, February 2015

3 **Abbas A.**, Ihsanullah, Abussaud B.A., Al-Baghli N.A.H., Atieh M.A., Study involving batch and column operation for removal of benzene from water using aluminum oxide nanoparticles impregnated CNTs (Under Writing)

Seminars and Presentations

1 Presented graduate seminar on “Benzene, toluene and xylene removal from water using carbon nanomaterials”

2 Presentation on “Application of raw and modified carbon nanotubes for removal of benzene from water” KFUPM internal conference for SSC 6 presenters selection.